Adkins, Harvey John

AN INVESTIGATION OF THE INTERACTION OF AMINOACYL-TRANSFER RNA WITH ELONGATION FACTOR TU USING SITE-SPECIFIC FLUORESCENT PROBES

The University of Oklahoma PH.D. 1982

THE UNIVERSITY OF OKLAHOMA

GRADUATE COLLEGE

AN INVESTIGATION OF THE INTERACTION OF AMINOACYL-TRANSFER RNA WITH ELONGATION FACTOR Tu USING SITE-SPECIFIC FLUORESCENT PROBES

A DISSERTATION

SUBMITTED TO THE GRADUATE FACULTY

in partial fulfillment of the requirements for the

degree of

DOCTOR OF PHILOSOPHY

BY

HARVEY JOHN ADKINS

Norman, Oklahoma

1982

AN INVESTIGATION OF THE INTERACTION OF AMINOACYL-
TRANSFER RNA WITH ELONGATION FACTOR Tu USING
SITE-SPECIFIC FLUORESCENT PROBES

APPROVED BY

Arthur E. Johnson

John Lorsch

Edward Smith

Donald R. Soll

Jeneane M. Murphy

DISSERTATION COMMITTEE

ACKNOWLEDGEMENT

I wish to express my sincere gratitude to my mentor and friend Dr. Arthur E. Johnson, whose guidance and advice was invaluable to me during the completion of this research project. I can only hope that my contribution to his research program partially repays the debt I owe him.

Secondly, I wish to thank Drs. J. H. Lancaster, E. C. Smith, B. A. Roe, J. W. Murphy, and D. R. Bone for the helpful criticism they provided during the conduct of this research and preparation of this manuscript.

Thirdly, the support and encouragement of my parents during my post-graduate period was very important to my continuing education. It is my greatest sadness that my mother did not live to share this achievement of which she would have been so proud.

Finally, without the self-sacrifice and loving support provided by my wife, this research project would not have been completed.

TO GAIL, CHRISTOPHER, AND EMILY

TABLE OF CONTENTS

LIST OF TABLES

LIST OF ILLUSTRATIONS

LIST OF ILLUSTRATIONS (CONT.)

AN INVESTIGATION OF THE INTERACTION OF AMINOACYL-TRANSFER RNA WITH ELONGATION FACTOR Tu USING SITE-SPECIFIC FLUORESCENT PROBES

CHAPTER I

GENERAL INTRODUCTION

The Protein Synthesis System

The protein synthesizing apparatus of a cell is a very complicated system. Synthesis requires ribosomes, messenger RNA (mRNA), transfer RNA (tRNA), initiation factors, elongation factors, termination factors, and numerous small molecules (eg.--nucleotides). A recent review of the structure and function of these components has been published (1). Even when we focus on protein chain elongation, a complicated process is evident. A schematic representation of the minimum number of steps that must be involved is illustrated in figure 1 (2). In step 1 an appropriate aminoacyl-tRNA (aa-tRNA) in a ternary complex with the non-ribosomal protein elongation factor Tu (EF-Tu) and GTP diffuses to the A (or possibly recognition (R) (2,3)) site on the ribosome where the anticodon of the tRNA hydrogen bonds to the codon of the mRNA. In step 2 recognition of the proper aa-tRNA results in GTP hydrolysis, and EF-Tu·GDP then leaves the ribosome. The aminoacyl terminus of the aa-

Figure 1. Diagram of the steps involved in protein chain elongation of the ribosome. This represents the minimum number of steps necessary for a single aa-tRNA molecule to cycle on and off the ribosome. (Abbreviations: PEP, peptide; AA, amino acid; Tu, Elongation Factor Tu; Ts, Elongation Factor Ts; GTP, guanosine-5'-triphosphate; GDP, guanosine-5'-diphosphate; ATP, adenosine-5'-triphosphate; AMP, adenosine-5'-monophosphate; EF-G, Elongation Factor G; Syn, specific aminoacyl-tRNA synthetase.) (After Johnson, et al, ref. 2)

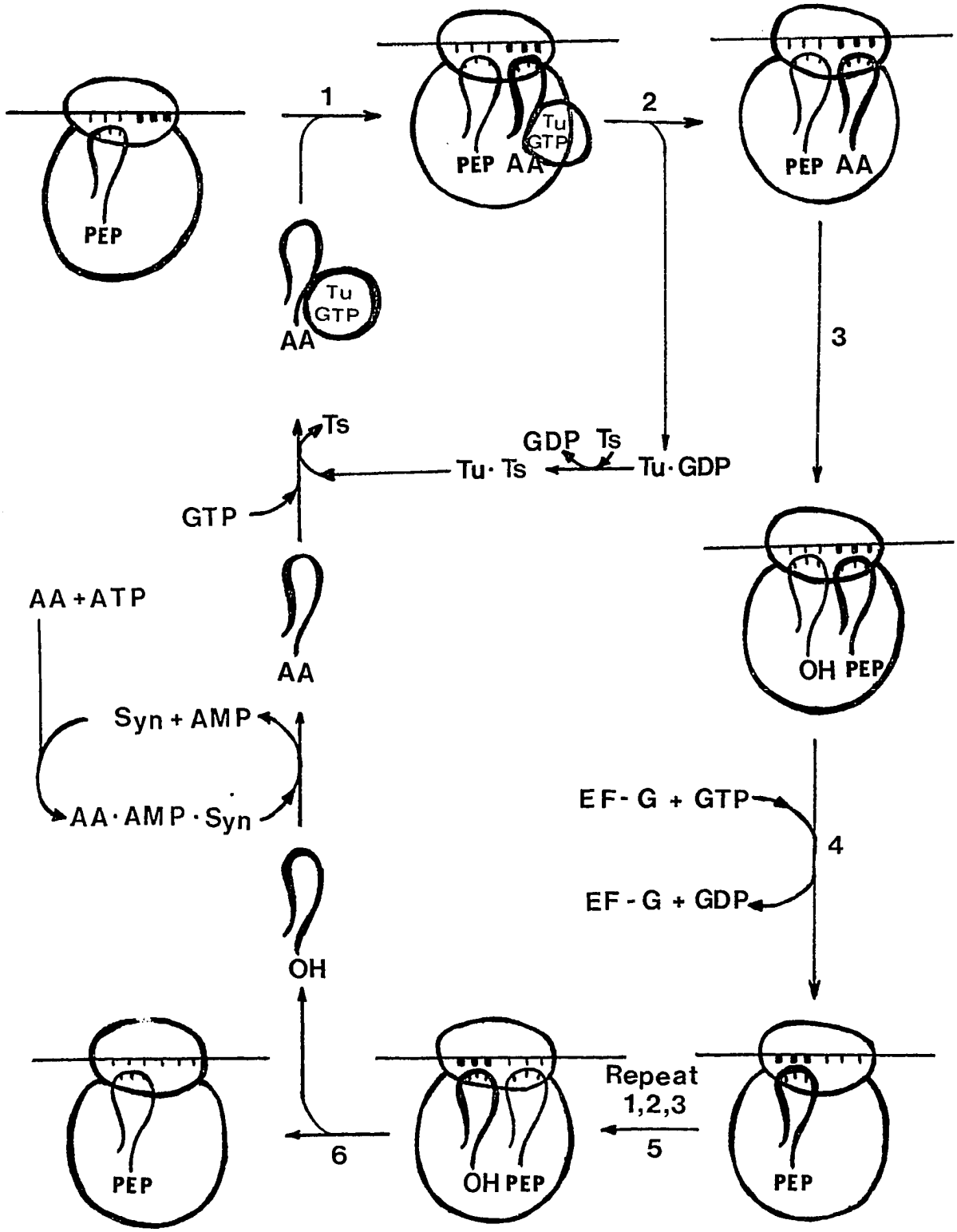
PEP
1
Tu
GTP
AA
PEP AA
2
PEP AA
3
Ts
GDP Ts
Tu·Ts
Tu·GDP
GTP
AA+ATP
AA
OH PEP
Syn+AMP
AA·AMP·Syn
EF-G + GTP
4
EF-G + GDP
OH
PEP
6
OH PEP
Repeat
1,2,3
5
PEP

tRNA in the A site will now be in position for transpeptidation which will occur spontaneously in step 3. In step 4 elongation factor G catalyzes translocation of the newly-formed peptidyl-tRNA from the A site to the P site. GTP is also hydrolyzed in this step, and the deacylated tRNA initially in the P site is ejected from the ribosome. For the tRNA now in the P site to cycle off the ribosome, this series of steps must be repeated following recognition of a second aa-tRNA. As noted earlier, this is the minimum number of steps necessary to complete one cycle. There may be others as well. Step 4, for example, is accomplished in stages (4). A complete understanding of this process will require an understanding of each of the individual steps in the cycle.

Elongation Factor Tu

EF-Tu is the most abundant protein found in *E. coli*. Estimates for *E. coli* B indicate that it may comprise as much as 6% of the total cell protein (5). This fact alone suggests that this protein must perform an important function. The protein is known to catalyze protein synthesis (6). How it performs this function is not understood. Some possibilities for the primary function of EF-Tu include (7,8):

1) It may interact with the ribosome to facilitate binding of aa-tRNA to the ribosome.
2) It may cause the aa-tRNA to adopt a particular, uniform conformation prior to recognition.

3) It may cause conformational changes in the ribosome necessary for recognition or peptide bond formation.

4) It may employ a combination of these and other as yet undetermined mechanisms.

It has also been suggested that EF-Tu prevents premature peptide bond formation by holding the amino acid in an unreactive position (8).

The aa-tRNA·EF-Tu·GTP Ternary Complex

Topological studies of the ternary complex. As noted, EF-Tu carries out its primary function in protein synthesis as part of a ternary complex with aa-tRNA and GTP. The three-dimensional structure of this complex has not been determined, although a number of laboratories throughout the world have been investigating this problem. The reason that this is an important question to answer is that if the structure is determined, insight will be gained into what parts of the aa-tRNA, EF-Tu, or both are available to interact with ribosomal components.

One way to determine the structure would be to use x-ray crystallography. Unfortunately, attempts to crystallize the complex have been unsuccessful due to the non-covalent nature of the interaction between the aa-tRNA and the EF-Tu. The ternary complex dissociates in the solvents used to date for crystallization. As a result, investigations of the three-dimensional topology of the ternary complex have focused upon solution studies. Ternary

complex structure has been examined by the ability of EF-Tu·GTP to protect aa-tRNA from ribonuclease degradation (9,10, Wilkman, et al, personal comm.), by low-angle x-ray scattering (11), and by kethoxal reaction with single-strand regions of the aa-tRNA (Bertram and Wagner, personal comm.). The low-angle x-ray scattering technique is of limited usefulness, since it only provides a general idea of the relative mass distribution (asymmetry) of the complex. And at present, there is a great deal of disagreement between authors using enzymatic and chemical modification techniques as to what parts of the aa-tRNA interact directly with the EF-Tu and what parts do not.

Several different experimental approaches have shown that the EF-Tu interacts with the aminoacyl terminus of the aa-tRNA. Alkaline hydrolysis of the aminoacyl ester bond of the aa-tRNA is greatly retarded when the complex is formed (12,13). Also, EF-Tu binds much more strongly to aa-tRNA than to peptidyl-tRNA, unacylated tRNA, or some aa-tRNAs modified at their aminoacyl termini (reviewed in 14). In addition, studies using normally aminoacylated tRNAs with different types of side chains, misacylated tRNAs, or a mutant suppressor tRNA which can be aminoacylated with either glutamine or tryptophan show that the efficiency of ternary complex formation is sensitive to the amino acide side chain (15-17). Analogs of the 3' terminus have been shown to complex weakly with EF-Tu·GTP (18,19). The high efficiency of affinity labeling of EF-Tu·GTP using N^{ϵ}-bromoacetyl-lysine-tRNA is further indication of a direct interaction between the protein

and the aminoacyl terminus (20). Finally, the C-C-A end of the aa-tRNA has been shown to be protected from nuclease digestion when in the presence of EF-Tu·GTP (9).

Presumably, the anticodon will be uncovered and free to "read" the mRNA on the ribosome. This is supported by the fact that ternary complex formation does not prevent dimer formation between tRNAs with complementary anticodons (21). Also, the attachment of bulky probes in this region does not prevent ternary complex formation (22-24).

The actual extent of direct interaction along the aminoacyl acceptor stem and in the corner region of the aa-tRNA has not been determined. Even investigators utilizing similar techniques (eg.--enzymatic degradation (9,10, Wilkman, et al, personal comm.)) are in disagreement on this question. What is needed is a non-destructive approach to avoid ambiguities caused by alteration of the complex structure during the course of the experimental procedure.

Conformational changes upon ternary complex formation. The frequency of errors in the protein synthesis system has been estimated to be one wrong amino acid per every 3,000 incorporated (25). This is much lower than should be expected from the binding that characterizes codon/anticodon interactions (26). Several theories as to how this accuracy is achieved have been formulated. They include such ideas as thermodynamic descrimination on the basis of different association constants between correct and incorrect

codon/anticodon pairs (27). A second theory is that GTP hydrolysis creates a high-energy intermediate state allowing for a second check during recognition (28). This is referred to as kinetic proofreading. Finally, there is the proposal of Kurland, et al (29), that the interaction between a codon and its cognate anticodon causes a conformational change in the aa-tRNA which facilitates subsequent interactions with the ribosome during the recognition process.

A possibility that is consistent with each of the above hypotheses is that the aa-tRNA conformation is regulated by EF-Tu·GTP. Specifically, the association with EF-Tu·GTP may constitute a mechanism of assuring that every aa-tRNA begins the recognition process in the same conformation. This conformation could be a high-energy conformation, and relaxation to a lower energy form may power some or all of the recognition process, as suggested by Kurland, et al (29). If ternary complex formation does require a specific aa-tRNA conformation, one might expect to observe conformational changes in the aa-tRNA when it associates with EF-Tu·GTP. Spin labels attached to bases in the anticodon loop of aa-tRNA are sensitive to ternary complex formation (22,23). This has been interpreted as the result of a conformation change. It is, however, conceivable that the increased rotational correlation times of the spin labels resulted largely (or only) from an increase in the size of the particle upon association of the protein and nucleic acid. Other studies using NMR (30), tritium exchange (31), and oligonucleotide binding (32) gave no indication of a gross

change in aa-tRNA conformation. However, small changes undetectable by these methods could not be ruled out.

The Use of Site-Specific Fluorescent Probes to Investigate the aa-tRNA·EF-Tu·GTP Complex

Our understanding of how aa-tRNA interacts with EF-Tu·GTP has been inhibited by the limitations of the techniques used to study the complex. What is needed is a nondestructive technique which will eliminate the ambiguities inherent in those techniques which alter the chemical structure of the aa-tRNA during the course of the investigation. Because fluorescence is very sensitive to the local environment and requires no alteration of structure during the course of an experiment, the use of site-specific fluorescence probes constitutes such a method. The method can be used to study both problems (topology and conformation) outlined above.

In practical terms, we desire to use a technique which would enable us to examine various aspects of ternary complex structure. Among the unknowns we would like to know are the following:

1) What is the initial conformation of the complex and/or aa-tRNA?
2) What, if any, conformational changes are taking place?
3) How large are these changes?
4) Do they require energy input?
5) When do the conformational changes take place?

6) How are these changes related to the various functional states of the complex?

7) What is the final conformation and how is it related to the initial one? (For example, is the final conformation of the tRNA such that it can be recycled?)

By monitoring the fluorescence characteristics of a site-specific fluorescent probe in the area of interest, insights into all of these questions can be obtained.

In order for a fluorescent probe to be of use, two criteria must be met:

1) The dye must not destroy biological function. This is important since the function of a macromolecule is inextricably interrelated with its structure. Loss of biological function strongly suggests that structure has been altered.

2) The dye must be sensitive to structural changes in the area of interest within the molecule or macromolecular complex.

In addition, determination of the exact position of the dye, while not completely necessary, is useful if maximum information is to be gained.

In studies involving tRNAs, several types of these site-specific fluorescent probes have been utilized. The fluorescence of a natural base in yeast $tRNA^{Phe}$, Y base, has been extensively studied (12,33-35). A second type of probe is one which has been covalently attached at a certain point on the tRNA by reaction with certain unusual bases or bases that have been chemically modified to make them reactive (36-40).

A third type is a chromophore which will form a tight, non-covalent complex at a specific position. Ethidium, for example, binds strongly to a single site on the tRNA molecule. However, the non-covalent nature of the interaction makes determination of the exact location of the site difficult. This question has been investigated primarily by NMR (41) and x-ray crystallography (42) and has not been resolved. Further investigations using fluorescence energy transfer (43) and nuclease digestion (44) have failed to clear up the picture. This question will be discussed in greater detail in chapter VI.

The fluorescence of a chromophore can be monitored in several ways:

1) Energy transfer between two appropriate chromophores can be used to measure the distance between them (2,40,43,45).
2) A variation in fluorescence intensity can be monitored. Such a change may be due to either a change in the molar extinction coefficient (ϵ) of the dye or to a change in the quantum yield (photons emitted/photons absorbed). This is strikingly illustrated by the binding of ethidium (Et) to nucleic acids. Upon binding the fluorescence intensity will increase on the order of 20-fold (46). A similar phenomenon is observed when 1-anilino-8-naphthalenesulfonate (ANS) binds to protein (47).
3) A shift in the wavelength of maximum excitation and emission, along with quantum yield changes, can give clues as to the type of environment in which the dye is located (eg.--polar or non-polar) (46,47).

4) Accessibility of the chromophore to the solvent can be determined by the ability of a solute to collisionally quench the fluorescence (48).

General Research Objective

The purpose of this research project was to study the corner region of the aa-tRNA during its interaction with EF-Tu·GTP. Two site-specific fluorescent probes were utilized:

1) A fluorescein moiety was covalently bound to the 4-thiouridine (s^4U) base of *E. coli* phenylalanine tRNA ($tRNA^{Phe}$) (40).
2) Ethidium was non-covalently complexed with unfractionated *E. coli* tRNA.

With the first probe, fluorescence intensity was monitored for both complexed and uncomplexed aa-tRNA in the presence and absence of collisional quenchers. In the case of Et, the ability of this dye to bind to complexed and uncomplexed aa-tRNA was investigated by observing changes in the fluorescence intensity of the dye.

Although the project was originally designed to investigate the topology of the ternary complex, we were aware that the probes might also detect conformational changes within the aa-tRNA. If such a change could be detected, this would represent an important finding. It could, for instance, help us to explain how the EF-Tu carries out its function of promoting the accurate recognition of the aa-tRNA for the binding site on the ribosome.

CHAPTER II

CHARACTERIZATION OF FLUORESCENT-LABELED tRNAs

Introduction

In order to investigate the interaction of aa-tRNA with EF-Tu·GTP, a fluorescent-labeled tRNA was required. Fluorescein-labeled *E. coli* $tRNA^{Phe}$ and AEDANS-labeled $tRNA_f^{Met}$ were prepared by reaction with 5-iodoacetamidofluorescein and 5-(2-(2-iodoacetamido)ethylamino)-1-naphthalenesulfonic acid (IAEDANS) respectively. Procedures for the synthesis and purification of these fluorescent tRNAs have been published (40). The resultant modified tRNAs were expected to have fluorescein or AEDANS covalently attached at the 4-thiouridine$_8$ (s^4U_8) position. However, in order for the new tRNAs to be of use in further investigations, the position of the label had to be determined. Also, it was necessary to determine if more than one site on the tRNA had been labeled.

The labeling reaction employs a nucleophilic attack on a primary alkyl halide (49). Both of these tRNAs have two sites at which such a reaction is likely to occur (49). The likely targets are the s^4U base at position 8 on both tRNAs and the pseudouridine base at positions 32, 39, and 55 on $tRNA^{Phe}$ or at position 56 on

$tRNA_f^{Met}$ (see figure 2). The much better nucleophile of the two (s^4U) would be expected to have the fastest reaction rate. In the three dimensional conformation of the tRNA, this base is located in the corner region of the L-shaped molecule. The crystal structure of yeast $tRNA^{Phe}$ is pictured in figure 3.

Only the $tRNA^{Phe}$-fluorescein was utilized for studies reported in this thesis. The $tRNA_f^{Met}$-AEDANS was used in studies involving energy transfer to the $tRNA^{Phe}$-F when the two tRNAs were located at adjacent sites on the ribosome (40). In this chapter the results of experiments done to characterize both of these tRNAs are reported.

Figure 2. The cloverleaf structures of $tRNA^{Phe}$ and $tRNA_f^{Met}$. Figure 2A shows the 2-dimensional structure for E. coli $tRNA^{Phe}$ (Uziel and Gassen, Ref. 50). Figure 2B is the secondary structure of E. coli $tRNA_f^{Met}$. (Dube, et al, ref. 51)

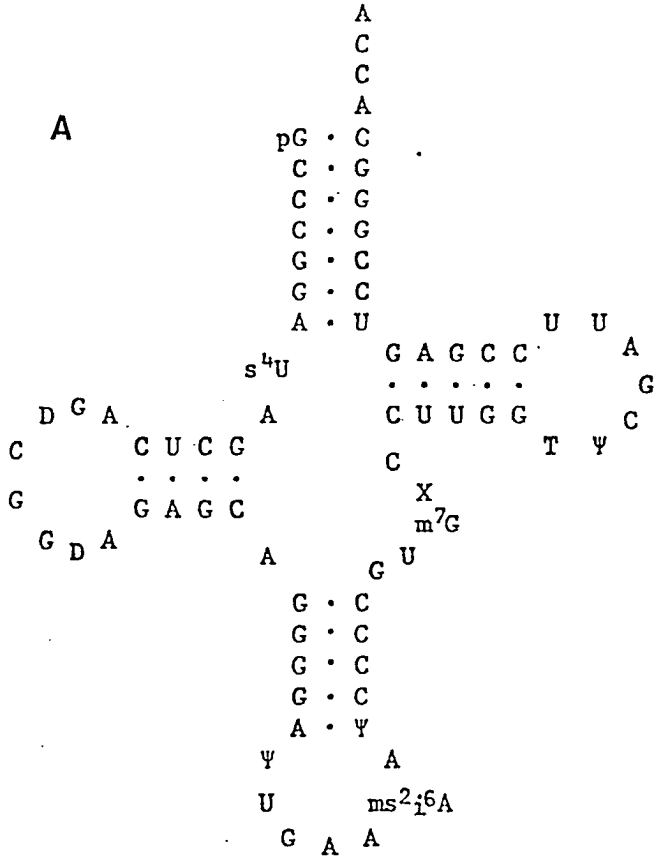
A
pG
s4U
D G A
C U C G
G A G C
G D A
G A A
G A G C C
C U U G G
T Ψ
X
m7G
G U
ms2i6A

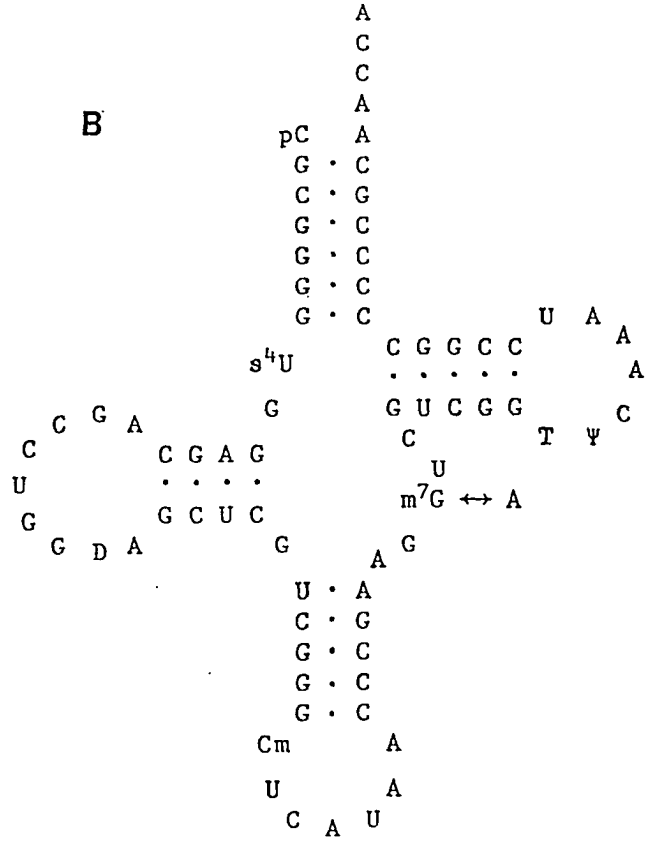
B
pC
s4U
C G G C C
G U C G G
T Ψ
C G A
C G A G
G C U C
G D A
U
m7G ↔ A
Cm
U
C A U

Figure 3. The three-dimensional conformation of tRNA. This figure represents the three-dimensional conformation of yeast $tRNA^{Phe}$ as determined by x-ray crystallography. (after Rich and Kim, ref. 52).

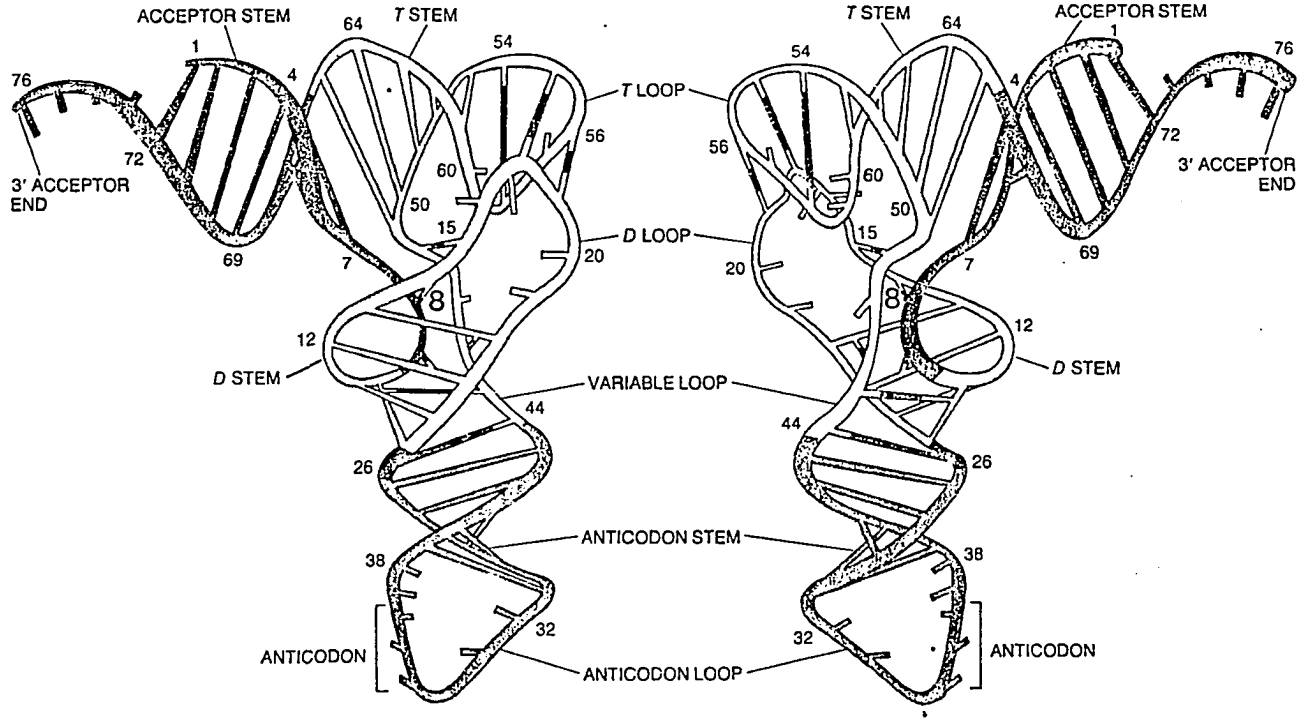
ACCEPTOR STEM
T STEM
T LOOP
D LOOP
D STEM
VARIABLE LOOP
ANTICODON STEM
ANTICODON
ANTICODON LOOP
3' ACCEPTOR END
1
4
7
12
15
20
26
32
38
44
50
54
56
60
64
69
72
76
78

Experimental

Preparation and purification of fluorescent-labeled tRNAs. Purified *E. coli* $tRNA^{Phe}$ (Plenum Scientific) and $tRNA_f^{Met}$ (Oak Ridge) were reacted with 5-iodoacetamidofluorescein (IAAF) or radioactive 5-(2-(2-iodoacetamido)ethylamino)-1-naphthalenesulfonic acid (1,5-IAEDANS) respectively. Fluorescent species from both reacted tRNAs were subsequently purified by reverse-phase anion exchange chromatography over RPC-5 resin. The procedures for this reaction and purification were done in accordance with previously published procedures (40).

Separation of fluorescent reagents and nucleosides. A variety of solvent conditions were tested for their abilities to separate s^4U, Ψ, IAAF, and IAEDANS by thin-layer chromatography (TLC). Silica gel plates (Analtech GHLF, pre-scored analytical TLC plates, 250 microns thickness) were predeveloped one time in methanol and dried for 30 mins. in air at room temperature. The purified nucleosides of s^4U (Sigma) and Ψ (Sigma) were dissolved in distilled H_2O to a concentration of 0.15M. The fluorescent reagents were dissolved to saturation in distilled H_2O. Samples were spotted onto the prewashed TLC plates one cm above the bottom of the plate, typically in volumes of 2 microliters. Spotting was done by adding 0.5 microliters of sample at a time with an Eppendorf pipet and drying in a stream of N_2 until the complete sample had been added to the TLC plate. Separate samples were at least one cm apart. The above procedure was done under conditions of reduced lighting in order to avoid photodegradation of the samples. Spotted plates were developed as soon as possible in 500 ml beakers containing 20 ml of the solvent to be tested. The beaker was

covered with aluminum foil both to maintain vapor saturation within the container and to prevent photodegradation of the samples while they were being chromatographed. R_f values were determined by measuring the distance from the center of the origin to the leading edge of the sample spot.

Preparation of dye-nucleoside marker adducts. Purified nucleosides of s^4U and Ψ were reacted with both IAAF and IAEDANS under conditons similar to those previously described for similar adduct preparation (53). The s^4U reactions (30°C, 30 min.) were done in a final volume of 100 microliters containing 1 mg of either IAAF or IAEDANS, 60% (v/v) methanol, 50mM phosphate buffer (pH7.4), and 15mM s^4U. For the Ψ reactions final volume was again 100 microliters and contained 1 mg of fluorescent reagent, 65% (v/v) methanol, 10mM carbonate buffer (pH9.0), and 15mM Ψ. These reaction mixtures were incubated at 60°C for 16 hours in order to get a significant yield of the products. All reactions were carried out in the dark in order to avoid photodegradation of either the reactants or the products.

Purification of dye-nucleoside marker adducts. The above reaction mixtures were evaporated to dryness in a stream of N_2 and then resuspended in 100 microliters of distilled H_2O. Sample preparations were streaked (by applying as spots very close together 1 cm above the bottom of the plate) onto TLC plates (Analtech GHLF, prescored analytical TLC plates, 250 microns thickness). Plates were broken so that each preparation was developed on a double (3"x4") plate. Sample was applied in 2 microliter aliquots with an Eppendorf pipet and dried in a stream of N_2. Typically,

it was necessary to develop two such plates in order to purify the adduct from the entire 100 microliter sample.

Optimal separation solvents were identified by spotting plates with both the nucleoside and the fluorescent reagent used in the particular reaction, as well as 2 microliters from the reaction suspension, and developing the plates with a variety of solvents. The objective was to obtain the best separation of the adduct from the reactants (see table 1), and hence obtain a pure adduct using a single solvent system. Adducts were located by visible detection of a new fluorescent spot (excited by long-wave UV using a Mineralight UVSL-25 fluorescent lamp). Association of the fluorescence with UV absorbance (expected from the nucleoside) was tested visually by shining short-wave UV light on the fluorescent TLC plate and looking for a dark spot coincident with the new fluorescent spot.

Once a solvent system had been decided upon the streaked plates were developed. The putative adduct (located as above) was scraped off the plate into a 13x100 mm assay tube with a razor blade. The new compound was eluted off the silica gel and into 100% ethanol by vigorous vortexing. Silica gel particles were allowed to settle out and the ethanol was removed carefully with a pasteur pipet. The eluted sample was evaporated to dryness in a stream of N_2 and resuspended in 1 ml of distilled H_2O.

Characterization of dye-nucleoside adducts. The adducts purified above were characterized by measuring their absorbances from 530-220 nm in 0.1M phosphate buffer (pH7.0) at 25°C. In addition, for the s^4U reactions, the course of the reaction was monitored by absorbance scans of samples removed from the reaction mixture at particular time intervals.

Fluorescent-labeled tRNA characterizations. Fluorescent-labeled tRNAs were completely digested to their nucleoside components by a slight modificaton of a published procedure (54). Digestion incubations (20 microliters, 22 hours, 37°C) contained: 1 microgram ribonuclease T_1 (Sigma); 40 micrograms ribonuclease A (Grand Island Biological); 4 micrograms snake venom phosphodiesterase (Worthington); 3.5 micrograms alkaline phosphatase (Sigma); 0.6 micromoles bicine (pH8.0); 0.2 micromoles magnesium acetate; and 0.2-0.3 A_{260} units of [^{3}H]AEDANS-labeled $tRNA_f^{Met}$ or 0.05 A_{260} units of fluorescein-labeled $tRNA^{Phe}$. Preparation of the reaction mix and the degradation itself were done under conditions of reduced lighting to avoid photodegradaton of the tRNAs or fluorescent dyes. In the case of the AEDANS-labeled tRNA, the incubation was done under N_2 in a capped microfuge tube to prevent decompositon of the fluorescent dye. After digestion the mixture was dried in a stream of N_2, resuspended in 2 microliters of distilled H_2O, and analyzed by silica gel TLC using the previously-described dye-nucleoside adducts as markers. The same TLC procedures were employed as described for marker purification. Fluorescein-containing spots and nucleoside-AEDANS markers were located visually by excitation with long-wave UV light. [^{3}H]AEDANS-labeled spots from the $tRNA_f^{Met}$ digestions were located by scraping 2 mm wide sections of the TLC plates into scintillation vials. To each vial was added 0.4 ml of distilled H_2O and 4 ml of Triton-containing scintillation cocktail (55). The samples were counted on a Beckman LS-100 liquid scintillation counter.

Analysis of the fluorescent-labeled tRNAs by TLC was carried out in those solvent systems which were found to best separate the pertinent marker adducts for the specific tRNA being analyzed (see table 2).

Results

Separation of dye-nucleoside adducts from reactants. Purification of the dye-nucleoside adducts from the reactions of s^4U or Ψ with either IAAF or IAEDANS was accomplished by the TLC method described in the experimental section. Table 1 shows the TLC R_f values of these components in various solvents. The solvent systems eventually chosen for the purification of preparative samples of the adducts or for fluorescent tRNA characterization are marked (*). Purification of s^4U-F in solvent number 4 (from table 1) required that the TLC plate be developed at least 5 times in order to move the adduct away from the origin. Table 2 lists R_f values obtained for pertinent compounds in those solvents used for preparative purification.

Characterization of dye-nucleoside adducts. The following absorbance maxima were expected for the various nucleosides and fluorescent dyes: s^4U = 331 nm, Ψ = 262 nm, fluorescein = 490 nm, AEDANS = 337 nm. Absorbance scans of all of the purified adducts showed them to have all of the expected maxima of both dye and nucleoside. In the cases of the s^4U adducts, the absorbance maximum for s^4U was shown to shift from 331 nm to 315 nm. This is consistent with previously published reports (53). An attempt was made to calculate the number of dye molecules per molecule of nucleoside by comparing the molar extinction coefficients at the maxima. In all cases there appeared to be slightly more than one dye per nucleoside molecule probably because the ϵ of the dye, the nucleoside, or both changed upon reaction.

Table 1. Thin-layer chromatography R_f values for bases, dyes, and their conjugates in various solvent systems. (Abbreviations: s^4U, 4-thiouridine; Ψ, pseudouridine; F, fluorescein; A, AEDANS; s^4U-F, adduct of 4-thiouridine and fluorescein; s^4U-A, adduct of 4-thiouridine and AEDANS; Ψ-F, adduct of pseudouridine and fluorescein; Ψ-A, adduct of pseudouridine and AEDANS; NT, not tested.)

Solvent system	R_f values							
	s^4U	Ψ	F	A	s^4U-F	s^4U-A	Ψ-F	Ψ-A
1. Chloroform:methanol (85 : 15)	.56	.21	.38	.11	NT	NT	NT	.69
2. 100% ethanol	.77	.68	.74	.69	NT	NT	NT	NT
3. Benzene:ethyl acetate:acetic acid (32 : 37 : 5)	.15	0	.62	0	NT	NT	NT	NT
4. *Benzene:pyridine:acetic acid: ethanol (16 : 6 : 1 : 5)	.77	.40	.82	0	NT	NT	.58	NT
5. *Benzene:pyridine:acetic acid: ethanol (65 : 25 : 4 : 6)	.57	.25	.66	NT	.33	NT	.18	NT
6. Ethyl acetate:methanol:H_2O: ammonia (10 : 2 : 1 : 1)	.15	.09	.12	.32	NT	NT	NT	NT
7. *Upper phase n-butanol:acetic acid: H_2O (4 : 1 : 5)	.72	.41	.96	.61	NT	.38	NT	.20
8. *Isobutyric acid:ammonia:H_2O (66 : 1 : 33)	.70	.54	.94	.57	NT	NT	NT	.45
9. Benzene:ethyl acetate:acetic acid: ethanol (32 : 37 : 5 : 3)	.43	0	.74	.07	NT	NT	NT	NT
10. Isopropanol:HCl:H_2O (70 : 15 : 15)	1	1	1	1	NT	NT	NT	NT
11. n-butanol:ethanol:H_2O (50 : 17 : 35)	.71	.52	.75	.75	NT	NT	NT	NT
12. *Benzene:ethyl acetate:acetic acid (32 : 36 : 7)	.20	0	.75	0	0	NT	NT	NT

Table 2. R_f values obtained in solvent systems used to purify samples of dye-nucleoside adducts.

	Solvent System	Compound	R_f
1.	Upper phase n-butanol:acetic acid:H_2O (4 : 1 : 5)	s^4U-AEDANS	0.38
		s^4U	0.72
		IAEDANS	0.61
2.	Isobutyric acid:ammonia:H_2O (66 : 1 : 33)	Ψ-AEDANS	0.45
		Ψ	0.54
		IAEDANS	0.57
3.	Benzene:ethyl acetate:acetic acid (32 : 36 : 7)	s^4U-F	0
		s^4U	0.20
		IAAF	0.75
4.	Benzene:pyridine:acetic acid: ethanol (16 : 6 : 1 : 5)	Ψ-F	0.58
		Ψ	0.40
		IAAF	0.82

Purified adducts were subjected to TLC in all of the solvents listed in table 1 in order to see whether the fluorescence and UV absorbance (determined visually by shining short-wave UV on the fluorescent plate) coincided. The fluorescence and UV absorbance was not separated in any of the solvents which indicates that the fluorescent dye and UV-absorbing base were covalently linked. No impurities were observed in any of the samples. Hence, we conclude that we have synthesized and purified the desired adducts.

Fluorescent-labeled tRNA Characterizations. RPC-5 anion exchange chromatographic elution profiles for both fluorescein-reacted $tRNA^{Phe}$ and AEDANS-reacted $tRNA_f^{Met}$ have been published (40). Fluorescein-labeled $tRNA^{Phe}$ eluted as a single peak. It had an A_{260}/A_{495} ratio of 12.3 indicating one dye per tRNA molecule (40). This tRNA was totally digested and analyzed using the procedure described in the experimental section of this chapter. On thin-layer chromatography using solvent number 5 (see table 1) inspection of the plate showed that the fluorescence of the digested tRNA sample migrated as a single spot and had the same R_f as the s^4U marker adduct. Even when the A_{260} of the digestion incubation was increased 5-fold to maximize the chances of observing other fluorescent species, none could be detected. A control in which TLC was carried out on undigested fluorescent tRNA showed that all fluorescence remained at the origin. Subjection of the marker adduct to the digestion procedure did not alter its R_f value. Thus, this tRNA is labeled with fluorescein at the s^4U_8 position and will be referred to as $tRNA^{Phe}\text{-}F^8$.

[^{3}H]AEDANS-labeled $tRNA_f^{Met}$ eluted from the RPC-5 column in two peaks, each with one dye per tRNA molecule. TLC analysis using solvent number 7 (from table 1) of the digestion products of one of the AEDANS-labeled tRNAs is shown in figure 4. Because the radioactive label had the same R_f as the synthesized s^4U-AEDANS marker, this tRNA will be referred to as $tRNA_f^{Met}$-AEDANS^8. The second AEDANS-labeled species was initially anticipated to be reacted at pseudouridine, since this is also a potential target for the reaction (49). However, this tRNA was also found to be labeled at the s^4U position. The separation of two $tRNA_f^{Met}$-AEDANS^8 species on the RPC-5 resin may result from the labeling of two different isoacceptors or from two different conformations of the same tRNA molecule that have different affinities for the RCP-5 resin.

Figure 4. Thin-layer chromatography of the digestion products of [^{3}H]AEDANS-labeled $tRNA_f^{Met}$. Marker adducts were 4-thiouridine-AEDANS (15-20 mm) and pseudouridine-AEDANS (6-13 mm).

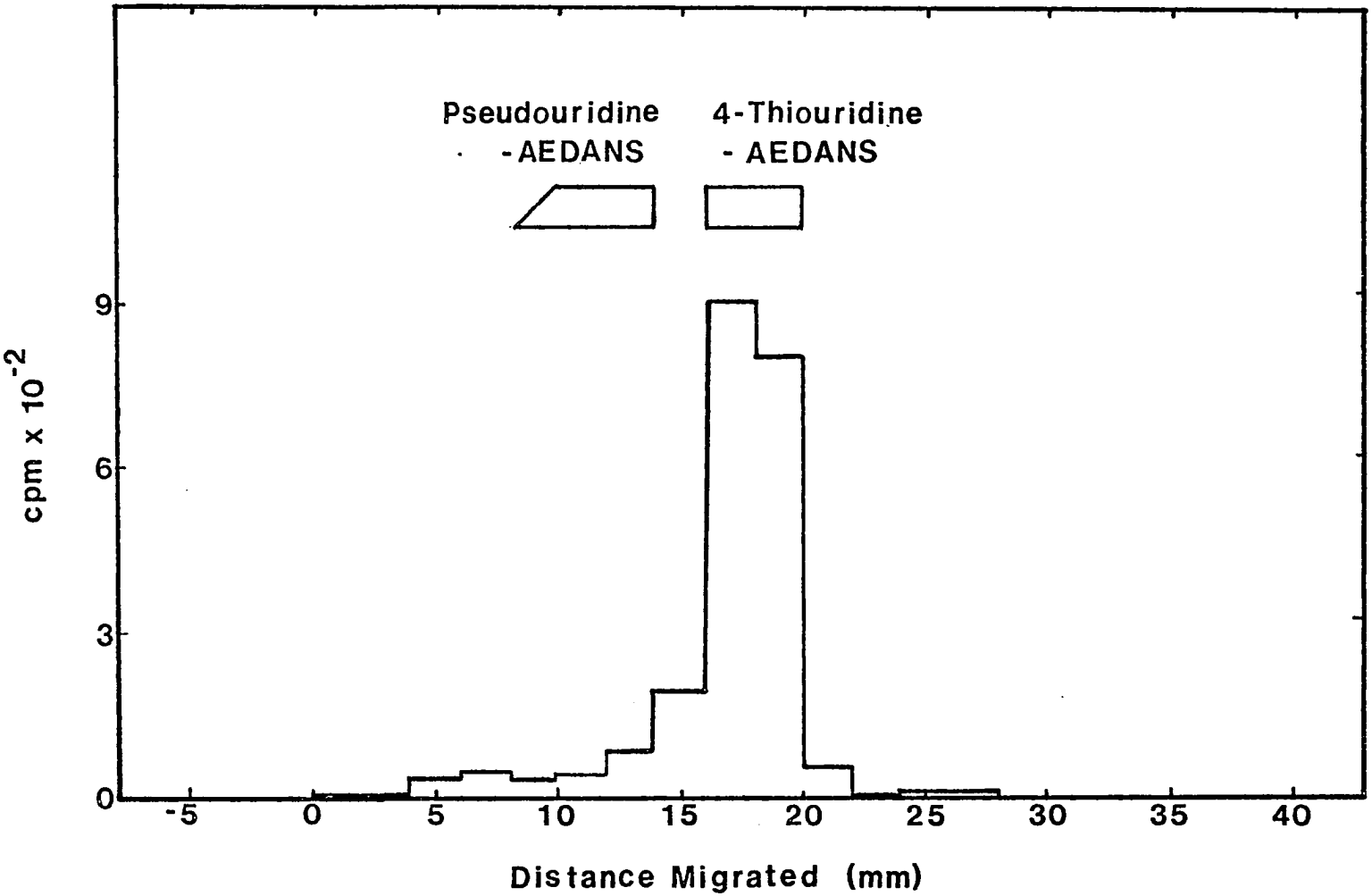
Pseudouridine
-AEDANS
4-Thiouridine
- AEDANS
cpm x 10^-2
9
6
3
0
-5
0
5
10
15
20
25
30
35
40
Distance Migrated (mm)

CHAPTER III

STABILITY OF THE Phe-tRNA^{Phe}-F^{8}·EF-Tu·GTP COMPLEX

Introduction

In order for the newly-synthesized fluorescent tRNA to be a useful tool in the study of the interaction between aa-tRNA and EF-Tu, the modified tRNA must retain its functional activity. Specifically, the aminoacylated tRNA must be able to form a ternary complex with EF-Tu·GTP. This activity can be tested, because ternary complex formation results in protection of the aminoacyl bond from alkaline hydrolysis (12). Formation of the complex can be demonstrated by a comparison of the rate of hydrolysis of amino acid from aa-tRNA in complex with EF-Tu·GTP to the rate of hydrolysis from uncomplexed aa-tRNA. A significantly slower rate of hydrolysis than would be expected for uncomplexed aa-tRNA demonstrates the presence of ternary complex.

A comparison of the rates of amino acid hydrolysis from EF-Tu-bound fluorescent and unmodified aa-tRNAs provides an indication of whether or not there are structural differences affecting function between the two species. Therefore, aminoacyl bond protection assays provide information on (i) whether the modified tRNA is functionally active and (ii) its activity relative to that of the unmodified species.

Finally, in order to study the ternary complex formed by the modified aa-tRNA, the presence of the complex must be demonstrated under the experimental conditions. Specifically, we wished to define the iodide ion concentration and ionic strength that we could employ in future experiments without disrupting the ternary complex.

This chapter reports the results of these experiments.

Experimental

Proteins. Crystalline EF-Tu·GDP (a gift from Dr. D. L. Miller) was purified from E. coli B by published procedures (56). S-100 enzymes were prepared from E. coli MRE600 as detailed previously (55). Pyruvate kinase from rabbit muscle was purchased from Sigma Chemicals.

Preparation of aminoacyl-tRNA. Preparative aminoacylation of $tRNA^{Phe}$ or $tRNA^{Phe}$-F^8 was accomplished in 5.0 or 6.0 ml incubations (37°C, 30 min.) containing 100mM HEPES (pH8.0); 20mM magnesium acetate; 5mM KCl; 4mM ATP; 10^{-4}M CTP; 1mM 2-mercaptoethanol; 10^{-5}M [^{3}H]Phe or [^{14}C]Phe (NEN, ICN, or Amersham); 300 or 360 micrograms of S-100 enzymes; and 2.5 to 6.6 A_{260} units of $tRNA^{Phe}$ or $tRNA^{Phe}$-F^8. Following phenol extraction and precipitation in high salt and ethanol, Phe-$tRNA^{Phe}$ or Phe-$tRNA^{Phe}$-F^8 was further purified by gel filtration on a Sephadex G-25 column (1.1 cm ID x 14 cm) equilibrated with 1mM potassium acetate (pH5.0) at 4°C. Following precipitation in high salt and ethanol, the pellet was resuspended in 1mM potassium acetate (pH5.0) and dialyzed against the same buffer. The sample was stored in liquid nitrogen. Absorbance was measured at 260 nm using a Cary 118 absorbance monitor in buffer containing 10mM Tris-Cl (pH7.4), 50mM NH_4Cl, and 10mM magnesium acetate. Concentration was determined assuming 1600 pmoles tRNA per A_{260} unit. The extent of aminoacylation was determined by a cold trichloroacetic acid precipitation assay. All samples used in this research were aminoacylated to a level between 750 and 1123

pmoles of [^{3}H]Phe or [^{14}C]Phe per A_{260} unit of tRNA (46.9 to 70.2% of theoretical).

Aminoacyl bond protection assays. Final incubations (160 microliters in 1.5 ml capped polypropylene tubes) contained: 10mM HEPES (pH7.4); 10mM magnesium acetate; 50mM NH_4Cl; 0.1mM dithiothreitol; 0.1mM $Na_2S_2O_3$; 10^{-5}M GDP; 1mM phosphoenolpyruvate (PEP); 3.1 micrograms pyruvate kinase; KI or KCl as indicated; EF-Tu as indicated; and aa-tRNA as indicated. Prior to addition of aa-tRNA, KI, and KCl, the samples were preincubated at 37°C for 10 min. to convert GDP to GTP with pyruvate kinase and PEP, and hence convert EF-Tu·GDP into EF-Tu·GTP. For EF-Tu·GDP (no ternary complex) controls, the PEP was omitted. Following the addition of the aa-tRNA and prior to any KI or KCl addition, samples were incubated in ice for 5 min. to allow ternary complex formation to occur. Immediately after KI or KCl addition, two 25 microliter aliquots were removed from each sample for assay, the sample was capped, and the sample was placed at 30°C. Duplicate 25 microliter aliquots were removed for assay as indicated. Each assay aliquot was precipitated in 1 ml of cold 10% (w/v) trichloroacetic acid, 3% (w/v) casamino acids (Difco Laboratories) for 10 min. in ice after the addition of 0.74 A_{260} units of ribosomal RNA in water to serve as carrier. Precipitates were collected on nitrocellulose triacetate filters (Gelman GA-6, 0.45 microns), then washed three times with 3 ml of cold 5% (w/v) trichloroacetic acid and once with 75% (v/v) ethanol. Dried filters were counted in a toluene-based

scintillator on either a Beckman LS-100 or LS-7500 liquid scintillation counter.

Results

The stability of the ternary complex formed with Phe-tRNA^{Phe}-F^{8} was compared with the stability of the ternary complex formed with Phe-tRNA^{Phe}. There is a small but reproducible difference in the rates of amino acid hydrolysis of the two complexes (see figure 5A). This may indicate one of two things:

1) The Phe-tRNA^{Phe}-F^{8} does not associate as strongly with EF-Tu·GTP as Phe-tRNA^{Phe} does because of the presence of the fluorescein probe.
2) The modification procedures may have damaged some of the tRNA in the Phe-tRNA^{Phe}-F^{8} making the sample heterogeneous. If the damaged tRNA had a reduced affinity for EF-Tu·GTP, a net increase in the rate of hydrolysis would result.

The net difference between modified and unmodified aa-tRNA was found to be sample dependent (data not shown). In addition, sham-reacted tRNA^{Phe} (subjected to the same modification reaction conditions as the Phe-tRNA^{Phe}-F^{8} except that IAAF was omitted) also showed a higher rate of hydrolysis than unmodified Phe-tRNA^{Phe} (data not shown). Both of the above suggest that the latter explanation (ii) is the correct one, but possibility (i) cannot be ruled out completely.

In the iodide quenching experiments (Chapter V), it was desired that all aa-tRNA would be complexed to EF-Tu·GTP throughout the experiments. For this reason a large molar excess of EF-Tu to tRNA was used in order to ensure that complex formation would be favored. Preliminary experiments had shown that a 5-fold excess of

EF-Tu (over 10^{-7}M aa-tRNA) would not be enough to hold the complex together at high concentrations of KI. Therefore, the molar excess of EF-Tu to tRNA was increased to 35-fold (equivalent to a 50-fold molar excess over aminoacyl-tRNA). The $[I^-]$ or $[Cl^-]$ dependence of complex formation was examined for both a 5-fold and a 35-fold excess of EF-Tu over total tRNA. Figure 5B shows that in the presence of a 9-fold molar excess of EF-Tu to total $tRNA^{Phe}$-F^8, the complex was destabilized at KI concentrations in excess of approximately 100mM. At a 53-fold excess of EF-Tu, the complex was very stable even in 125mM KI. We decided to use a 30-fold excess of EF-Tu in our iodide ion quenching experiments in order to force the equilibrium in favor of ternary complex formation.

Protection assays using chloride ions in place of iodide showed that high concentrations of Cl^- did increase the rate of amino acid hydrolysis (data not shown), but the effect was not nearly as pronounced as when I^- was added. This is not surprising in view of the chaotropic nature of the iodide ion (57).

Figure 5. Stability of the ternary complex. Figure 5A shows the rates of aminoacyl bond hydrolysis for Phe-tRNA^{Phe} (○no KI, ●100 mM KI) and for Phe-tRNA^{Phe}-F^{8} (□no KI, ■ 100 mM KI) in the presence of about a 4 fold molar excess of EF-Tu over aa-tRNA. The range of values obtained from parallel samples which lacked PEP is also shown, with the filled triangle indicating the average value. Figure 5B shows the rates of hydrolysis for Phe-tRNA^{Phe}-F^{8} in the presence of a 9 fold molar excess of EF-Tu over aa-tRNA (□no KI, ■125 mM KI) or a 53-fold molar excess of EF-Tu (○no KI, ● 125 mM KI). Incubations (160 μl), described in the Experimental section, contained: (A) 1.76 μg EF-Tu and either [^{3}H]Phe-tRNA^{Phe} (7,260 dpm/pmol Phe; 868 pmol Phe/A_{260} unit tRNA; .011 A_{260} units) or [^{3}H]Phe-tRNA^{Phe}-F^{8} (11,750 dpm/pmol Phe; 1085 pmol Phe/A_{260} unit tRNA; .010 A_{260} units); (B) [^{14}C]Phe-tRNA^{Phe}-F^{8} (899 dpm/pmol Phe; 905 pmol Phe/A_{260} unit tRNA; .012 A_{260} units) and either 4.1 μg or 24.4 μg of EF-Tu.

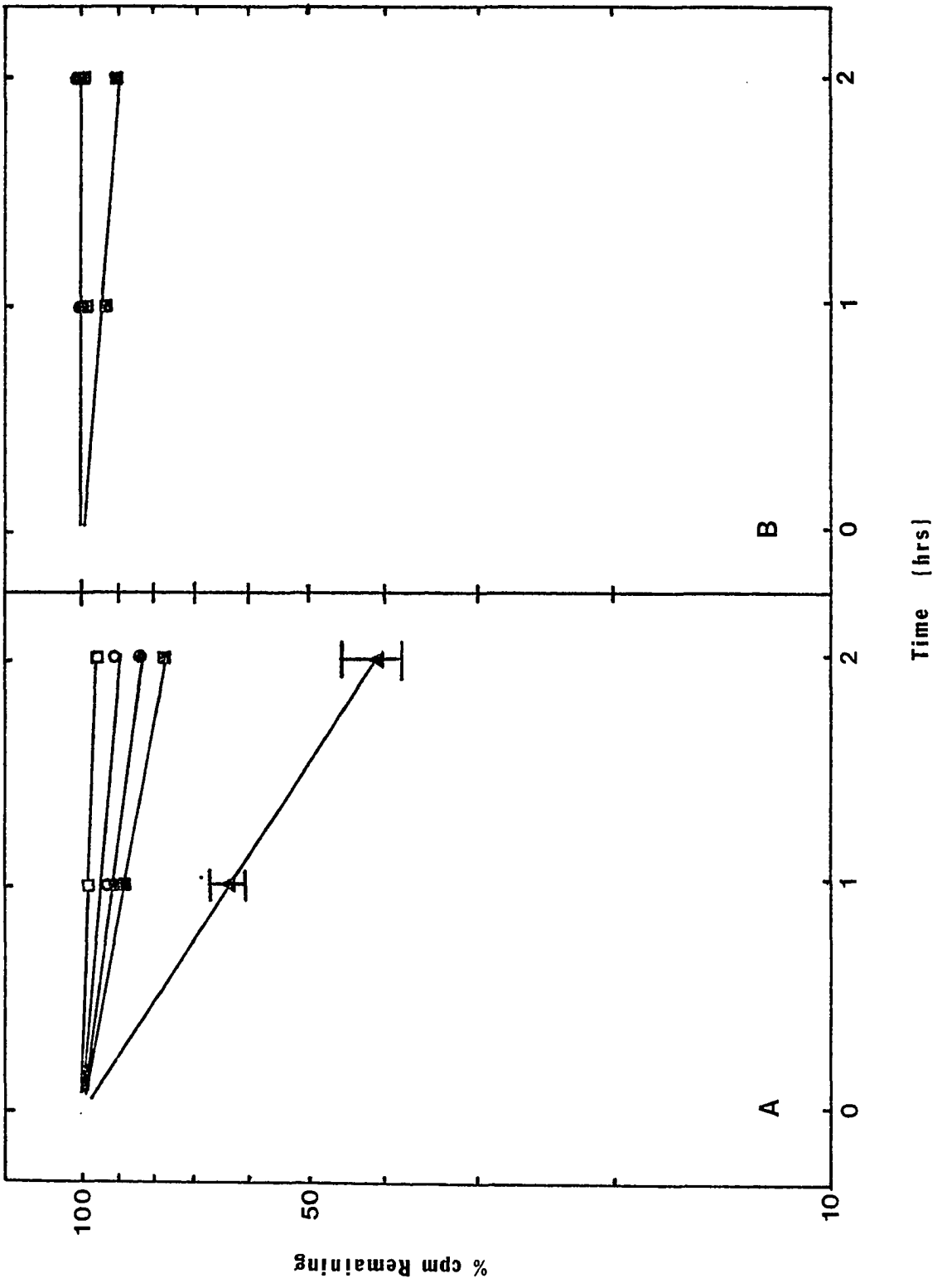
% cpm Remaining
100
50
10
A
B
0
1
2
Time (hrs)

CHAPTER IV

CHANGES IN THE FLUORESCENCE OF Phe-tRNA^{Phe}-F^{8} UPON ASSOCIATION WITH EF-Tu·GTP

Introduction

In chapter II we established that we had synthesized a tRNA with a site-specific fluorescent probe. In chapter III this modified aa-tRNA was shown to interact normally with EF-Tu·GTP. The question now becomes whether or not this tRNA will be a useful spectroscopic probe for interactions between Phe-tRNA^{Phe} and EF-Tu·GTP. In an attempt to answer this question, the fluorescence emission was monitored as Phe-tRNA^{Phe}-F^{8} was bound to EF-Tu·GTP because changes in the local environment of a fluorescent dye frequently cause the fluorescent signal to be altered. The experiments detailed in this chapter show that there is a change in the fluorescence intensity of the probe upon ternary complex formation.

Experimental

Fluorescence measurements. All fluorescence measurements were done on a Spex Fluorolog fluorescence spectrophotometer. Emission spectra for the experiments reported in this chapter were corrected for emission intensity using a standard lamp (Optronic Laboratories). For experiments reported in subsequent chapters, all emission spectra were uncorrected.

For fluorescein-containing samples, excitation was at 480 nm. Emission intensity was quantified by integration over the spectrum from 495 nm to either 600 nm (chapter V) or 680 nm (chapter IV). In all cases, for both ex and em, the band pass was 5 nm, which corresponds to slit widths of 1.25 mm (in), 1.25 mm, and 2.5 mm (out) in the Spex double monochromator arrangement. For ethidium-containing samples (chapter VI), excitation was at 520 nm and emission was quantified by integration from 540 to 750 nm. Slit widths were maintained as above, except at high concentrations of EtBr when they were reduced to 1.25-1.25-1.25(out)mm in order to reduce the intensity of emitted light impinging on the emission photomultiplier tube.

Samples were observed in 1 x 1 cm fluorescence cuvettes containing a final volume of at least 2 ml per cuvette (to ensure that the meniscus was not in the light path). Sample temperature was regulated using a Lauda K2R circulating bath attached to the cell holder. Lamp stability was tested for every experiment by measuring the H_2O Raman scatter (ex=350 nm, em=399 nm) both before and after the experiment.

Fluorescence intensity of $tRNA^{Phe}$-F^8 in different functional states. Fluorescence intensities of $tRNA^{Phe}$-F^8, Phe-$tRNA^{Phe}$-F^8, and Phe-$tRNA^{Phe}$-F^8·EF-Tu·GTP were compared directly usng an in situ aminoacylation in fluorescence cuvettes. Experiments were performed in buffer containing 100mM HEPES (pH8.0), 20mM magnesium acetate, 0.1mM dithiothreitol, 10^{-5}M [^{14}C]Phe (405 to 450 Ci/mol), 4mM ATP, 0.1 mM CTP, 10^{-5}M GDP, 11.4 micrograms pyruvate kinase, 1mM PEP, and 10^{-7}M $tRNA^{Phe}$-F^8 (based on 1600 pmoles per A_{260} unit). Total initial sample volumes were 2.25 ml. In most experiments a control containing no PEP (-complex) was run. In some experiments a control for fluorescence impurities was also run which contained no $tRNA^{Phe}$-F^8. Such controls were found to contribute no detectable fluorescence signal and were later omitted. Fluorescence measurements were made as described in the previous section. All spectra were obtained by measuring 1 nm increments at an integration time of 1 second.

Conduct of the experiment was as follows:

1) Components were added to cuvettes as indicated above.
2) The fluorescence emission of each sample (cuvette) was scanned as noted earlier. Also, a digital printout of the fluorescence intensity data was made in order to aid in the determination of the wavelength of maximum emission. All measurements were done at 30°C.
3) To each cuvette, 6 micrograms of Phe-tRNA synthetase (partially purified from E. coli MRE600 by a published procedure (58)) was added. The samples were incubated in the

Spex cell compartment at 30°C for 20 mins. during which time the tRNA was aminoacylated.

4) Fluorescence scans were done as in step (2).

5) Three 50-microliter aliquots were removed from each sample to assay for acid-insoluble radioactivity (described in chapter III) and thereby determine the extent of aminoacylation.

6) To each cuvette EF-Tu·GDP was added to a final concentration of 3.0×10^{-6}M, and the cuvettes were incubated for 15 mins. in the turret while ternary complex formation occurred.

7) Fluorescence scans were done as in step (2).

8) Samples were removed for assay as in step (5).

In some experiments, sample absorbance between 400 and 530 nm was measured after steps 4 and 6 using a Hitachi model 100-80 absorbance spectrophotometer. In these samples tRNA concentration was increased to 10^{-6}M in order to obtain an A_{480} of 0.05. Temperature was regulated to 30°C by a Haake model FK-2 circulating bath attached to the sample chamber. Measurements were done in the same 1 x 1 cm cuvettes utilized for the fluorescence measurements. Consistent scans were obtained only when the same face of the cuvette was oriented toward the light beam. Scan settings were as follows: scan speed = 1 nm per sec., response time = 1 sec., full scale = 0.1 or 0.2, chart speed = 20 nm per division. After scans were run in the wavelength scan mode, the wavelength program mode with auto print was used to obtain a digital reading of the absorbance at the excitation wavelength for fluorescence scans (480 nm).

Results

The purpose of these experiments was to determine the effect of aminoacylation and ternary complex formation on the fluorescence intensity of Phe-tRNA^{Phe}-F^{8}. Initially the fluorescence intensity of tRNA^{Phe}-F^{8} was measured. Addition of synthetase then converted the unacylated tRNA to Phe-tRNA^{Phe}-F^{8}. Again the fluorescence intensity was measured. Finally, upon addition of EF-Tu·GDP (which will be converted to EF-Tu·GTP in those samples containing PEP) ternary complex was formed and its emission measured. Since all steps were performed in the same cuvette, it was possible to compare directly the fluorescence emission in three different functional states: unacylated, aminoacylated, and complexed to EF-Tu·GTP.

Upon aminoacylation there was no increase in fluorescence intensity in samples containing 10^{-7}M tRNA^{Phe}-F^{8}. However, there was a slight increase (2%) in emission intensity in samples containing 10^{-6}M tRNA^{Phe}-F^{8} (fig. 6). This increase, seen only in high tRNA samples, probably results from a weak association of the tRNA with the synthetase enzyme.

Upon addition of EF-Tu to the cuvette (now containing aa-tRNA), the emission intensity increased significantly. A typical result is shown in figure 6. In this case the fluorescence intensity increased by 18.1%. Cold TCA precipitation assays showed that this sample was aminoacylated to a level of 1152 pmoles Phe per A_{260} unit tRNA. Thus, the fluorescence increase expected for a sample that is 100% aminacylated is 25.2%. The emission intensity

Figure 6. Corrected emission intensities of $tRNA^{Phe}$-F^8 (••••), Phe-$tRNA^{Phe}$-F^8 (---), and Phe-$tRNA^{Phe}$-F^8 in the presence of EF-Tu·GTP (——). Sample contents are described in Experimental, and include $tRNA^{Phe}$-F^8 at 1 μM. Excitation wavelength was 480 nm.

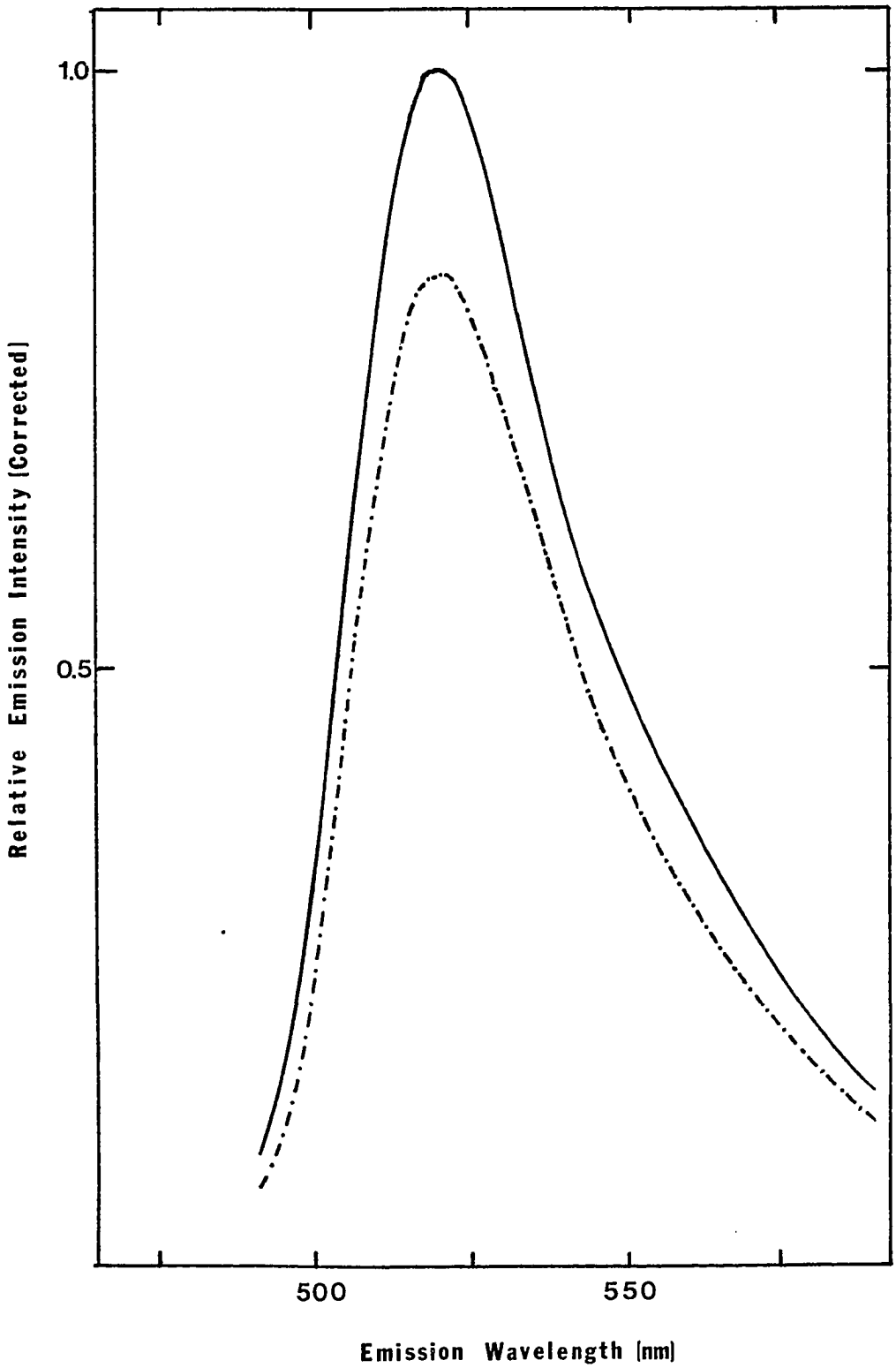
1.0
0.5
Relative Emission Intensity (Corrected)
500
550
Emission Wavelength (nm)

increases observed in our experiments ranged from 23% to 33% when normalized to 100% aminoacylation (aminoacylation levels varied from 56 to 72%). The average increase in fluorescence intensity of Phe-tRNA^{Phe}-F^{8} upon association with EF-Tu·GTP was 28%. These results were about the same as those obtained at a lower pH using different aminoacylation solvent conditions (58). In these experiments the average aminoacylation and fluorescence intensity increase were lower. When normalized to 100% aminoacylation, the average emission increase was 23%. Since the emission intensity of fluorescein is dependent upon pH, this difference was expected.

The magnitude of the change in fluorescence intensity is similar to the difference in emission intensity found when Phe-tRNA^{Phe}-F^{8} was added to parallel samples, one containing EF-Tu·GTP, the other EF-Tu·GDP. The fluorescence intensity of unacylated tRNA^{Phe}-F^{8} was not altered by the addition of EF-Tu·GTP.

Origin of the fluorescence intensity increase. An increase in the emission intensity of a fluorescent dye can be caused either by an increase in the quantum yield or by an increase in the molar absorptivity of the chromophore. Since the quantum yield is proportional to the fluorescence lifetime (59), one could measure the change in quantum yield by monitoring the change in fluorescence lifetime. We attempted to do this, but facilities available at the University of Oklahoma were found to be inadequate for our purpose. Thus, the effect of complex formation on the absorbance of the dye was measured instead. This was done using the same *in situ* procedure and samples used to obtain the data of fig. 6. Both

emission intensity and absorbance at 480 nm were measured for these samples. The total tRNA concentration was increased in order to obtain a significant dye absorbance (A_{480} approximately 0.05).

Absorbance changes paralleled the fluorescence changes upon aminoacylation and were small or zero (data not shown). However, upon addition of EF-Tu to the sample of figure 6, an absorbance increase of 14.8% (corrected to 100% aminoacylation as described for fluorescence intensity increase) was observed (see figure 7). Clearly, a large portion of the increase in the fluorescence intensity is due to an increase in the molar absorptivity of the chromophore. The average change in absorbance in our samples was 13% when Phe·$tRNA^{Phe}$-F^{8} associated with EF-Tu·GTP. Hence, absorbance changes account for approximately 50% of the increase in emission intensity upon ternary complex formation. This fact will become important in interpreting subsequent fluorescence quenching results.

Noteworthy problems encountered. Two problems were encountered during the conduct of these experiments. Both resulted in an apparent increase in the fluorescence intensity of samples which were expected to have no ternary complex formation and hence no change in fluorescence. In the case of samples containing high concentrations of tRNA (1.0×10^{-6}M) and EF-Tu·GDP (4.7×10^{-6}M), the fluorescence intensity increase in the EF-Tu·GDP-containing samples was nearly as great as in those containing EF-Tu·GTP. However, this fluorescence change was reversible upon addition of GDP, indicating

Figure 7. Fluorescein absorbance of Phe-$tRNA^{Phe}$-F^{8} before (---) and after (——) EF-Tu addition. The same sample was used to obtain the data in figures 6 and 7.

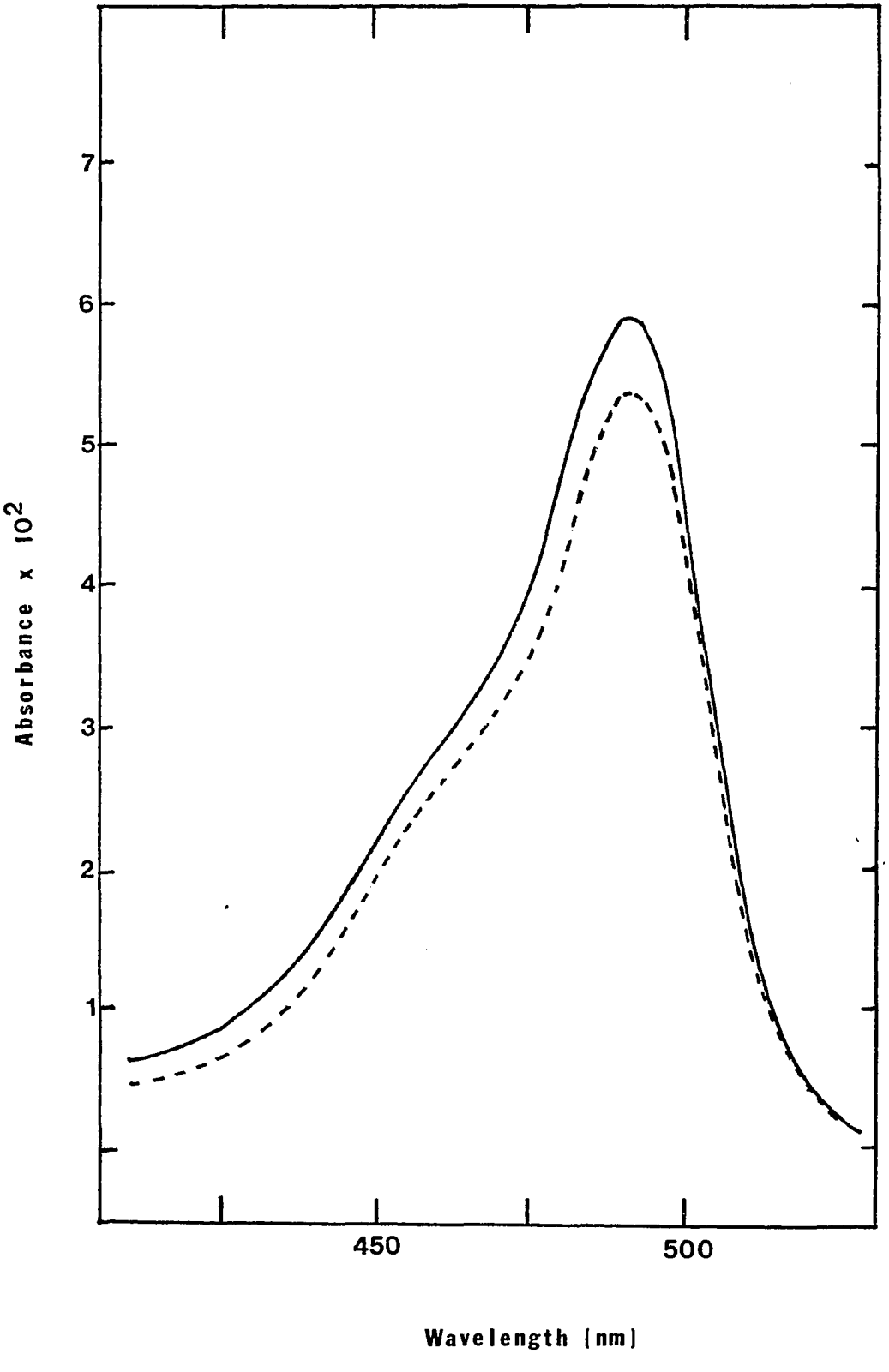
Absorbance x 10^2
7
6
5
4
3
2
1
450
500
Wavelength (nm)

that the fluorescence increase could not have been due to association of Phe-tRNA^{Phe}-F^{8} with EF-Tu·GDP. Since the sample also contained ATP, it is conceivable that the ATP was causing a low level of EF-Tu activation (enough to be detectable using the high concentration of very active EF-Tu sample). This possibility was ruled out by a control experiment which showed that ATP, under the experimental conditions, could not induce ternary complex formation to a detectable degree (data not shown). More likely, the partially purified synthetase preparation was contaminated with an enzyme such as nucleoside diphosphate kinase which was catalyzing the conversion of GDP to GTP from ATP.

In the other case, a sample lacking Phe and presumably unable to aminoacylate tRNA^{Phe}-F^{8} showed an increased intensity when EF-Tu·GTP was added to it. The most likely explanation was that our sample was contaminated with Phe, added with either the synthetase or the pyruvate kinase preparations as a degradation product. To test this interpretation, a sample containing Phe, AMP (4mM) and PP_i (0.05mM), but no ATP, was examined. No aminoacylation was possible in this sample since under these conditions the synthetase will catalyze the deacylation reaction: Phe-tRNA^{Phe} + AMP + PP_i $\longrightarrow$ ATP + Phe + tRNA^{Phe}. As expected, there was no increase in fluorescence when this control was run (data not shown). Thus, the experiment demonstrates that unacylated tRNA^{Phe} does not associate with EF-Tu·GTP.

In order to show unambiguously that the increase in the emission intensity of Phe-tRNA^{Phe}-F^{8} was due to its association

with EF-Tu·GTP, the reversibility of the fluorescence change was investigated. As has already been mentioned, reversibility by addition of GDP had already been tested. In addition, the fluorescence change should be reversible upon addition of non-fluorescent aa-tRNA, since this will complete for EF-Tu binding sites with the modified tRNA. When a large excess of non-fluorescent aa-tRNA was added to a sample containing Phe-tRNA^{Phe}-F^{8} in the presence of EF-Tu·GTP, the emission intensity decreased to the same level found in a control sample (data not shown). When an intermediate amount of aa-tRNA was added, the amount of fluorescence intensity decrease was consistent with the amount of Phe-tRNA^{Phe}-F^{8} expected to be displaced from the ternary complex. Thus, reversibility with both GDP and unmodified aa-tRNA indicate that the fluorescence intensity increase for Phe-tRNA^{Phe}-F^{8} in the presence of EF-Tu·GTP must be due to ternary complex formation.

CHAPTER V

COLLISIONAL QUENCHING OF FLUORESCENCE

Introduction

Data presented in the previous chapter showed that the fluorescence intensity of Phe-tRNA^{Phe}-F^{8} increases upon ternary complex formation. This change could be due to a direct interaction between the dye moiety and EF-Tu. Alternatively, the binding of EF-Tu at a site on Phe-tRNA^{Phe}-F^{8} distant from the fluorescein may cause a conformational change in the aa-tRNA molecule which alters the local environment of the dye.

A direct interaction would require that the protein bind to the aa-tRNA where the dye is covalently attached. The dye is located in a groove in the tRNA molecule, based on the three-dimensional conformation around its point of covalent attachment. When fully extended the dye would reach to the edge of the groove of the tRNA. The protein may bind so as to cover this region, in which case the chromophore would become inaccessible to the solvent. On the other hand, the protein could bind at a distant point on the aa-tRNA and exert an allosteric influence upon the dye. In this case the chromophore's accessibility to solvent would be unaltered.

One can test whether or not the fluorescein is accessible to solvent by measuring the sensitivity of its fluorescence emission to collisional quenchers dissolved in the solvent. Iodide ion is an efficient quencher of fluorescein fluorescence. Thus, if the fluorescein moiety is covered up by EF-Tu in the ternary complex, the ability of I^- to quench fluorescein fluorescence will be significantly decreased.

These experiments also provide information about the three-dimensional topology of the ternary complex, since one can determine whether the dye position is covered by or free of protein. This in itself is important, because as noted earlier, it is important to know the relative orientations of the protein and the nucleic acid in the complex and hence what regions are available for interaction with the ribosome during the recognition and binding process.

In these fluorescence quenching experiments, we have examined the efficiency of iodide ion quenching of Phe-$tRNA^{Phe}$-F^8 fluorescence in the presence of both EF-Tu·GTP and EF-Tu·GDP. The ability of I^- to quench the fluorescence of free fluorescein (5-iodoacetamido fluorescein), s^4U-fluorescein, unacylated $tRNA^{Phe}$-F^8, and Phe-$tRNA^{Phe}$-F^8 in the absence of EF-Tu was also examined. Finally, the abilities of Tl^+, Cs^+, acrylamide, NO_3^-, and SCN^- to quench fluorescein emission were tested. Only Tl^+ was found to be an efficient quencher (data not shown), and it was not used in any of these experiments due to problems caused by the insolubility of thallium salts.

Experimental

Fluorescence Quenching. Initially, samples contained buffer A (10mM HEPES (pH7.4), 10mM magnesium acetate, 50mM NH_4Cl, and 0.1mM dithiothreitol), 0.1mM $Na_2S_2O_3$ (to prevent I_3^- formation) and 10^{-7}M fluorescein, added as disodium fluorescein or 5-iodoacetamido fluorescein, $tRNA^{Phe}$-F^8, Phe-$tRNA^{Phe}$-F^8, or the covalent adduct of s^4U and IAAF as indicated. EF-Tu-containing samples also contained 1mM PEP (where indicated), 10^{-5}M GDP, 19.2 micrograms pyruvate kinase, and 2.0×10^{-6}M EF-Tu·GDP. All samples were incubated in the cell compartment at 30°C for 15 mins. to allow for temperature equilibration and for the formation of GTP and the ternary complex in those samples containing PEP. The cuvettes were shaken gently several times during this period to obtain a stable F_o measurement. This probably minimized the O_2 (a quencher) dissolved in the solution. Samples were titrated with iodide (or chloride) ions by sequential addition of (usually) 10-microliter aliquots of buffer A containing 4M KI (or 4M KCl). Fluorescence emission was measured 5 mins. after each addition of KI (or KCl) as detailed in the experimental section of chapter IV. Before and after each quenching experiment involving Phe-$tRNA^{Phe}$-F^8, two 20-microliter samples were removed from each cuvette and assayed for cold TCA precipitable radioactivity. This procedure typically required at least 4 hours.

Gel filtration chromatography. Samples (approx. 2 ml) were taken from cuvettes following spectral scans and cold TCA assays and then applied directly to a 1.8 cm ID x 30 cm column of Ultrogel AcA-44 equilibrated with buffer containing 50 mM Tris-Cl (pH7.4), 10mM

magnesium acetate, 50mM NH_4Cl, and 1mM 2-mercaptoethanol. Fractions of the eluant (25 drops, 1.35 ml) were collected at room temperature. Aliquots of 0.4 ml were removed from each fraction and placed into scintillation vials. To each vial 4 ml of Triton-containing scintillation cocktail (55) was added. Radioactive samples were counted on a Beckman LS-100 or LS-7500 liquid scintillation counter. Radioactive peaks were identified and their respective molecular weights determined (60) by comparison with the elution volumes of known species (BSA, 68,000 d.; EF-Tu·GDP, 44,000 d.; and fMet-$tRNA_f^{Met}$, 25,000 d.). Excluded and included volumes were determined by the elution positions of blue dextran and [^{3}H]lysine respectively. The K_{AV} for molecular weight determinations was calculated by the equation:

$$K_{AV} = \frac{V_e - V_o}{V_t - V_o},$$

where V_e is the elution volume of the unknown peak, V_o is the excluded volume, and V_t is the included volume. Elution volume of an individual peak was measured at the peak center.

Data analysis. Iodide ion quenching data was analyzed according to the Stern-Volmer relation (48):

$$\frac{F_o}{F} - 1 = K_{sv}[X],$$

where F_o is the initial fluorescence in the absence of quencher, F is the fluorescence measured at a particular concentration of added quencher, [X] is the concentration of quencher, and K_{sv} is the Sterm-Volmer quenching constant. K_{sv} is experimentally determined by measuring the slope of a plot of $(F_o/F) - 1$ vs. [X]. Further:

$$K_{sv} = k_q \tau_o,$$

where k_q is the bimolecular quenching rate constant and τ_o is the fluorescence lifetime in the absence of quencher. The k_q value of a dye covalently attached to a macromolecule depends upon the steric accessibility of the quencher to the dye. The lower the accessibility, the lower the value of k_q. In the case of a charged quencher, such as the one used in these experiments, the electrostatic environment of the dye will also be important. A major change in macromolecular topology or conformation is likely to cause a detectable change in the value of k_q.

Three types of Stern-Volmer plots are seen. They may be linear, upward curving, or downward curving. The three types indicate strictly collisional quenching, static plus collisional quenching, and a heterogeneous population of chromophores respectively (48,61). Except for plots of free dye and s^4U-F, all Stern-Volmer plots obtained in this study were linear.

Results

Initial fluorescence quenching observations. Iodide ion was found to quench the fluorescence of free (disodium) fluorescein, IAAF, s^4U-fluorescein, $tRNA^{Phe}$-F^8, and Phe-$tRNA^{Phe}$-F^8. Figure 8 shows the results of iodide ion quenching of these species in buffer A. Stern-Volmer plots of the quenching of disodium fluorescein and s^4U-fluorescein had similar slopes and corresponded closely with previously published results (62). Although it is not visible in the figure, these plots became non-linear at I^- concentrations above 50mM. The upward-curving plots that resulted indicate that static quenching became significant at high quencher concentration. Static quenching results when chromophore and quencher form a "dark complex" (48). In this case the local concentration of quencher around the fluorescent dye is such that a much higher efficiency of quenching of fluorescence is found than should be expected.

As expected, the quenching of the fluorescence of the $tRNA^{Phe}$-F^8 was greatly reduced in comparison to free dye (see fig. 8). This is due both to protection of the dye by the physical presence of the tRNA and to electrostatic repulsion between the tRNA (a poly-anion) and the negatively charged iodide ions. The Stern-Volmer plot was linear up to iodide concentrations of 279mM, indicating that only collisional quenching was occurring. The fact that the tRNA is negatively charged may explain why the plots for quenching of tRNA species did not curve upward as they did for free dye species. Repulsion of the I^- by the tRNA may not allow local concentrations of quencher high enough to form a dark complex.

Figure 8. Iodide ion quenching of free fluorescein (●, ○), $tRNA^{Phe}$-F^8 (■, □), and Phe-$tRNA^{Phe}$-F^8 (◆, ◇) fluorescence. Unfilled symbols represent controls for ionic strength effects in which chloride is added in place of iodide, as described in the experimental section of this chapter.

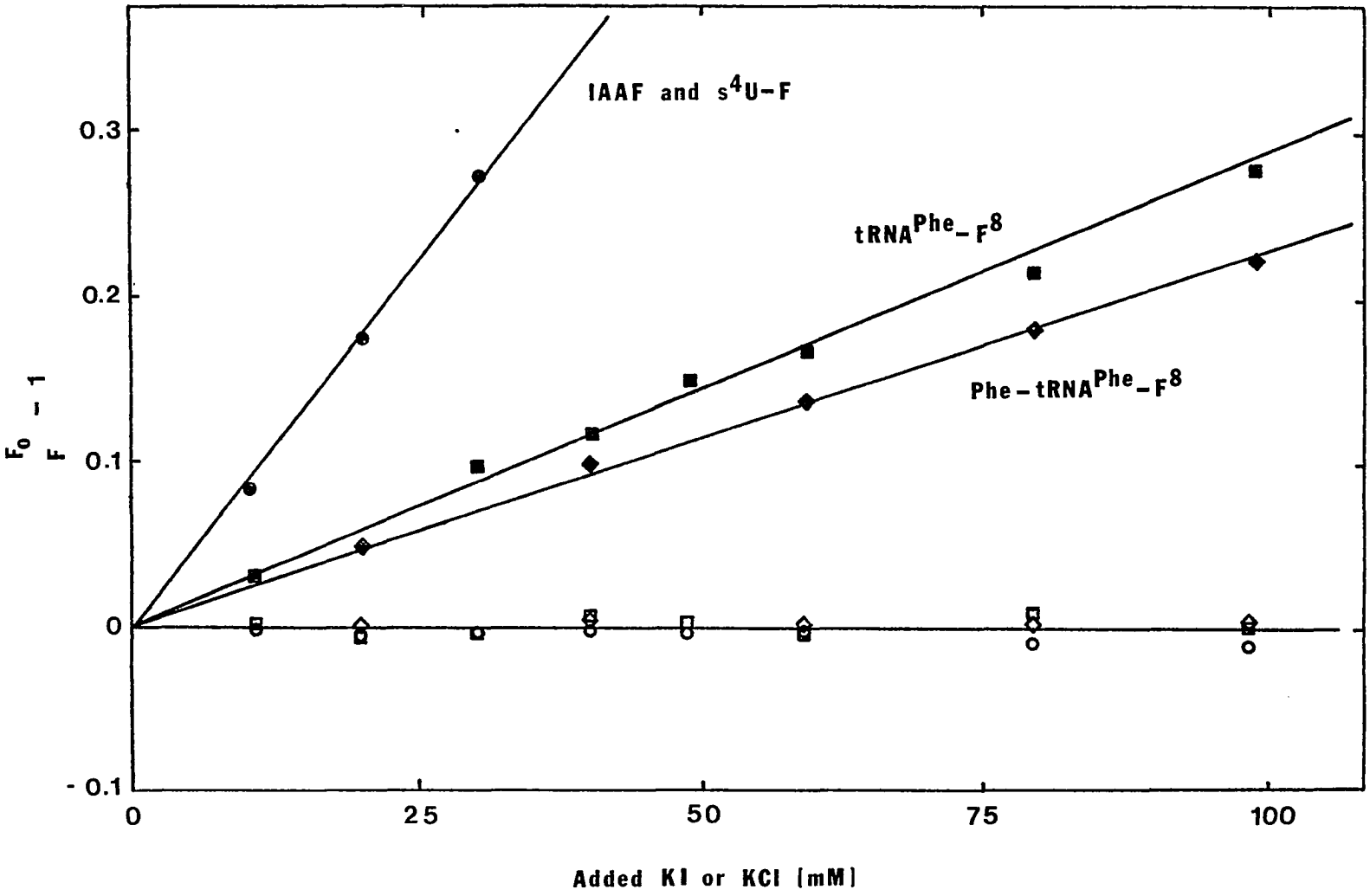
IAAF and s4U-F
tRNAPhe-F8
Phe-tRNAPhe-F8
F0 - 1
F
0.3
0.2
0.1
0
- 0.1
0
25
50
75
100
Added KI or KCl [mM]

When the fluorescence of Phe-tRNA^{Phe}-F^{8} was quenched it was expected to have the same K_{sv} as the unacylated tRNA. In fact, the quenching was not as efficient (see fig. 8). The experiment has been repeated with three different samples of tRNA^{Phe}-F^{8} and their aminoacyl derivatives and has been found to be reproducible. The lower quenching efficiency of the aa-tRNA may be a result of the fact that it is stored in a different buffer (1mM potassium acetate (pH5.0)) than is unacylated tRNA (H_2O). The change may also be an artifact induced during the aminoacylation procedure or due to intercalation of the amino acid (an aromatic) into the aminoacyl acceptor stem. Finally, there is a possibility that the technique utilized is actually detecting a difference in the conformations of the two species.

When tRNA^{Phe}-F^{8} and Phe-tRNA^{Phe}-F^{8} fluorescence was quenched under conditions favorable for ternary complex formation except for the omission of EF-Tu, the slopes of their respective Stern-Volmer plots increased (see figure 9). In addition, although there was still a difference between the two, the K_{sv}'s were much more similar than had been previously observed. The question of whether a conformational difference between the two has been detected or not remains unresolved and is worthy of future investigation.

In all cases, when chloride ion (a non-quencher) was substituted for iodide as a test for the effect of ionic strength on fluorescein fluorescence, no detectable change was observed (see fig. 8).

Figure 9. Iodide ion quenching of fluorescence of $tRNA^{Phe}$-F^8 in the presence of GTP (●) or GDP (■) and Phe-$tRNA^{Phe}$-F^8 in the presence of GTP (○) or GDP (□) under conditions favoring ternary complex formation. All components necessary for complex formation except EF-Tu have been added to the same concentrations utilized in ternary complex quenching experiments.

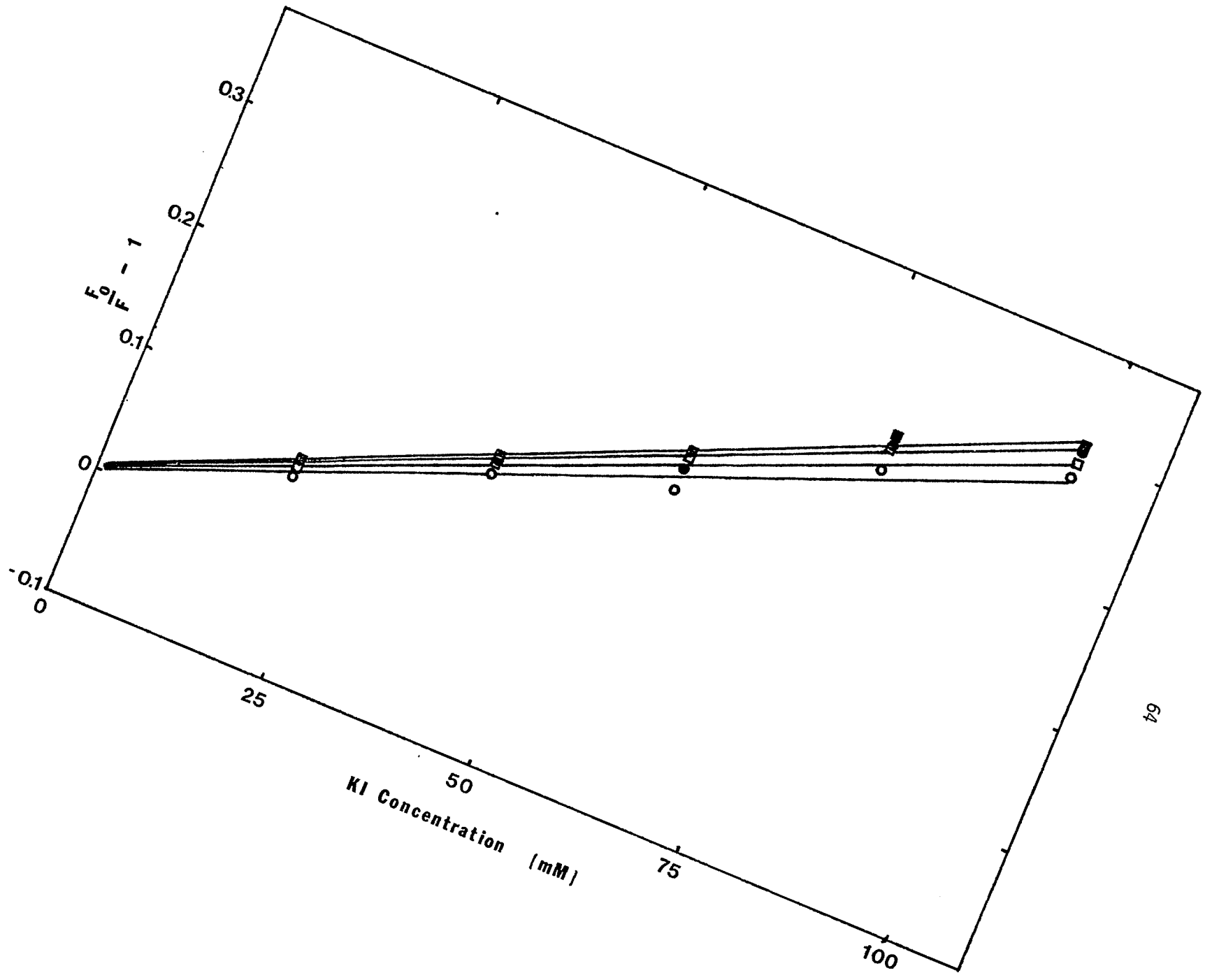
0.3
0.2
0.1
0
-0.1
$F^o/_F - 1$
0
25
50
75
100
KI Concentration (mM)
64

Fluorescence quenching of Phe-tRNA^{Phe}-F^{8} in ternary complex. Collisional quenching of the fluorescence emission of Phe-tRNA^{Phe}-F^{8} by iodide ion was measured in the presence of either EF-Tu·GTP or EF-Tu·GDP. Results are shown in figure 10. Both complexed and uncomplexed aa-tRNA have equal slopes, and hence equal Stern-Volmer constants (K_{sv}). This is an indication that the chromophore is equally accessible to solvent whether or not the aa-tRNA is complexed with EF-Tu. Consequently, the s^4U_8 position is not covered up by the protein when ternary complex is formed. Here again, as with the other quenching experiments, chloride ion (in place of iodide) had no effect on fluorescence (see fig. 10). Fluorescence intensity decrease is iodide-specific.

In addition to the above experiment, a control experiment was run in which the total added salt concentration ([KI] + [KCl]) was kept constant at 118mM. The KI concentration was varied from 0 to 118mM and the change in relative fluorescence was plotted as a function of [KI]. The Stern-Volmer constant obtained using this procedure was exactly the same as before (data not shown). This method confirms that the change in fluorescence intensity was strictly dependent upon I^- concentration and not due to a change in the ionic strength of the solution.

The final interpretation of this data is not completely straightforward, because $K_{sv} = k_q \tau_o$. As shown in chapter IV, the fluorescence intensity of Phe-tRNA^{Phe}-F^{8} increases by 33% upon ternary complex formation (fig. 6). A large portion (16%) of this increase is due to a change in the molar absorptivity of the

Figure 10. Iodide ion quenching of Phe-tRNA^{Phe}-F^{8} fluorescence in the presence of either EF-Tu·GTP (●,○) or EF-Tu·GDP (■,□). Unfilled symbols represent chloride controls for ionic strength effects. The inset shows the fraction of aa-tRNA remaining at the end of the experiment. Sample contents are described in the experimental section and each includes .133 A_{260} units of [^{14}C]Phe-tRNA^{Phe}-F^{8} (932 dpm/pmol Phe; 1170 pmol Phe/A_{260} unit tRNA).

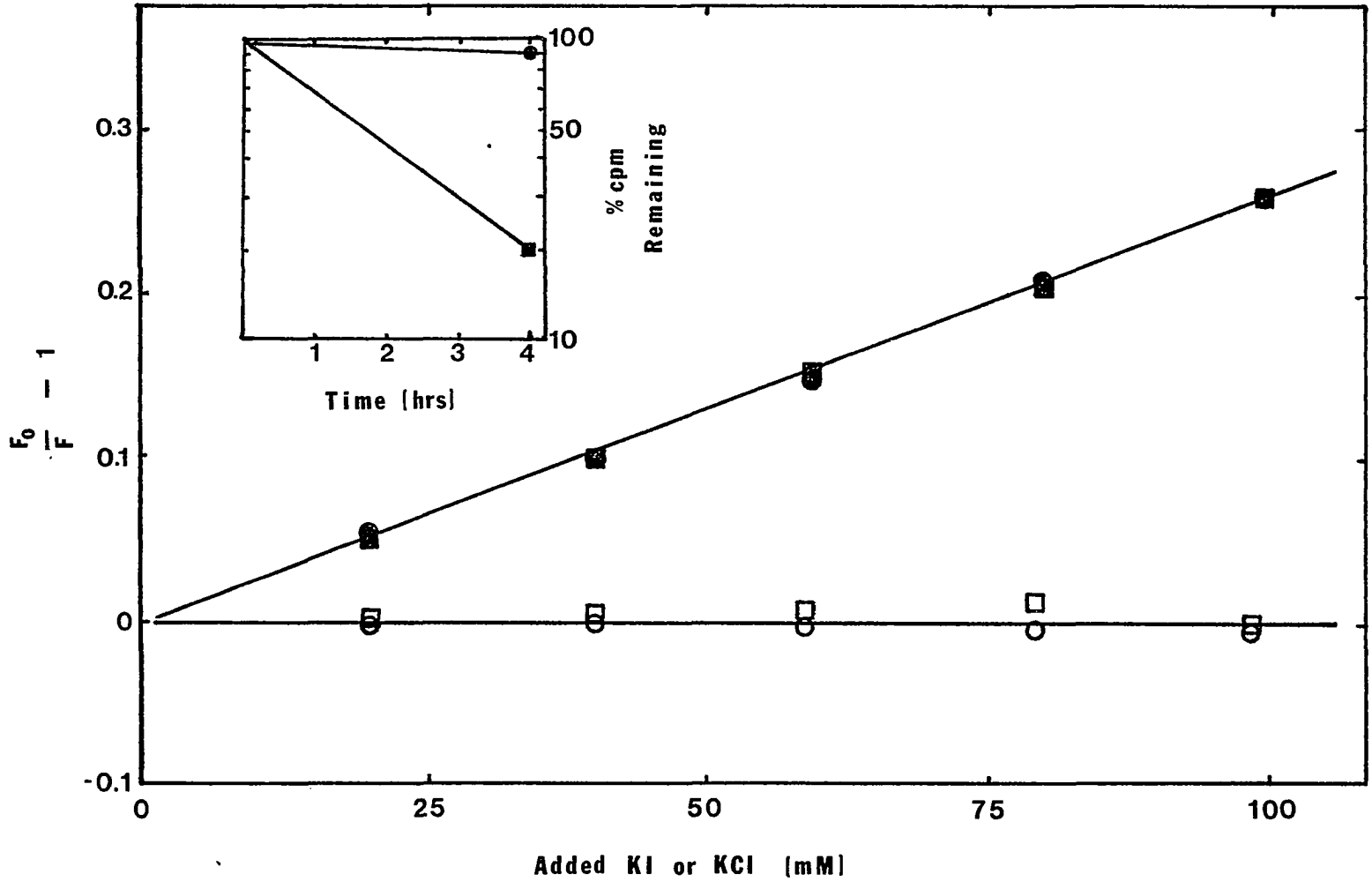
0.3
0.2
0.1
0
-0.1
$F_o/F - 1$
0
25
50
75
100
Added KI or KCl (mM)
100
50
10
% cpm Remaining
1
2
3
4
Time (hrs)

chromophore (see fig. 7), but it is likely that the fluorescence lifetime is also increased slightly. If this is the case, then the k_q values may differ by as much as 15% for Phe-tRNA^{Phe}-F^8 in the presence of EF-Tu·GTP. This difference is small enough that one can rule out the possibility of Tu covering a significant amount of this region of the aa-tRNA. More likely, this slight difference in k_q arises from a conformational change in the aa-tRNA discussed earlier (see chapter I). The positions of the negative phosphate charges on the aa-tRNA are probably altered sufficiently in the conformation change to alter the electrostatic environment of the dye and, therefore, the collision rate with the negative iodide ions.

A summary of K_{sv} values obtained for all fluorescence quenching experiments is shown in table 3.

Confirmation of ternary complex formation. The presence of ternary complex at the end of the long (typically four hours) fluorescence quenching experiments was confirmed by gel filtration chromatography (figure 11) and by aminoacyl bond protection assays (figure 10, inset).

Gel filtration of samples containing GDP resulted in the elution of two radioactive peaks (fig. 11). The higher molecular weight species eluted at the same elution volume as fMet-tRNA$_f^{Met}$. The lower molecular weight species eluted at the same position as lysine. The majority of the radioactive counts (80-90%) were contained in the low molecular weight peak. This indicates a high

Table 3. Summary of fluorescence quenching results. Results of iodide quenching experiments are expressed in terms of the slopes obtained from the respective Stern-Volmer plots (K_{sv}). Slopes are the averages of between 2 and 10 experiments (depending upon the species tested). K_{sv} values for individual species were reproducible to within 0.1 M^{-1}. The correlation coefficient is an indication of how well the data points correlate to a straight line (correl. coeff = 1.0000).

Iodide Quenching Summary

	Species	Buffer	K_{sv} (M^{-1})	Correlation Coefficient	λ_{max} Emission (nm)
1)	IAAF	A	9.8	.999	517
2)	Disodium fluorescein	A	10.2	.998	515
3)	s^4U-fluorescein	A	9.8	.997	517
4)	$tRNA^{Phe}$-F^8	A	2.9	.999	519
5)	Phe-$tRNA^{Phe}$-F^8	A	2.2	.999	519
6)	$tRNA^{Phe}$-F^8	A + TC	3.1	.999	519
7)	Phe-$tRNA^{Phe}$-F^8	A + TC	2.9	.999	519
8)	Phe-$tRNA^{Phe}$-F^8 + EF-Tu·GDP	A + TC	2.7	.999	519
9)	Phe-$tRNA^{Phe}$-F^8·EF-Tu·GTP	A + TC	2.7	.998	519

Notes: i) A + TC denotes experiments done in buffer A plus components for ternary complex formation (GDP, PEP, and pyrvuate kinase).

ii) For species 1 thru 3, Stern-Volmer plots become non-linear at KI concentrations above 50mM. The correlation coefficients for these species refer to KI concentrations from 0 to 50mM.

Figure 11. Gel filtration of Phe-tRNA^{Phe}-F^{8} in the presence of EF-Tu·GTP (●) or EF-Tu·GDP (○). These results were obtained by gel filtration of samples of fig. 10 following I^- quenching experiments (described in the experimental section of this chapter).

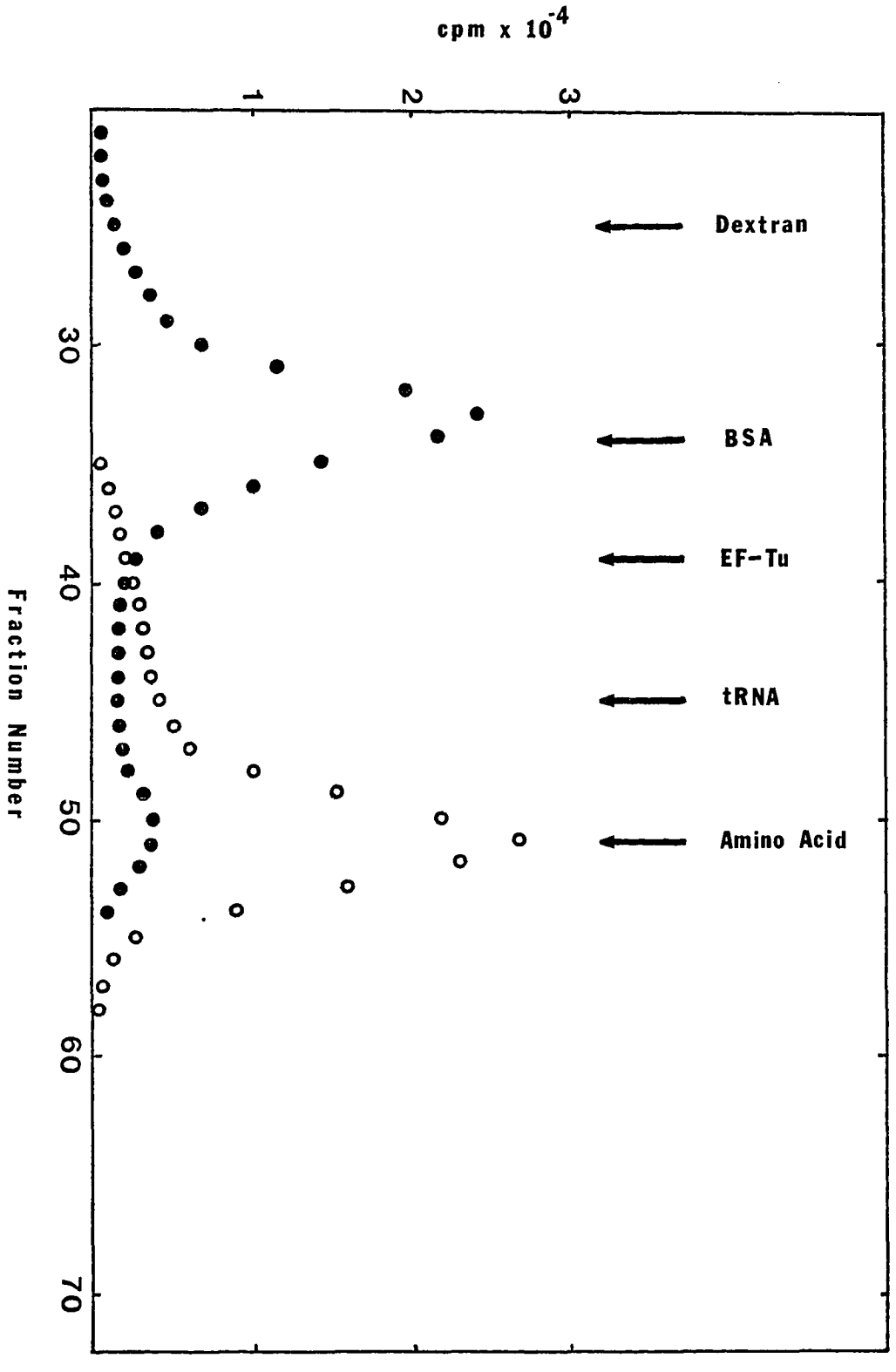
cpm x 10^-4
1
2
3
30
40
50
60
70
Fraction Number
Dextran
BSA
EF-Tu
tRNA
Amino Acid

rate of amino acid hydrolysis in this sample, as expected for uncomplexed aa-tRNA. In the GTP-containing cuvettes two peaks were also observed. The low molecular weight species again had the same elution volume as lysine and typically contained less than 7% of the total net cpm. The high molecular weight species eluted at an elution volume corresponding to a molecular weight equal to approximately 70,000 d. (see figure 12). More than 90% of the total net cpm were found to be in this peak. No peak could be detected at the elution of aa-tRNA, indicating that all of the aa-tRNA present was complexed with EF-Tu·GTP.

Protection assay results agree with the gel filtration data. Cold TCA precipitation assays taken before and after the quenching experiments show that aminoacyl bond hydrolysis is much slower in the cuvettes containing GTP than in those containing GDP (fig. 10, insert). Therefore, two independent methods confirm that virtually all of the aa-tRNA was associated with EF-Tu·GTP throughout the lengthy fluorescence quenching experiments.

Figure 12. Standardization of gel filtration column. This figure shows the molecular weight determination for the high molecular weight species from the GTP-containing sample of figure 11. The elution positions of bovine serum albumin (68,000 d., K_{av} = .32), EF-Tu·GDP (44,000 d., K_{av} = .50) and fMet-$tRNA_f^{Met}$ (25,000 d., K_{av} = .74) are also shown. Elution volume was measured to the center of the peak.

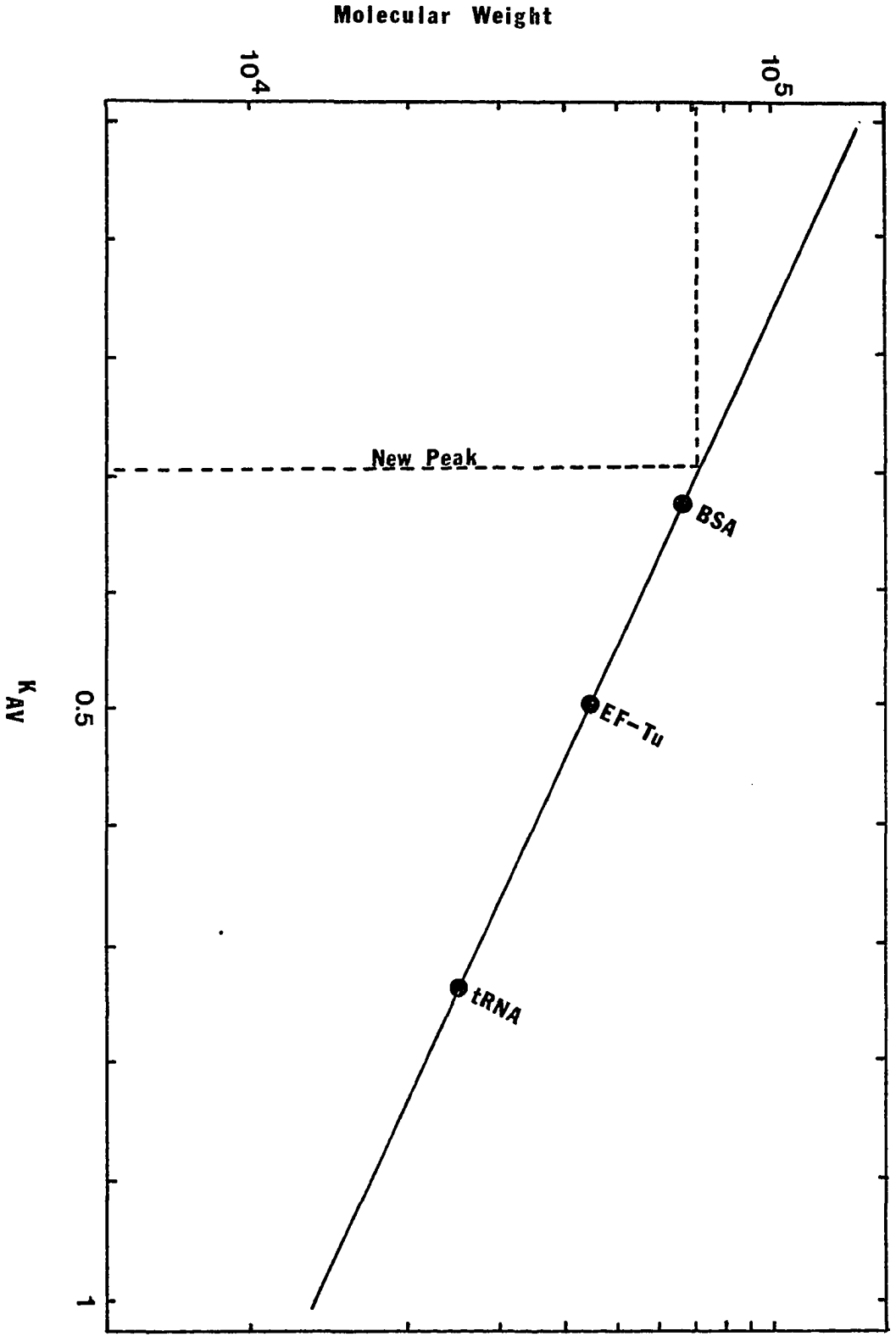
Molecular Weight
10^4
10^5
New Peak
BSA
EF-Tu
tRNA
K_{AV}
0.5
1

CHAPTER VI

ETHIDIUM BROMIDE BINDING TO UNFRACTIONATED tRNA

Introduction

In order to obtain further data concerning the topology and possible conformational change in the corner region of the aa-tRNA upon association with EF-Tu·GTP, another probe was utilized. Ethidium (Et) binding to unfractionated aa-tRNA in the presence of EF-Tu·GTP or EF-Tu·GDP was investigated. Transfer RNA has one strong binding site for ethidium (K_a approximately $3x10^6 M^{-1}$) (43). This system provides us with certain advantages over the one employing the modified tRNA. First, the tRNA is unmodified. This has the obvious advantage of eliminating the possibility that a covalently attached probe has perturbed the structure of the tRNA. Secondly, the unfractionated tRNA contains all the species of tRNA. Therefore, our interpretation is not limited to a particular tRNA. Even so, we must be careful in making a general interpretation since small, individual differences may be obscured. Finally, the position of the strong binding site for ethidium is known to be within our region of interest.

The exact Et binding site has not been established unambiguously, nor has the mechanism of its binding been determined

(41-44). NMR studies indicate that the dye intercalates between base pairs AU_6 and AU_7 along the aminoacyl acceptor stem (41). Others disagree that this is the position of the site or the binding mechanism (42,44). X-ray crystallographic analysis indicates that the Et stacks partially on the uridine or s^4U base found at position #8 (42). This binding is apparently stabilized by hydrogen bonding to phosphates P8 and P15. Either location is consistent with experiments which measured the fluorescence energy transfer between the Et and a fluorescent dye covalently attached to the 3' terminus of a tRNA (43). In either case, the binding site for Et is very near the corner of the tRNA molecule and the s^4U_8 base. The lack of certainty as to the exact position is counterbalanced by the advantages listed above.

In this chapter the binding of Et to aa-tRNA was examined in the presence of either EF-Tu·GTP or EF-Tu·GDP, as well as in the absence of EF-Tu.

Experimental

Titration of ethidium with unfractionated tRNA. Titration of 10^{-6}M EtBr was carried out in 1 x 1 cm fluorescence cuvettes (initial volume 3 ml, 10°C). The titrations were done in buffer A (see experimental, chapter V) plus an additional 125mM NaCl (to minimize the amount of non-specific, electrostatic binding of the dye to tRNA (41)). In all cases, prior to addition of the EtBr to the cuvette, background fluorescence was measured for each cuvette. This was subtracted from each subsequent fluorescence measurement. In all cases A_{520} was less than 0.01, so there was no inner filter effect.

The relative emission intensities of free Et (F_F) and of tRNA-bound Et (F_B) were determined as follows. Unfractionated tRNA or aa-tRNA (as indicated) was added in small aliquots (typically 1 to 10 microliters) until the fluorescence intensity was the same for at least two consecutive readings. The highest fluorescence intensity value obtained constituted F_B. The initial fluorescence in the absence of tRNA constituted F_F. F_B/F_F for our conditions was measured at both 10°C and 30°C by this method. Determination of the binding constants and amounts of bound dye is described in the data analysis portion of this section.

Titration of ethidium with ternary complex. 10^{-6}M EtBr was titrated with either aa-tRNA·EF-Tu·GTP or aa-tRNA + EF-Tu·GDP at 10°C. Cuvettes initially contained (in 2.0 ml) 10^{-6}M EtBr, buffer A + 125mM NaCl, 19.2 micrograms pyruvate kinase, and either 10^{-5}M GTP plus 1mM PEP (in ternary complex samples) or 10^{-5}M GDP (negative complex). Titrant, prepared in a polypropylene microfuge tube, contained: buffer A + 125mM NaCl, 168

micrograms EF-Tu, 4.8 micrograms pyruvate kinase, and either 10^{-5}M GTP plus 1mM PEP (plus complex) or 10^{-5}M GDP (minus complex). The titrant solution was incubated 10 mins. at 37°C, and unfractionated aa-tRNA (0.69 A_{260} units; totally aminoacylated with a mixture containing 15 [^{3}H]amino acids (see section on aa-tRNA preparation)) was added to complete the titration mixture (50 microliter total volume). This mixture was subsequently added to the sample in the fluorescence cuvette in 5 to 10 microliter aliquots, and fluorescence was measured as detailed earlier.

Titration of ethidium·aa-tRNA with activated EF-Tu. Samples containing 10^{-6}M EtBr and 5.5×10^{-7} M aa-tRNA ($\epsilon_{260} = 6.25\times10^{5}M^{-1}cm^{-1}$) were titrated with either EF-Tu·GDP or EF-Tu·GTP as above. These titrations differed from the above in that the aa-tRNA was added to the cuvette initially, and no aa-tRNA was present in the titrant.

Titration of ternary complex with ethidium. Titrations of aa-tRNA in the presence of either EF-Tu·GTP or EF-Tu·GDP were done at 30°C. Fluorescence cuvettes contained (in 2.0ml) the same concentrations of salts and ternary complex components (GTP or GDP, PEP where applicable, and pyruvate kinase) as for the 10°C titrations above, as well as 2.7×10^{-6}M aa-tRNA and 4.2×10^{-6}M EF-Tu. EtBr in H_2O was added in 1 microliter aliquots (from 10^{-4}M to 10^{-2}M stock solutions) up to a final concentration of 1.46×10^{-5}M. Initial fluorescence readings for the varying concentrations of EtBr were obtained from a control sample which contained no aa-tRNA or EF-Tu but to which the same amount of EtBr was added during the titration. Background fluorescence was subtracted as before.

The effect of EtBr on ternary complex stability. Ethidium effects on the protection of the aminoacyl bond were examined as described in chapter III, except that the solvent also contained 125mM NaCl and KI or KCl was replaced by EtBr. Samples containing 1.9×10^{-5}M EtBr (more than was used in the fluorescence experiments) were compared with samples lacking EtBr.

Aminoacyl bond stability during the above titrations was determined by gel filtration and acid-insoluble radioactivity as described in chapter V. In the ethidium binding experiments, the final time point was typically taken 7 hours after the initial one.

Preparation of unfractionated aa-tRNA. Unfractionated E. coli MRE600 tRNA (Boehringer) was totally aminoacylated in a 2.0 ml incubation containing 100mM HEPES (pH8.0), 10mM magnesium sulfate, 10mM KCl, 1mM dithiothreitol, 4mM ATP, 0.1mM CTP, 100 A_{260} units of tRNA, 200 micrograms of S-100 enzymes, 19 non-radioactive amino acids (-Phe) at 8.3×10^{-6}M, and a 1:20 dilution of a mixture of [^{3}H] amino acids (NET-250, New England Nuclear). After a 37°C, 30 min. incubation, this unfractionated aa-tRNA was processed as described previously for the Phe-$tRNA^{Phe}$-F[8] (see experimental, chapter III).

Data analysis. The fluorescence intensity of free Et at a given concentration is defined to be F_F. The fluorescence intensity of the same Et sample when the dye is totally bound to tRNA is defined to be F_B. F_B is the maximum possible intensity of the sample, while F_F is the minimum intensity. When the fraction of bound dye is set equal to x, then the fraction of unbound dye will equal (1-x). Therefore (43):

$$F = xF_B + (1-x)F_F,$$

where F is the measured fluorescence intensity of the sample. Upon substitution and rearrangement, the equation becomes:

$$x = \frac{\left(\frac{F}{F_F} - 1\right)}{\left(\frac{F_B}{F_F} - 1\right)}$$

F_B/F_F is assumed to be constant and is determined as described earlier. Since F and F_F can be measured, the fraction of bound Et can be calculated. Knowing x we can now calculate the total pmoles of Et_{Bound} (since it is known how much was added) and the amount of Et_{Free}, as well as the amount of complexed aa-tRNA (since this must equal the amount of Et_{Bound} if we are observing binding only to the strong site). Finally, since the total pmoles of tRNA added is known, the pmoles of unbound tRNA can be calculated. Hence, all of the data necessary to do a Scatchard analysis is available.

A Scatchard plot is derived from the well-known Scatchard equation (63):

$$\frac{\bar{\nu}}{c} = -K\bar{\nu} + Kn$$

where $\bar{\nu}$ is the average occupancy of receptor binding sites by ligand, c is the concentration of free ligand, K is the intrinsic binding constant, and n is the number of binding sites per receptor molecule. In the derivation of this equation, the titrant is defined to be the ligand, and

the receptor is the species which is titrated. The relation of x to $\bar{\nu}$ (assuming tRNA is the receptor) will be:

$$\bar{\nu} = (x \cdot \text{total pmoles EtBr}) / \text{total pmoles tRNA}$$

When a plot is made of $\bar{\nu}/c$ vs. $\bar{\nu}$ a straight line will result if and only if the system is in equilibrium and binding sites are identical and independent. In the case of Et binding to tRNA upward-curving Scatchard plots have been observed, indicating that there are two distinct types of binding sites (64).

Results

Determination of F_B. Upon binding to tRNA the fluorescence intensity of ethidium has been shown to increase on the order of 20-fold (41,43) (See figures 13 and 14). In order to characterize the binding of Et to tRNA, the relative emission intensities of free and tRNA-bound ethidium must be determined. This is done by the titration of EtBr with tRNA, as described in the experimental section. Figure 15 shows the saturation curves obtained for titrations at 10°C (F_B/F_F = 18.0 ± 0.4) and at 30°C (F_B/F_F = 16.2 ± 0.4).

Titration of Et with unfractionated tRNA and aa-tRNA. The association constant between Et and tRNA (or aa-tRNA) at 10°C was determined by titration of EtBr with tRNA (or aa-tRNA). Results are shown in figure 16. In addition, the same type of titration was done under the high salt conditions described by other researchers (43), and the binding constant obtained ($3.3 \times 10^6 M^{-1}$) was the same as had been previously reported (data not shown). Under our salt conditions, the binding constant for tRNA is $1.5 \times 10^6 M^{-1}$. When all 20 amino acids are added to the tRNA, the binding constants for both tRNA and aa-tRNA are very similar ($1.1 \times 10^6 M^{-1}$). It is worth noting that in this titration tRNA is the titrant, and the Et constitutes the "receptor". Hence n must always equal 1 since it refers to the "binding sites" on the ethidium.

Scatchard plots for these titrations show some upward curvature where the Et concentration is equivalent to or greater

Figure 13. Fluorescence changes accompanying the binding of EtBr to tRNA. This figure shows the increase in fluorescence intensity of EtBr when it binds to unfractionated tRNA. This is an excitation scan (emission at 610 nm) of free EtBr (——) or EtBr in the presence of a large excess of unfractionated tRNA (----). Spectra were taken in the ratio made (E/R) to eliminate lamp intensity variations.

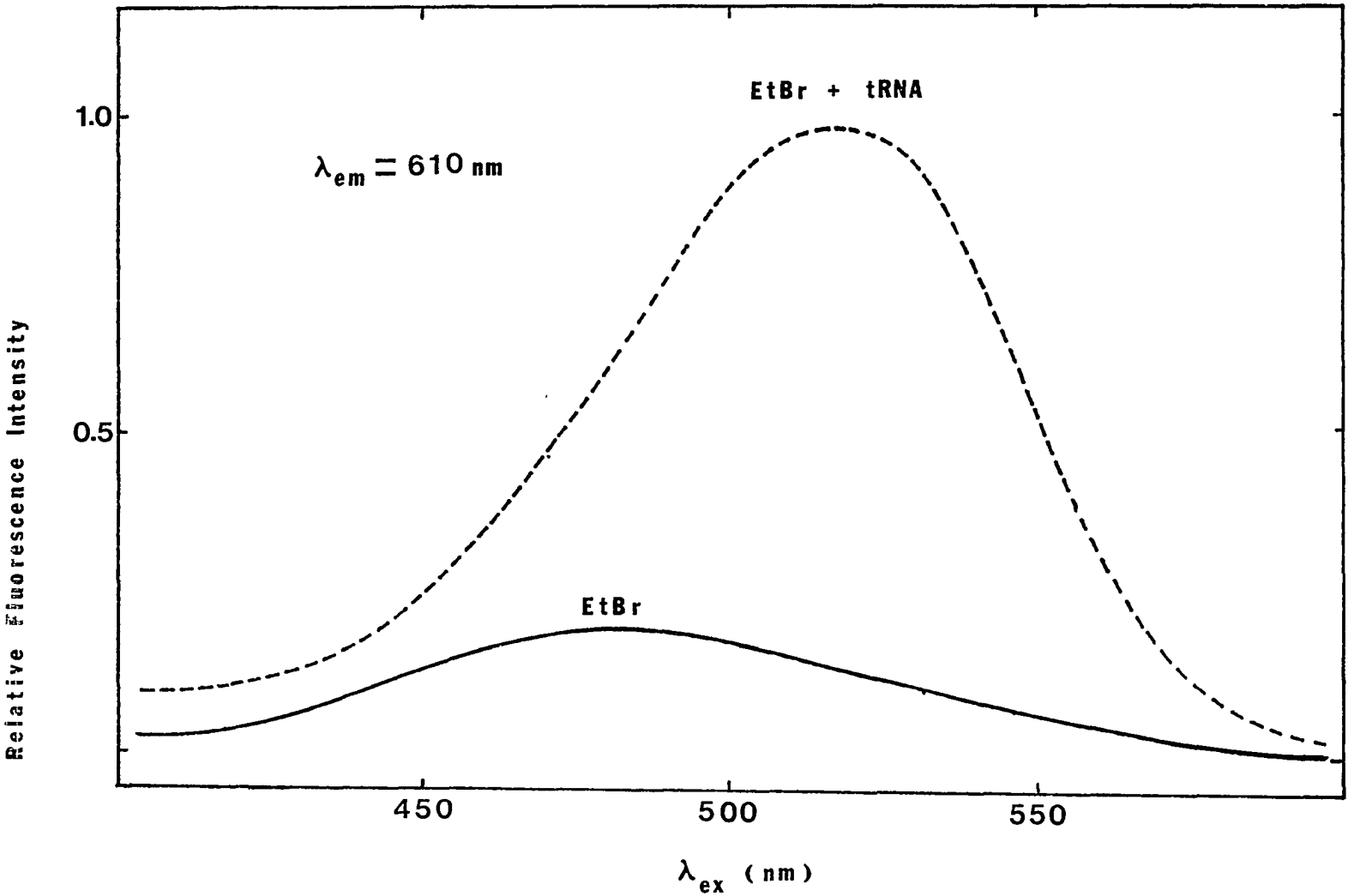
EtBr + tRNA
λ_{em} = 610 nm
EtBr
1.0
0.5
Relative Fluorescence Intensity
450
500
550
λ_{ex} (nm)

Figure 14. Emission spectra (uncorrected) of free EtBr (——) or EtBr in the presence of a large excess of unfractionated tRNA (– – –).

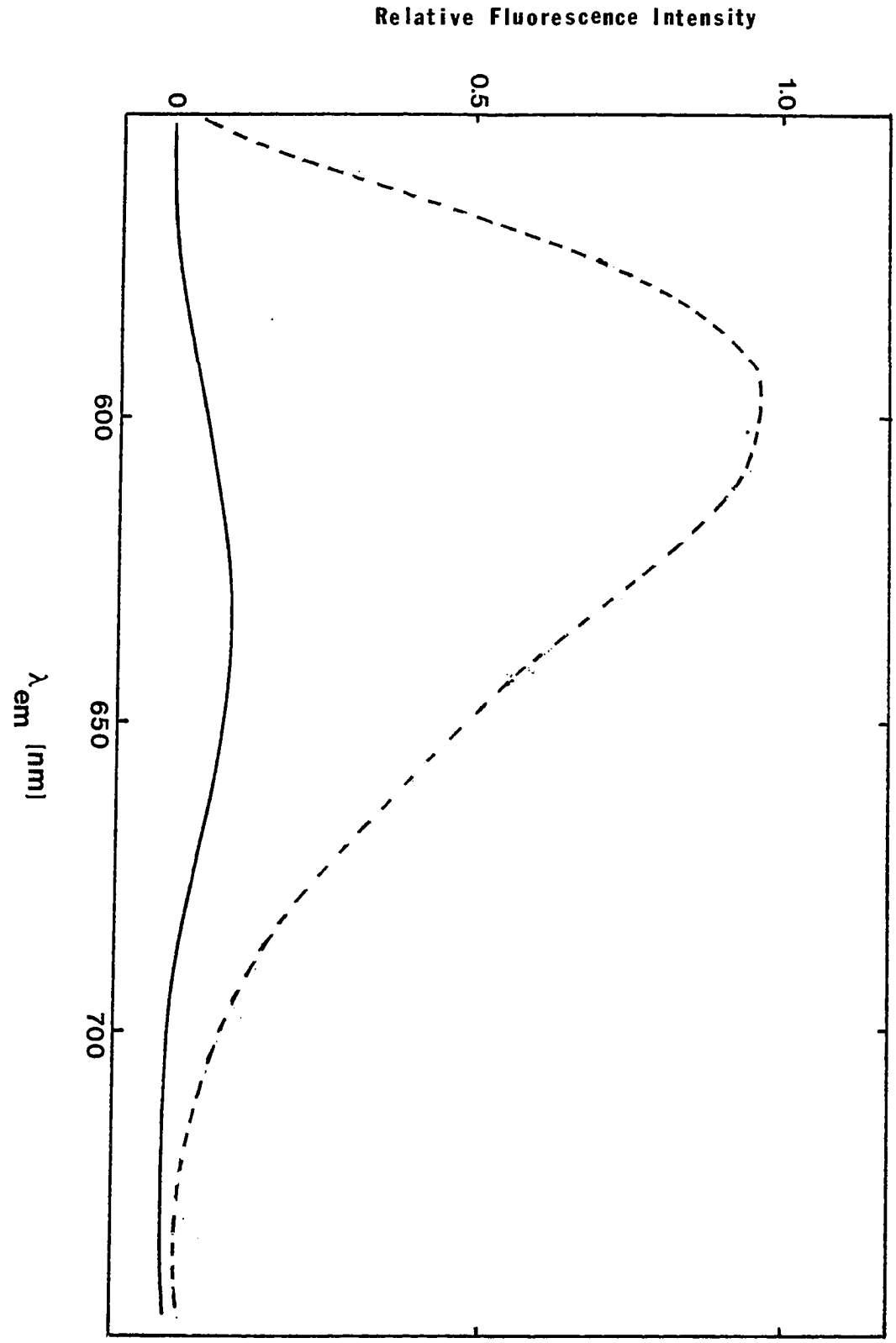
Relative Fluorescence Intensity
0
0.5
1.0
600
650
700
λem [nm]

Figure 15. Experimental determination of F_B/F_F. This plot shows the fluorescence intensity changes obtained when EtBr is titrated with unfractionated tRNA at 10°C (●) or 30°C (■). See experimental section for details.

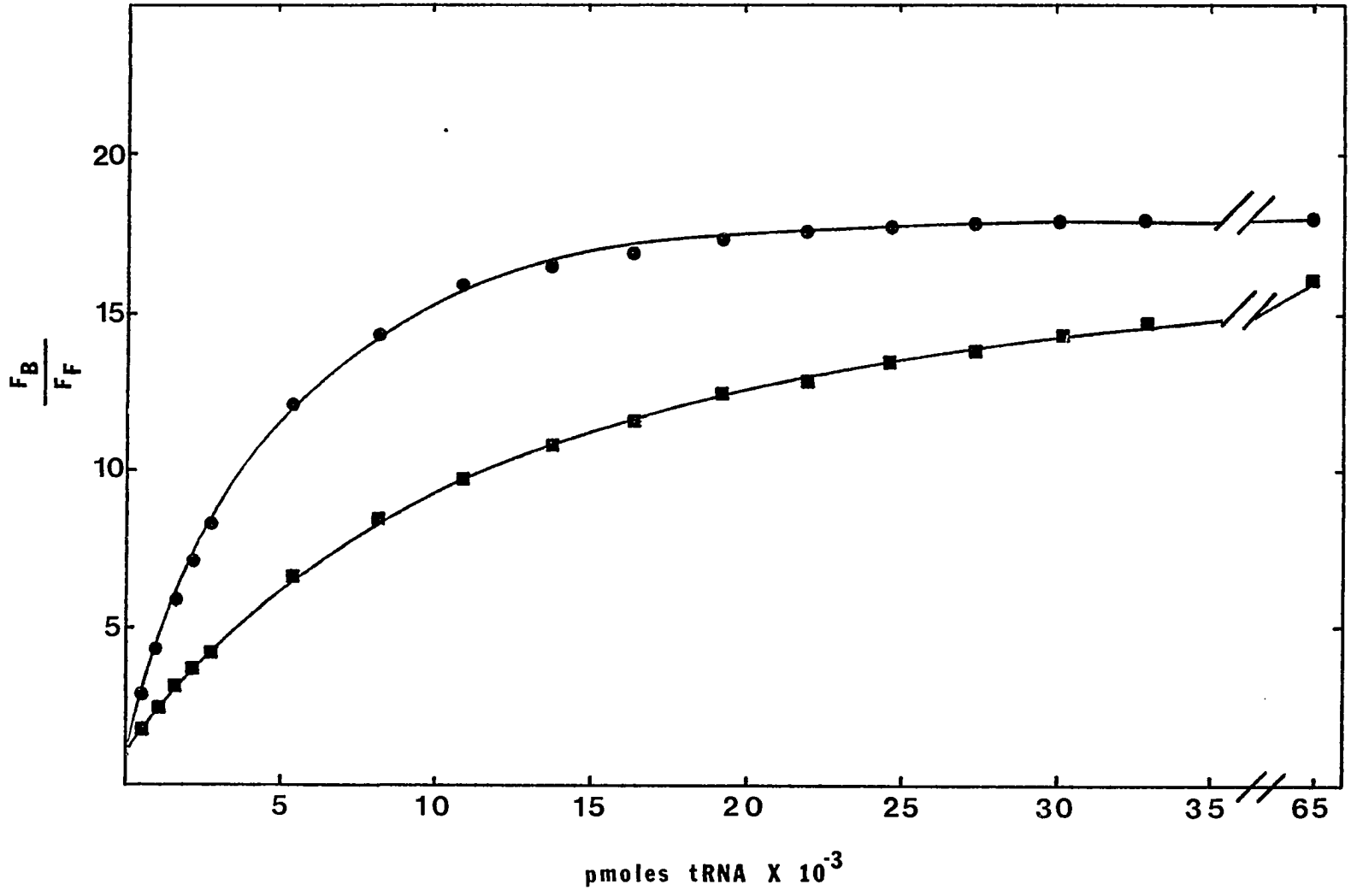
20
15
10
5
$\frac{F_B}{F_F}$
5
10
15
20
25
30
35
65
pmoles tRNA X 10^{-3}

Figure 16. Titration of EtBr with tRNA, aa-tRNA, and tRNA in the presence of amino acids. This figure shows Scatchard Plots for titrations similar to those of fig. 15. EtBr (10^{-6}M) was titrated with unfractionated tRNA (●), unfractionated aa-tRNA (■), or unfractionated tRNA and 20 amino acids, each at .05 the concentrations of the tRNA (▲). The experiment was done at 10°C as described in Experimental.

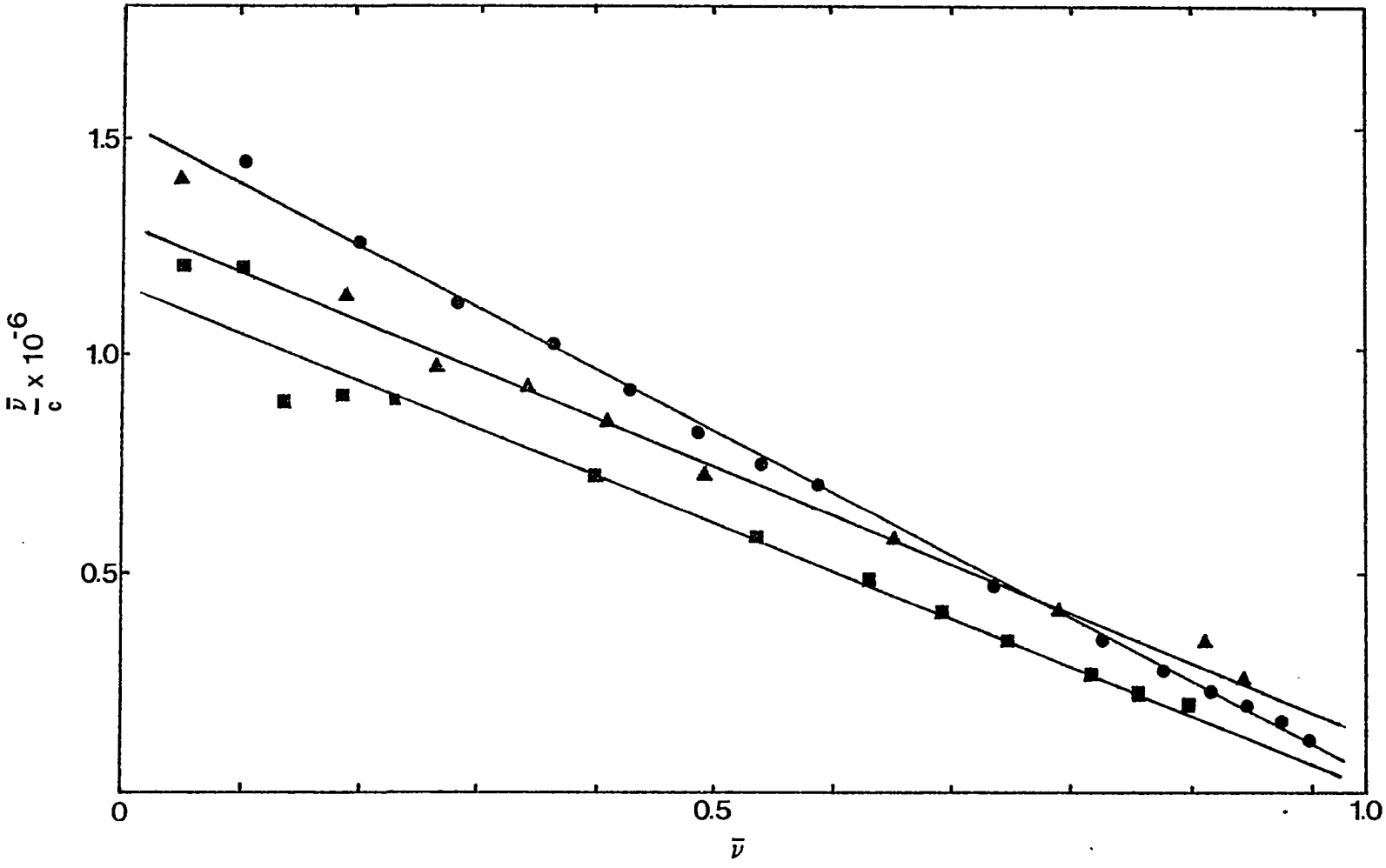
1.5
1.0
0.5
0
0.5
1.0
$\frac{\bar{\nu}}{c} \times 10^{-6}$
$\bar{\nu}$

than the tRNA concentration. This indicates that there is secondary binding at high [Et]/[tRNA]. This has also been observed previously by others (64).

Titrations of tRNA and aa-tRNA with Et. Figure 17 shows the results of titrations of tRNA and aa-tRNA with Et at 30°C. Because of the high [Et]/[tRNA], the Scatchard plots are curved, although not nearly as much as when the titrations were done at 10°C (data not shown). To rule out the possibility that intercalation of amino acids in the aa-tRNA preparation was causing artifactual results, a control sample containing tRNA in the presence of all amino acids was also tested. The curve obtained for this sample was the same as that for tRNA. Thus, it is clear from the data in figure 17 that tRNA and aa-tRNA have a different conformation.

It is possible that the above differences resulted from differences in the storage buffer of the various tRNA preps (H_2O; 1mM KAc (pH5.0); 1mM KAc (pH5.0) plus 1mM Mg^{++}; or 1mM KAc (pH5.0) plus 5mM Mg^{++}). In fact we observed differences in the initial binding of Et for tRNA samples stored in (or dialyzed into) different buffers. However, after incubation at 30°C in high (10mM) Mg^{++} for a short time (typically 15 min.), the amount of bound Et stabilized. This suggests that the incubation allowed any tRNA which had been unfolded due to a lack of Mg^{++} or a low pH to return to its native structure. When Et was titrated with tRNA or aa-tRNA which had been preincubated, no difference was observed in the titrations (fig. 16). On the other hand, when preincubated tRNA or

Figure 17. Titration of tRNA and aa-tRNA with EtBr. This figure shows Scatchard Plots for titrations of unfractionated tRNA (●), unfractionated tRNA in the presence of 20 amino acids (▲), or unfractionated aa-tRNA (■). The experiment was done at 30°C to minimize the curvature of the plot.

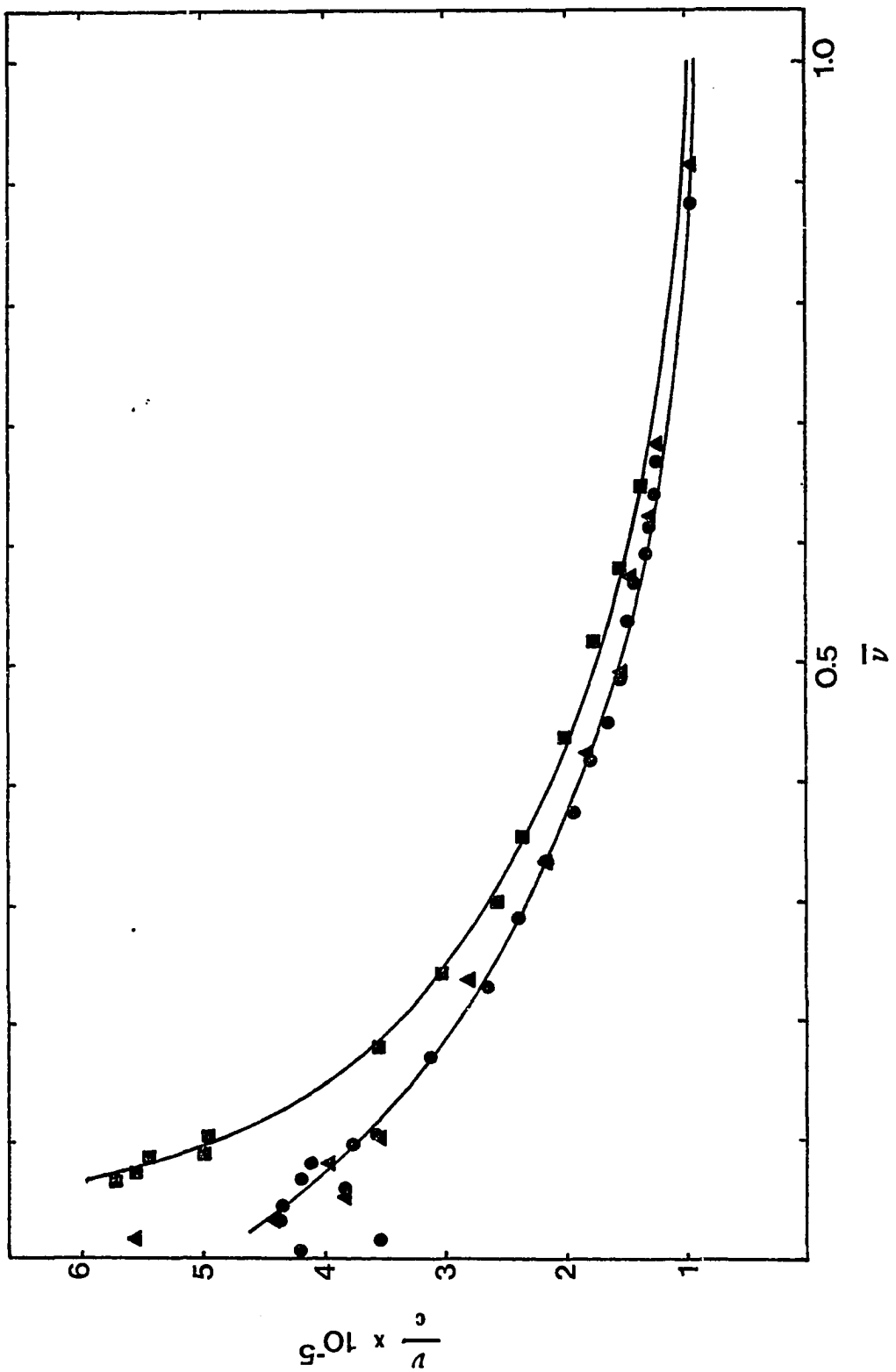
$\frac{v}{c} \times 10^{-5}$
1
2
3
4
5
6
0.5
1.0
$\bar{\nu}$

Figure 18. Titrations of EtBr with ternary complex components. Et binding to aa-tRNA in the presence of either EF-Tu·GTP (●) or EF-Tu·GDP (■) is illustrated. Figure 15A shows the results of titrations of EtBr with aa-tRNA · EF-Tu · GTP or aa-tRNA plus EF-Tu·GDP. In figure 15B, EtBr + aa-tRNA was titrated with EF-Tu·GTP or EF-Tu·GDP. Et binding to (or release from) aa-tRNA was monitored as an increase (or decrease) in fluorescense intensity as described in the experimental section of chapter IV. The experiments were carried out at 10°C.

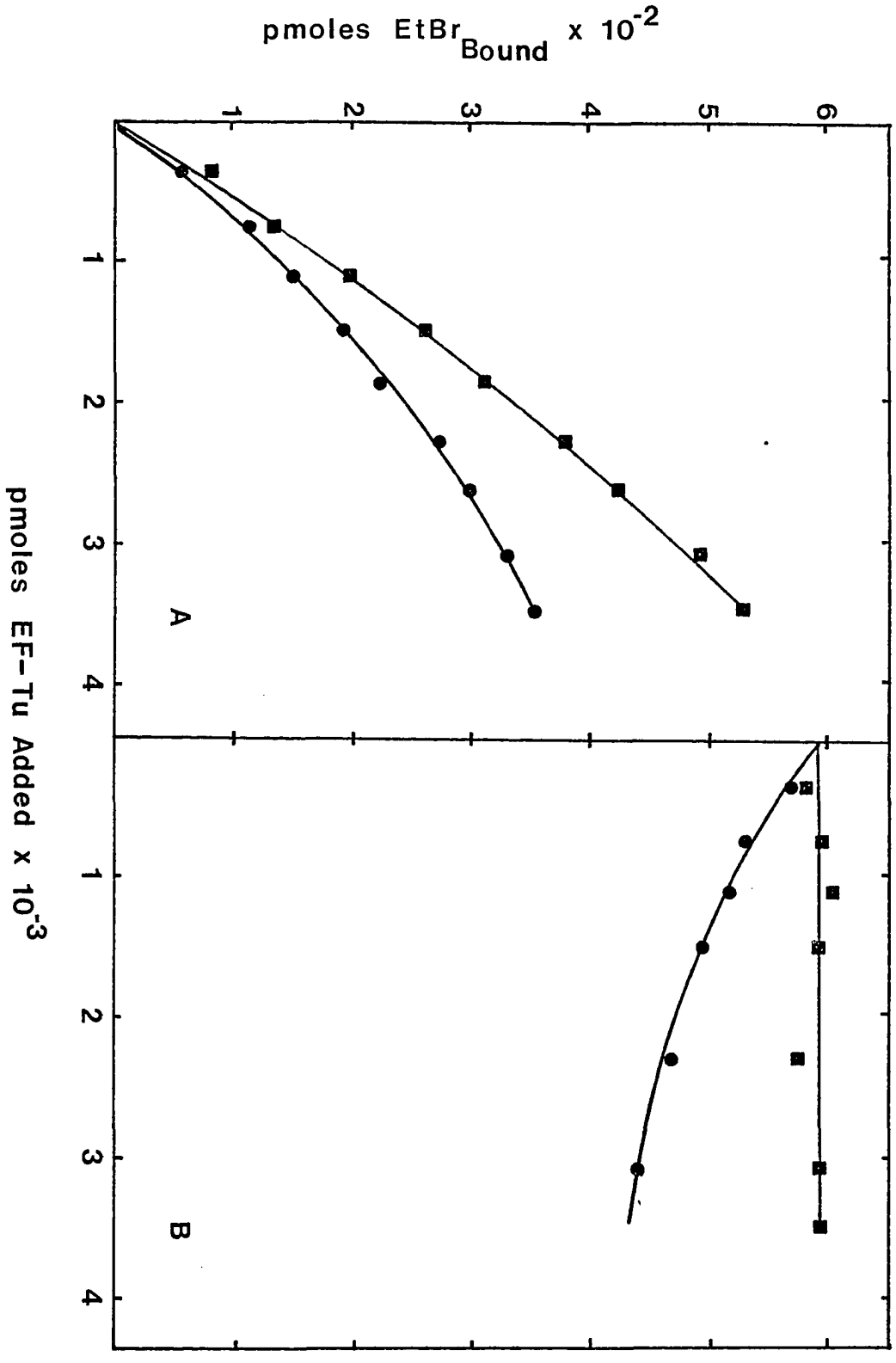
pmoles EtBr Bound x 10-2
1
2
3
4
5
6
pmoles EF-Tu Added x 10-3
1
2
3
4
A
B

aa-tRNA was titrated with Et, differences were observed (fig. 17). It therefore appears that there is a conformational difference between tRNA and aa-tRNA not caused by the difference in storage conditions. Since the difference is seen only when the concentration of Et is greater than or equal to that of tRNA, it suggests that the putative conformation change affects only the secondary binding sites on the tRNA, and does not alter the binding of Et to its strong site.

Titrations of Et with ternary complex components. Two types of titrations of Et with ternary complex components show that formation of the complex reduces the amount of bound dye (see figure 18). In one case, 10^{-6}M EtBr was titrated with aa-tRNA·EF-Tu·GTP (pre-formed ternary complex) or aa-tRNA + EF-Tu·GDP. In both titrations the fluorescence increased (see fig. 18A), but the total increase was lower in the case of the complexed aa-tRNA.

The second type of titration was one in which either EF-Tu·GTP or EF-Tu·GDP was added to a cuvette containing aa-tRNA and EtBr (pre-complexed aa-tRNA·Et). Based on the above results, the fluorescence intensity should decrease in the sample to which EF-Tu·GTP is added. Indeed, that is exactly what happens (fig. 18B). It is also interesting to note that the fluorescence intensities of comparable samples in figures 18A and 18B are approaching the same final values. In both types of titrations, therefore, the inhibition of Et binding to aa-tRNA due to ternary complex was the same.

The data from figure 18A is replotted as a Scatchard plot in figure 19. Due to the limitation of our EF-Tu supply and the difficulty in obtaining pure ternary complex, only a small range of ternary complex concentrations could be investigated. From figure 19, the binding constant for aa-tRNA in the presence of EF-Tu·GDP is $1.5 \times 10^{6} M^{-1}$. This agrees with the binding constant derived for aa-tRNA (fig. 16).

Due to the curvature of the plot for aa-tRNA in the presence of EF-Tu·GTP (fig. 17), the binding constant can only be estimated. However, the apparent association constant is clearly different from that obtained for uncomplexed aa-tRNA. Three problems hinder our interpretation of this data. First, the possibility that the fluorescence increase in the plus ternary complex cuvette may have been due, at least in part, to Et binding to unacylated tRNA or uncomplexed aa-tRNA cannot be ruled out. Second, the curvature of the plot indicates that there are two or more types of binding sites. Third, it is possible that F_B (and therefore F_B/F_F in the equation) may be different for aa-tRNA·EF-Tu·GTP than for free aa-tRNA. In any case, the binding of Et to ternary complex appears to differ from its binding to uncomplexed aa-tRNA. This may result from changes in the binding of Et either to its strong site or to secondary sites. (Note that in this experiment, the concentration of Et was greater than that of aa-tRNA; see above).

Titration of ternary complex with Et. The Et titrations of

Figure 19. Titrations of EtBr with either aa-tRNA·EF-Tu·GTP or aa-tRNA·EF-Tu·GDP. This figure shows the data from figure 18A replotted as a Scatchard Plot. The extrapolation is justified on the basis of previous observations (see figure 16).

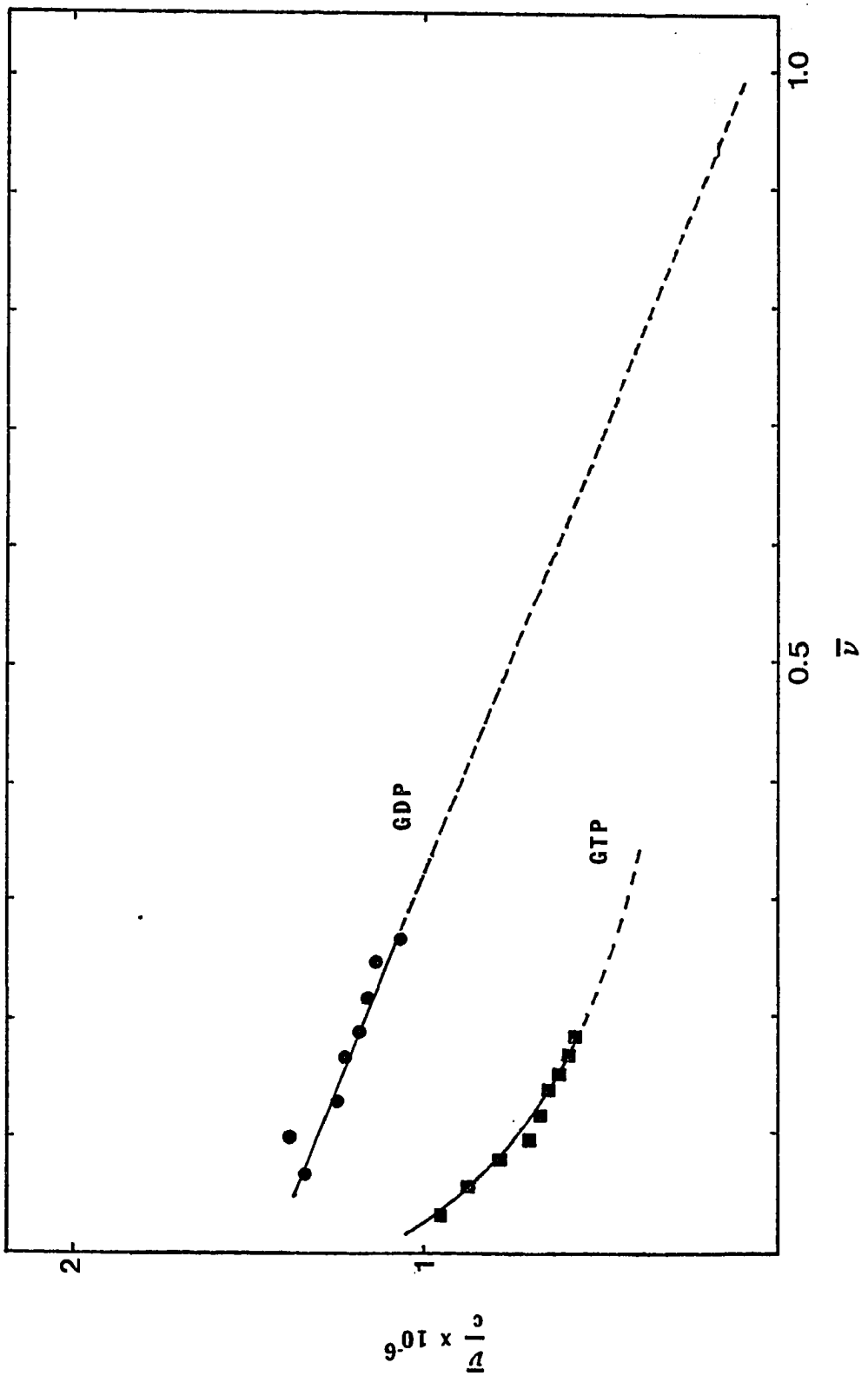
GDP
GTP
1.0
0.5
$\bar{\nu}$
2
1
$\frac{[V]}{c} \times 10^{-6}$

aa-tRNA·EF-Tu·GTP and aa-tRNA + EF-Tu·GDP were done at 30°C. Figure 20 shows the results of these titrations. The dotted line represents the total number of tRNA binding sites in the sample (based on one site per tRNA, 1600 pmoles per A_{260} unit). It is apparent that the total number of bound Et molecules approaches the total number of available sites in both cases. From this the important conclusion can be made that the strong binding site for Et is not covered up by the protein.

As seen earlier (fig. 18), the formation of ternary complex appears to inhibit the binding of Et to aa-tRNA. This can be seen even more clearly in a Scatchard plot (figure 21). As noted above, an unqualified interpretation of this data cannot be made.

EtBr effect on ternary complex stability. EtBr concentrations greater than those used in the above binding experiments were found to have no effect on ternary complex stability (see figure 22).

Confirmation of ternary complex formation. The presence (or absence) of ternary complex formation during the above Et binding experiments was tested both by aminoacyl bond protection assays and gel filtration over Ultrogel AcA-44 (see experimental, chapter V). Figure 23 shows the results of a typical gel filtration (following a seven-hour titration). The results are similar to those obtained following ternary complex quenching experiments (fig. 11) except that the total per cent cpm of the hydrolyzed amino acid was higher here due to the lower molar ratio of EF-Tu to aa-tRNA and the longer time (7 hours as opposed to 4 hours for the I^- quenching

experiments). Likewise, the aminoacyl bond protection in ternary complex samples was similar to that in I^- quenching experiments (data not shown).

Figure 20. Ethidium occupation of binding sites on aa-tRNA at 30°C in the presence of either EF-Tu·GTP (●) or EF-Tu·GDP (■). The dotted line represents the total number of pmoles of aa-tRNA added (total number of strong binding sites). Sample contents are described in Experimental. The amount of ethidium bound was determined as outlined in Experimental, assuming that F_B was the same for Et·aa-tRNA and Et·aa-tRNA·EF-Tu·GTP.

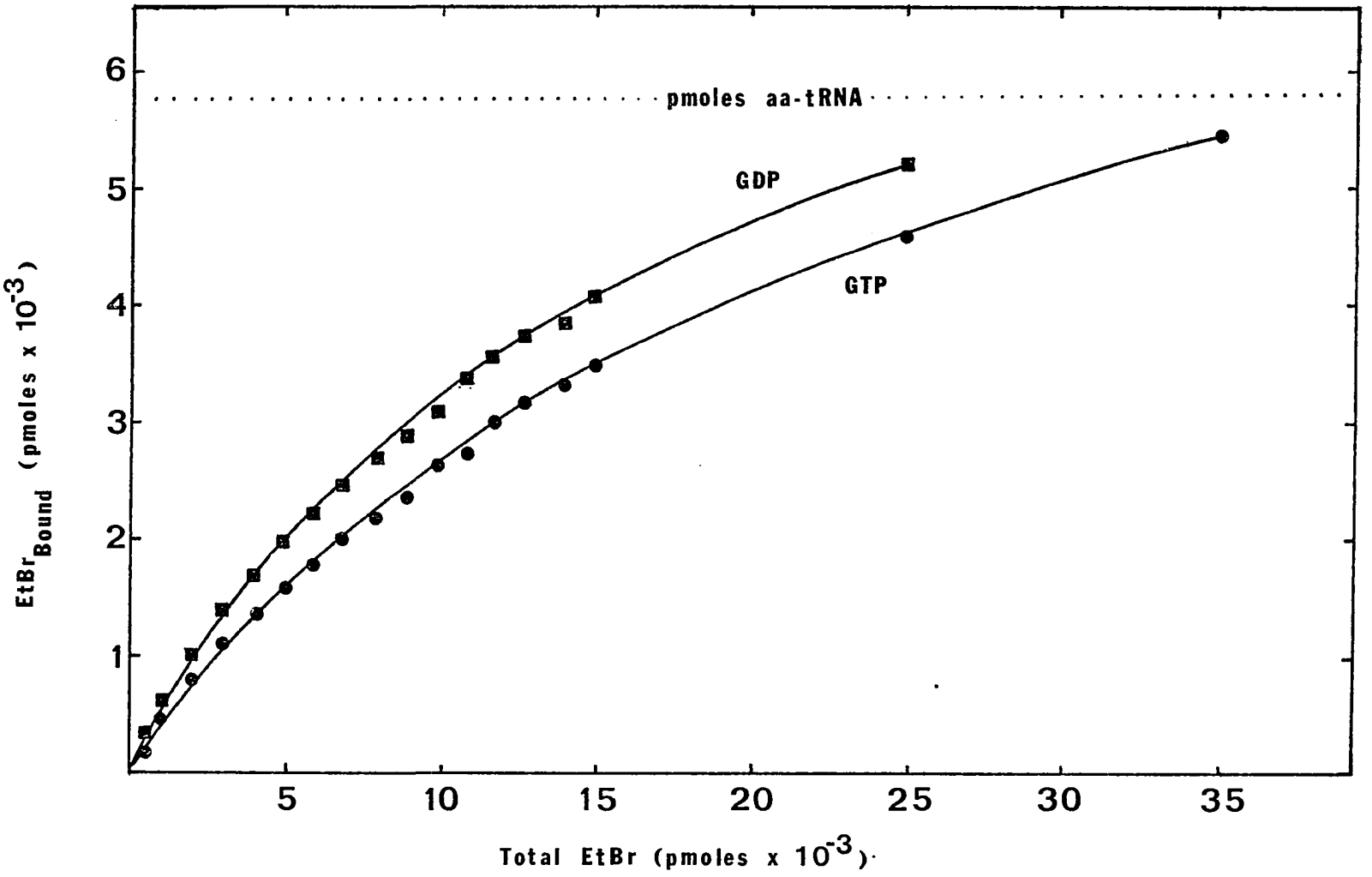
pmoles aa-tRNA
GDP
GTP
$EtBr_{Bound}$ (pmoles x 10^{-3})
Total EtBr (pmoles x 10^{-3})
1
2
3
4
5
6
5
10
15
20
25
30
35

Figure 21. Titration of aa-tRNA in the presence of EF-Tu·GTP (■) or EF-Tu·GDP (●) with EtBr. This Scatchard Plot was constructed using the data from the experiment of fig. 20.

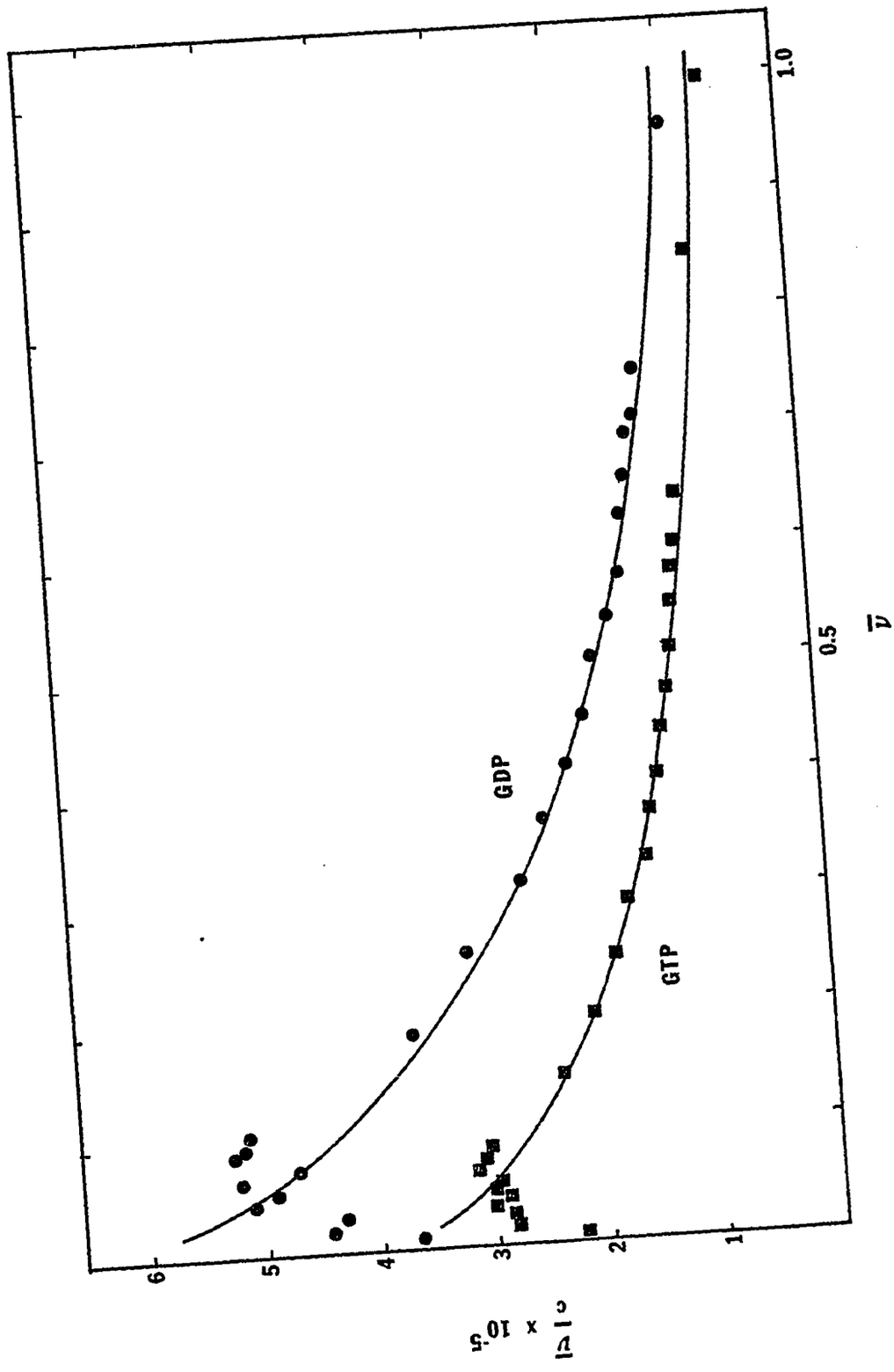
GDP
GTP
0.5
1.0
1
2
3
4
5
6
$\bar{\nu}$
c | v | x 10^{-5}

Figure 22. EtBr effect on ternary complex stability. The rate of hydrolysis of amino acid from unfractionated tRNA aminoacylated with 15 tritiated amino acids is shown in the absence (●) or presence (▲) of 1.9×10^{5}M EtBr. Unfilled symbols represent incubations of aa-tRNA in the presence of EF-Tu·GDP. Filled symbols are incubations in the presence of EF-Tu·GTP. Incubations were at 30°C as described in the experimental section of this chapter and included .268 A_{260} units of the aa-tRNA preparation. Acid-insoluble radioactivity at t = 0 totaled approximately 10,000 cpm.

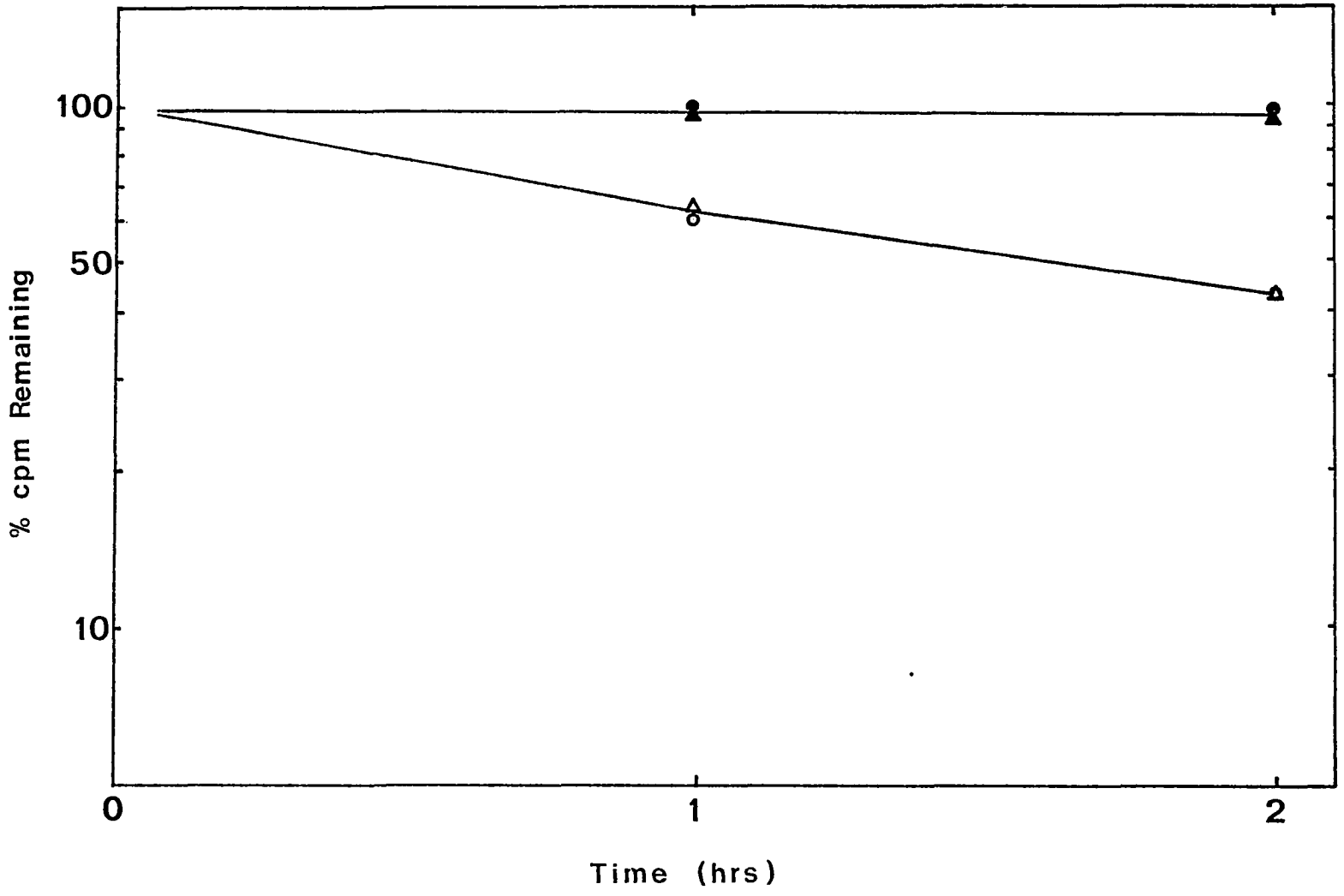
100
50
10
% cpm Remaining
0
1
2
Time (hrs)

Figure 23. Gel filtration of unfractionated aa-tRNA in the presence of EF-Tu·GTP (●) or EF-Tu·GDP (○) following Et binding experiments.

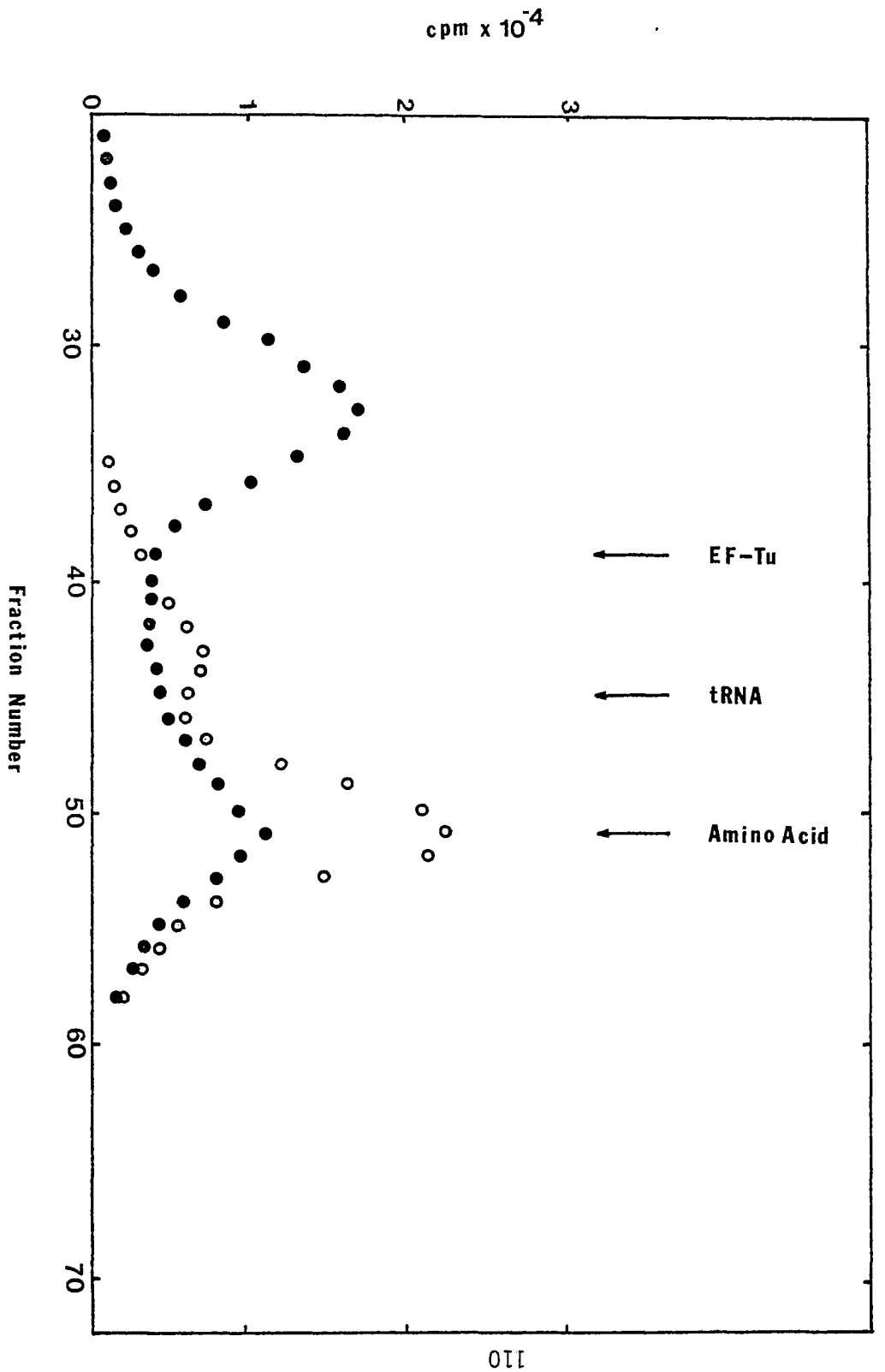
cpm x 10^-4
0
1
2
3
30
40
50
60
70
110
Fraction Number
EF-Tu
tRNA
Amino Acid

CHAPTER VII

THE EFFECT OF GLYCEROL ON aa-tRNA

Introduction

Originally we wished to examine the ternary complex formed with eukaryotic elongation factor T (eEF-T) and elongation factor Tu (eEF-Tu), the eukaryotic equivalent of EF-Tu. eEF-T is usually isolated as a multi-subunit protein and is considerably larger than prokaryotic EF-Tu (180,000 d. vs. 44,000 d.) (65). Besides a subunit which appears to be functionally equivalent to EF-Tu, EF-T contains what is thought to be an analog of EF-Ts and also a third subunit, designated the β chain, which has an unknown function. The eukaryotic factor has a weaker binding constant for aa-tRNA than does the prokaryotic analog (66).

When attempts were made to study the complex between aa-tRNA and eEF-Tu, the data was inconsistent and uninterpretable. No direct evidence that ternary complex was formed could be obtained, either by a change in fluorescence intensity or by aminoacyl bond protection assays. Indeed, rather than protect the bond, the addition of the eEF-Tu appeared to be catalyzing the bond's hydrolysis. When the problem was investigated more closely, both the eEF-Tu preparation and the buffer in which the protein was

stored were found to exhibit this effect. This buffer contains 20% (v/v) of glycerol, which has been found necessary for maintenance of the protein's activity (67). In this chapter evidence is presented that glycerol, even to concentrations as low as 1% (v/v), has a profound effect on the aa-tRNA. This fact alone may help to explain conflicting reports in the literature concerning this protein.

Experimental

Aminoacyl bond hydrolysis assays. Rates of hydrolysis of amino acid from aa-tRNA were measured using the cold TCA precipitation assay as before (see chapter III, experimental). Incubations (100 microliters, 30°C, 2 or 4 hours, as indicated) contained buffer B (20mM Tris-Cl (pH7.6), 5mM $MgCl_2$, 50mM KCl) glycerol concentrations as indicated, and radioactive aa-tRNA as indicated.

Effect of glycerol on prokaryotic ternary complex. The effect of glycerol on prokaryotic ternary complex was tested using the aminoacyl bond protection assay described in chapter III, except that glycerol, as indicated, was substituted in place of potassium iodide. Final incubation volumes for this assay were 125 microliters.

Fluorescence quenching. Fluorescence intensity quenching with iodide ion was carried out at 15°C as described in the experimental section of chapter V.

Results

Problems were encountered during the conduct of experiments designed to examine the iodide ion accessibility of the fluorescein in the Phe-tRNA^{Phe}-F^{8} complex with eEF-T·GTP and eEF-Tu·GTP. Specifically it was observed that:

1) Stern-Volmer plots of iodide ion quenching were not reproducible and frequently had much greater slopes than anticipated.
2) Rather than protecting the aminoacyl ester bond, addition of eEF-T or eEF-Tu (in the presence of either GTP or GDP) seemed to enhance hydrolysis. This phenomenon had been previously noted during studies involving the affinity labeling of eEF-Tu with N$^{\epsilon}$-bromoacetyl-lysine-tRNA^{Lys} (A. E. Johnson, personal comm.).

In addition, fluorescence observations and protection assays gave no clear evidence of ternary complex formation.

The possibilities of nuclease and/or synthetase contamination were ruled out when it was shown that the effect could be duplicated by adding the buffer in which the protein was stored to the samples in place of the elongation factor preparations. Eventually, the cause of the problem was narrowed down to the glycerol in which the proteins are stored to maintain their activity. Both commercial analytical grade glycerol and ultrapure redistilled glycerol (from BRL) were found to exert this effect equally (see figure 24) on both prokaryotic (fig. 24A) and eukaryotic (fig. 24B) aa-tRNA. As can be seen the effect is significant at glycerol concentrations even as low as 1% (v/v).

Figure 24. Glycerol stimulation of amino acid hydrolysis from aa-tRNA. This plot shows the results of adding 0 (●), 1 (x), 2 (■), or 3 (▲) per cent (v/v) of glycerol to incubations of aa-tRNA at 30°C. Figure 24A was obtained using E. coli (prokaryotic) unfractionated tRNA aminoacylated with 15 (^{3}H) amino acids (.344 A_{260} units per assay, t = 0 cpm approx. 10,000). Figure 24B was obtained using unfractionated yeast (eukaryotic) [^{14}C]lysine-tRNA (.977 A_{260} units per assay, 555 dpm/pmol Lys, 69.7 pmol Lys per A_{260} unit tRNA).

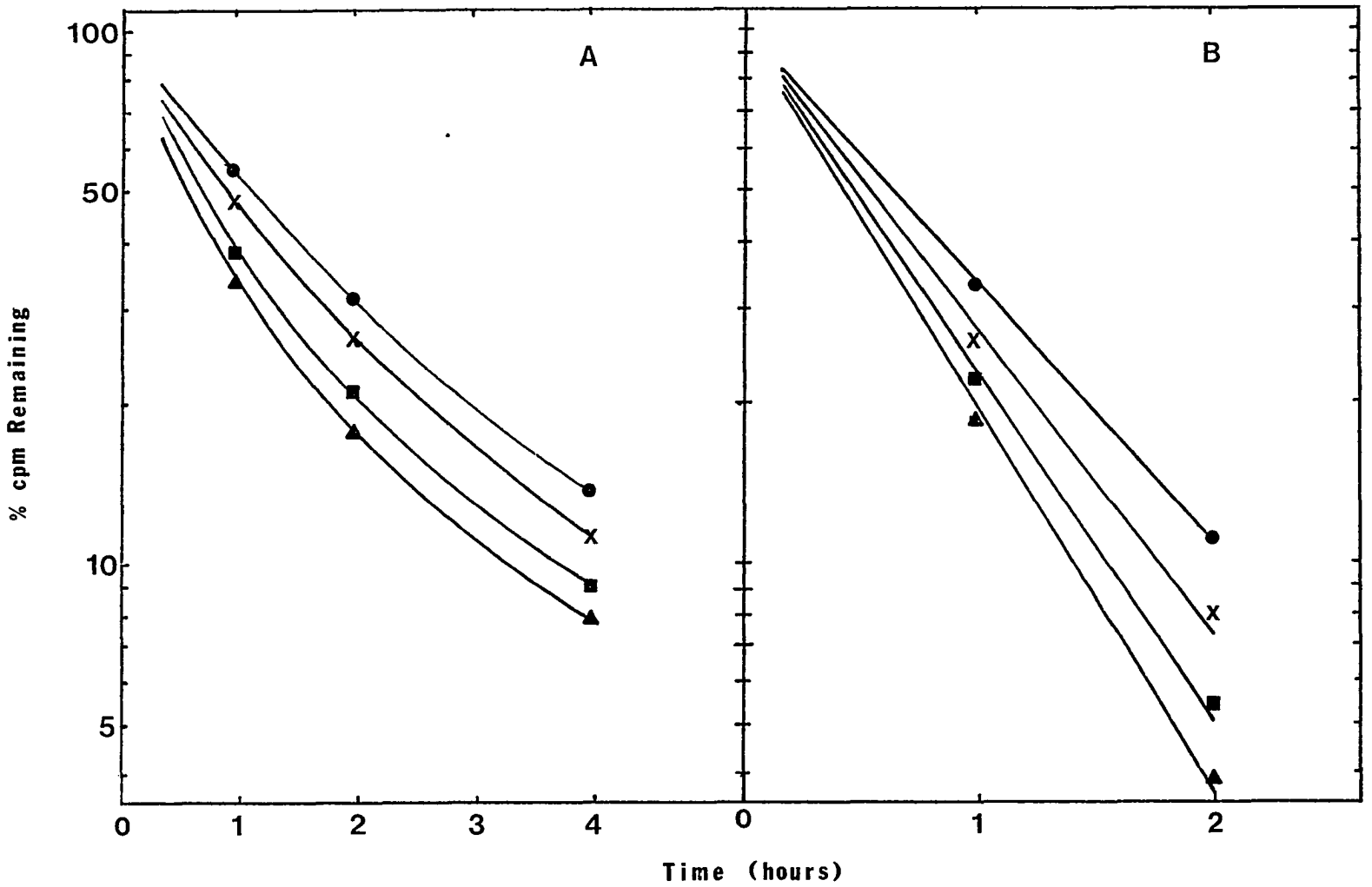
100
50
10
5
% cpm Remaining
A
B
0
1
2
3
4
0
1
2
Time (hours)

Next, the effect of varying concentrations of glycerol on prokaryotic ternary complex was examined. Figure 25 shows that the complex is disrupted (the rate of amino acid hydrolysis increases) at glycerol concentrations as low as 2% (v/v). The increase in the rate of hydrolysis is observed in both GTP and GDP containing samples as should be expected if the glycerol is exerting its effect directly on the aa-tRNA molecule.

When I^- quenching of $tRNA^{Phe}$-F^8 in glycerol (4%) was tested, the K_{sv} from its Stern-Volmer plot was greatly increased in comparison to that which had been seen previously (results, chapter V). The results are shown in figure 26. This would seem to indicate that the tRNA had denatured (unfolded) to some extent. However, a measurement of absorbance at 260 nm before and after addition of glycerol showed no hyperchromicity (data not shown). Also, titration of unfractionated tRNA with EtBr showed only a very small change in the binding constant at 5% (v/v) glycerol (data not shown). These observations would seem to suggest that if there is denaturation, it does not involve a major portion of the tRNA molecule.

It is clear that the effect of glycerol on aa-tRNA and the ternary complex is significant, but the mechanism of the effect has not yet been identified. Glycerol has been shown to have non-specific effects in certain experimental systems, particularly in the stimulation of tubulin association in the absence of GTP (68), but in this case the concentrations of glycerol were 10 to 30 times higher than in our experiments. A more likely related observation

was that low concentrations of glycerol were found to inhibit methylene blue sensitized degradation of guanosine (69). The authors found that the glycerol was somehow affecting the ribose moiety of the nucleotide (possibly hydrogen bonding to it). They did not follow up this observation.

Figure 25. Effect of glycerol on prokaryotic ternary complex. This figure illustrates the effect of addition of 0 (●), 2 (■), or 5 (▲) percent (v/v) of glycerol to unfractionated aa-tRNA labeled with 15 tritiated amino acids (.030 A_{260} units per assay, t = 0 cpm approx. 1,000) in the presence of either EF-Tu·GTP (figure 25A) or EF-Tu·GDP (figure 25B). The difference in the rates of hydrolysis between complexed and uncomplexed aa-tRNA in these experiments than in those of figure 5 was because [EF-Tu]/[aa-tRNA] was 1.1 here and at least 4 earlier.

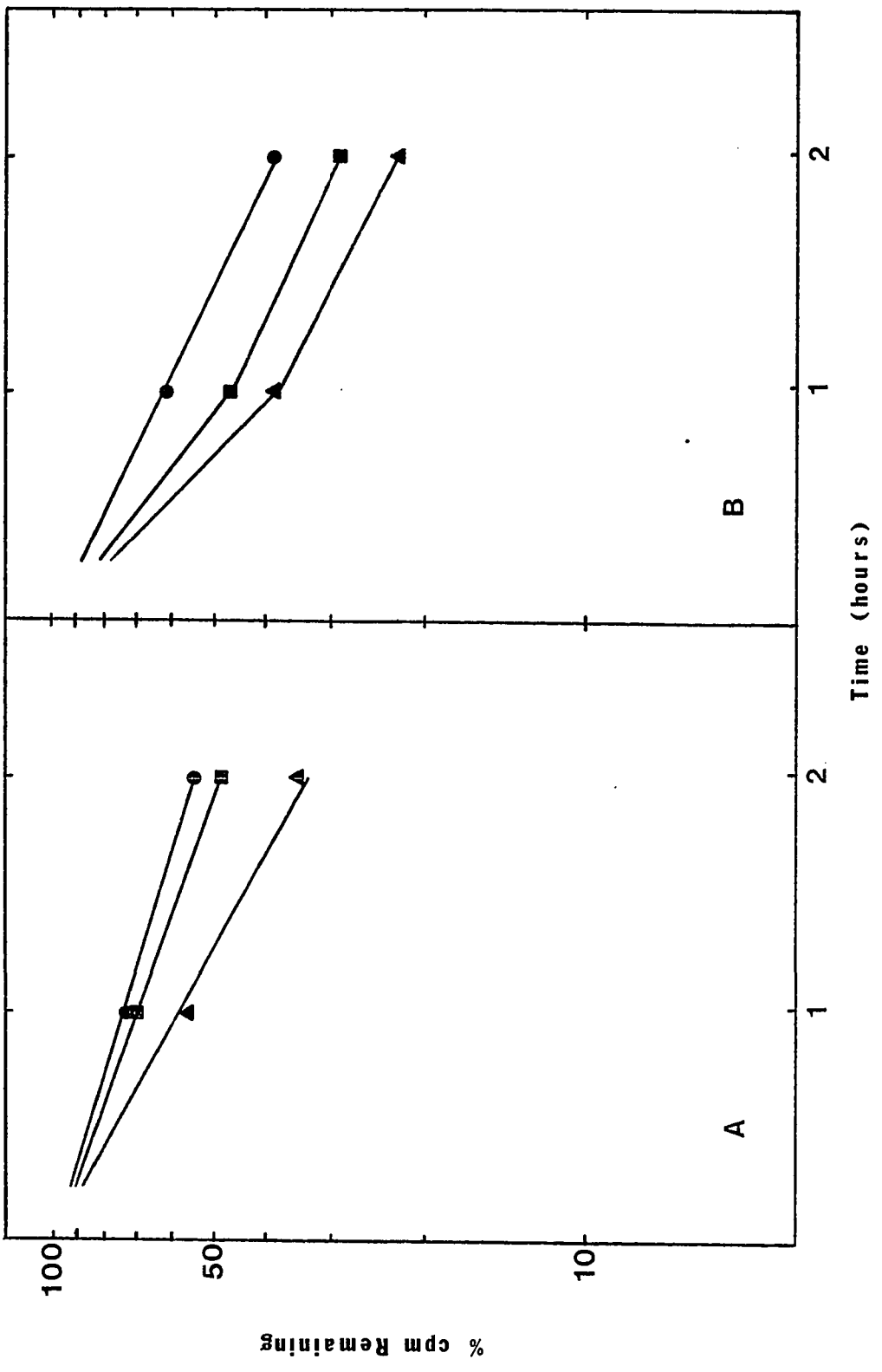
% cpm Remaining
100
50
10
A
B
1
2
1
2
Time (hours)

Figure 26. Effect of glycerol on the iodide ion quenching of $tRNA^{Phe}$-F^{8} fluorescence. The figure shows results of fluorescence quenching in the presence of 4% (v/v) of glycerol at 15°C (●). For comparison the dotted line represents quenching of the fluorescence of the same tRNA at 30°C from previous experiments (see table 3).

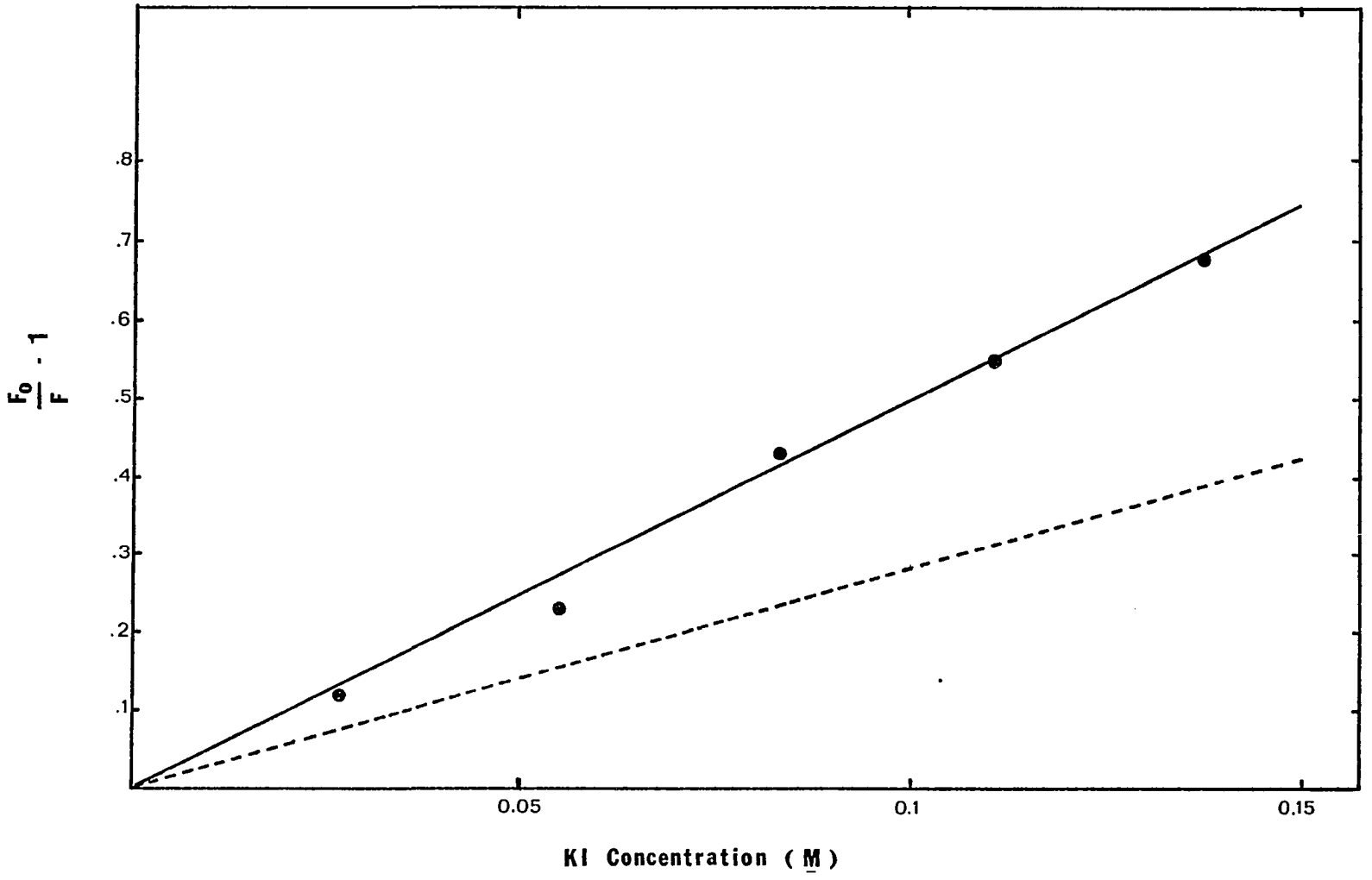
$\frac{F_o}{F} - 1$
.8
.7
.6
.5
.4
.3
.2
.1
0.05
0.1
0.15
KI Concentration (M)

CHAPTER VIII

DISCUSSION

During the course of this research project, the ternary complex formed between aa-tRNA, EF-Tu, and GTP has been studied using site-specific fluorescent probes. In one case the probe was covalently attached to a modified $tRNA^{Phe}$, while in the second case, unmodified tRNA was examined using a non-covalently bound probe. In both cases, studies centered primarily on two aspects--topology of the complex and the possible involvement of conformational changes in its function.

Because the emission properties of fluorescent probes are, in general, very sensitive to changes in their environment, structural changes near the probe can be detected by changes in its fluorescence signal. A particular advantage of this approach is that it is non-destructive. Thus, one can monitor macromolecular structure throughout a lengthy experiment. Because one can demonstrate that the ternary complex is intact at the end of the experiment, interpretation of the results is straightforward. In contrast, topological studies involving enzymatic digestion and chemical modification procedures, upon which much of our knowledge of ternary complex structure is currently based, alter the

macromolecules during the experiment. This makes interpretation of the results difficult, and indeed, there is disagreement between investigators using similar techniques as to the topological structure of the complex (9,10, Wilkman, et al, personal comm.)

Both of the probes utilized in these studies were bound in the corner region of the tRNA. In the case of the modified $tRNA^{Phe}$, a fluorescein moiety was covalently attached to the 4-thiouridine base at position #8. In the case of the unmodified, unfractionated tRNA, the binding of ethidium to its strong binding site was studied. Although the project was initially designed to study the topology of the ternary complex, the possibility that the probes would be sensitive to conformational changes within the corner region was not overlooked. Indeed, if such a change could be detected, it was recognized that the fluorescent probes may provide an important tool in our attempts to understand how EF-Tu carries out its primary function as a catalyst of protein synthesis.

Our results show that the conformation of aa-tRNA changes when it associates with EF-Tu·GTP. This change was detected by both probes. In the studies involving Phe-$tRNA^{Phe}$-F^8, the change in conformation caused a 28% increase in the emission intensity of the fluorescein (fig. 6). Fluorescence quenching studies with the collisional quencher, iodide ion, indicate that this fluorescence change was not due to a direct interaction between EF-Tu and fluorophore, since the solvent accessibility of the fluorescein was not altered significantly by complex formation (fig. 10). This conclusion is further supported by the fact that ternary complex

formation altered the nature of the strong binding site for Et on unmodified, unfractionated aa-tRNA (figs. 18 thru 21). Thus, ternary complex formation causes a conformation change in aa-tRNA.

The conformational flexibility of the aa-tRNA molecule is well-established (reviewed in 70). A mutation distant from the anticodon of $tRNA^{Trp}$ altered the tRNA's ability to read its cognate codon (71,72). The mutant aa-tRNA can read not only its normal codon but also the nonsense codon UGA. Photocrosslinking of the s^4U_8 with C_{13} subsequently altered the decoding properties of this nonsense supressor $tRNA^{Trp}$ (73). This seems to indicate that aa-tRNA structure near the s^4U is somehow involved in the decoding process. Therefore, in view of our data, it seems likely that one function of EF-Tu in protein biosynthesis is to ensure that every aa-tRNA begins the process in a particular (possibly the same) conformation. In this way, EF-Tu would serve as a regulatory element in the process.

The exact nature of the conformational change in the corner region of the aa-tRNA which occurs upon ternary complex formation is presently unknown. However, since the emission intensity change (fig. 6) was due in large part to a change in the molar absorptivity of the fluorescent dye, and since the absorbance of the dye is very sensitive to pH (74), it seems likely that a change in the electrostatic environment of the dye is involved. It is probable that the locations of the negatively-charged phosphates are slightly altered with respect to the fluorescein moiety. This could lead to a change in either the local pH or the pKa of the carboxyl group on the fluorescein.

Topologically, the fluorescence quenching results presented in chapter V demonstrate that the s^4U position of Phe-$tRNA^{Phe}$-F^8 is not covered up by the protein. This can be ascertained from the fact that the K_{sv} for the quenching of ternary complexed Phe-$tRNA^{Phe}$-F^8 was the same as that for uncomplexed Phe-$tRNA^{Phe}$-F^8 (fig. 10). The conditions were such that the complex was not destroyed during the course of the experiment (figs. 10, inset and 11). Consistent with this finding is the fact that the binding of Et to its strong site (near the s^4U) is not blocked by formation of the ternary complex (fig. 20).

The above results are in apparent disagreement with recent experiments studying EF-Tu protection from nuclease (10, Wilkman, et al, personal comm.) and kethoxal reaction rates with guanine residues in single-strand regions (Bertram and Wagner, personal comm.). The former technique seems to indicate that this region is protected from nuclease cleavage by complex formation. Also, kethoxal reaction rates are slower in the corner region with complexed as compared to uncomplexed aa-tRNA. However, both of these techniques are sensitive to changes in conformation; both rely on the accessibility of particular tRNA components (a guanine or a phosphodiester bond) for optimal reaction, and any conformation change which alters the accessibility can yield ambiguous results. In addition, the methods themselves may induce conformational changes. Reaction at one site may cause structural changes that can alter subsequent interactions of the enzyme or reagent with the tRNA. Finally, it is possible that the ternary

complex may be disrupted following the first enzyme cut or chemical reaction. For these reasons, the results of such techniques must be interpreted with caution. Since we have found that association with EF-Tu·GTP alters the conformation of aa-tRNA, it is likely that the difference in reactivity near s^4U that others observe is due to the conformation change and not to EF-Tu covering this region in the ternary complex. Our fluorescence quenching data is not subject to ambiguity in interpretation, since it can be demonstrated that aa-tRNA is complexed to EF-Tu throughout the experiments. From our results it is clear that the EF-Tu does not cover the s^4U region of the aa-tRNA in the ternary complex.

On the other side of the tRNA, fluorescamine attached to X_{47} showed no change in fluorescence intensity upon ternary complex formation (75). In addition the X base could be cross-linked to EF-Tu only when the photoaffinity label was at least 20 Å long (Kao, Miller, and Ofengand, in preparation). These findings and those reported in this thesis are consistent with a model in which EF-Tu binds to aa-tRNA at the aminoacyl terminus and the aminoacyl acceptor stem. The entire anticodon stem and corner region would then be free to interact with components of the ribosome.

Unless and until a solved crystal structure is obtained for the aa-tRNA·EF-Tu·GTP complex, we shall be forced to visualize its topology on the basis of the individual three-dimensional structures of tRNA (fig. 3) and EF-Tu (76-78). Recent affinity labeling experiments (24,79) provide a fixed point of reference for the orientation of the nucleic acid and protein relative to one

another. The data presented herein will serve to further restrict the possible arrangements of EF-Tu and aa-tRNA in the complex.

Another question of importance touched on during this research is whether or not there is a conformational difference between tRNA and aa-tRNA. Considering the large increase in fluorescence intensity observed when Phe-$tRNA^{Phe}$-F^8 complexed with EF-Tu·GTP, it is interesting that there was little or no change seen when $tRNA^{Phe}$-F^8 was aminoacylated. We did, however, observe a small, but reproducible difference in the rate of collisional quenching with I^- (fig. 8). This is consistent with a structural change in this region which persists even after dissociation of the aa-tRNA from the synthetase enzyme. Further support is provided in the case of the unmodified, unfractionated aa-tRNA, since the binding properties for Et are different between the two species (fig. 17). This difference is most obvious when Et is in excess over tRNA suggesting that whatever the difference is, it affects only the secondary binding of the dye. Other researchers using photocrosslinked (80,81) and fluorescent-labeled (82) tRNAs have reported that the conformation of the tRNA near s^4U is altered upon association with its cognate synthetase. Also, studies of the binding of oligonucleotides complementary to TΨC (83) as well as laser light scattering during deacylation (84) suggest that a conformational change does persist in the aa-tRNA. On the other hand, early NMR studies (85) failed to detect any difference due to an effect on the exchangeable proton spectrum. Presently, the current literature is about evenly divided on this issue,

apparently depending on the technique used to study the question (70).

The possibility must be considered that our results were caused by the different storage buffers for the two species or by the aminoacylation reaction and procedures. At least in the case of Et binding experiments, the storage buffer conditions were ruled out as a cause (chapter VI, results). Another possibility suggested by Dr. Paul Schimmel is that phenylalanine intercalates somewhere within the aminoacyl acceptor stem and induces the different conformations observed for $tRNA^{Phe}$-F^{8} and its aminoacylated counterpart. This idea can be tested by misacylating this tRNA and seeing if the difference is still observed. In any case our initial observations suggest a structural difference between aa-tRNA and tRNA, and are interesting enough to merit future study.

Finally, during our attempts to study the ternary complex formed with eukaryotic elongation factors, it was noticed that the glycerol in the storage buffers of these proteins exhibits a profound effect on the aa-tRNA. For reasons not presently understood, glycerol in very low concentration (1% (v/v)) catalyzed the hydrolysis of the aminoacyl ester bond. In addition, large changes in the K_{sv}'s of our fluorescein-labeled $tRNA^{Phe}$ were seen (fig. 26) as well as significant disruption of prokaryotic ternary complex (fig. 25). Interestingly, no change in A_{260} was observed upon addition of glycerol to tRNA, indicating that no extensive unstacking of bases was occurring.

Non-specific effects of glycerol on the association of tubulins has been reported (68). However, in those experiments the concentrations of glycerol utilized were from 10 to 30 times as great as in our experiments. A related report (69) showed the the presence of glycerol in low concentrations inhibited the methylene blue sensitized degradation of guanosine. Their interpretation was that the glycerol interacted (possibly by hydrogen bonding) with the ribose moiety of the nucleoside. If such was the case, it seems likely that the glycerol could interact with the same component of the aa-tRNA. Just how this would catalyze amino acid hydrolysis is difficult to visualize. In any event, our observation is important, since the results of any experiment in which aa-tRNA was observed in the presence of glycerol must be viewed with caution. More specifically, conclusions concerning the interaction of eukaryotic elongation factors (which are stored in glycerol-containing buffer) with aa-tRNA may need to be re-evaluated in light of this discovery.

In conclusion, the results of this research project have shown that the aa-tRNA undergoes a conformational change when it associates with EF-Tu·GTP. Therefore, it is likely that this is the mechanism by which EF-Tu promotes recognition and binding of the aa-tRNA to the ribosome. The position of 4-thiouridine in the corner region of the aa-tRNA is not covered up by the protein in the ternary complex, which leaves the anticodon stem and the corner region of the aa-tRNA available to interact with ribosomal components during recognition.

CHAPTER IX

SUMMARY

The interaction of aa-tRNA with EF-Tu·GTP was investigated using site-specific fluorescent probes located near the corner region of the aa-tRNA.

E. coli $tRNA^{Phe}$ was labeled with fluorescein. The dye was shown to be covalently attached (one dye per tRNA) at the 4-thiouridine position. The attachment of the dye did not significantly alter the ability of this modified aa-tRNA to associate with EF-Tu·GTP.

The emission intensity of Phe-$tRNA^{Phe}$-F^8 increased substantially (28%) when the aa-tRNA complexed with EF-Tu·GTP. Collisional quenching of the fluorescence of the Phe-$tRNA^{Phe}$-F^8 in the ternary complex demonstrated that the fluorescence change was not due to a direct interaction between the protein and the fluorescent dye moiety.

Upon ternary complex formation the binding of Et to aa-tRNA is apparently inhibited, even though the binding site is not blocked by the protein. This observation is consistent with the putative conformation change in the corner region of the aa-tRNA.

Important topological information was provided by collisional quenching and Et binding studies. In the fluorescence quenching experiments, the intensity of the fluorescein emission was quenched whether or not the Phe-tRNA^{Phe}-F^{8} was complexed with EF-Tu·GTP. In the Et binding experiments, it was shown that the strong binding site could be filled even when the aa-tRNA was associated with EF-Tu·GTP. Thus, the region near s^4U is not covered by EF-Tu in the ternary complex.

In addition, our studies provide evidence that there is a conformational difference between unacylated tRNA and aa-tRNA. These two species differed both in their affinity for Et and in the iodide ion quenching efficiency of a fluorescent dye covalently attached to s^4U.

Finally, we found that very low concentrations of glycerol (down to 1% (v/v)) will catalyze the hydrolysis of amino acid from aa-tRNA. The reason for this has not been determined. However, this observation is important in that it makes suspect results of experiments in which low concentrations of glycerol are in contact with aa-tRNA. In particular, investigations into the characteristics of eukaryotic elongation factors (which are stored in a glycerol-containing buffer) may need to be re-evaluated.

Thus, this research shows that association with EF-Tu·GTP induces a conformational change in the aa-tRNA. This may be the primary means by which EF-Tu promotes protein biosynthesis. Topological data from this research, when combined with results from other researchers, indicate that the entire anticodon stem, as

well as the corner region of the aa-tRNA are available to interact with ribosomal components during the recognition process.

BIBLIOGRAPHY

1. Grunberg-Manago, M., Buckingham, R. H., Cooperman, B. S., and Hershey, J. W. B. (1978) Symp. Soc. Gen. Microbiol. 28, 27-110.

2. Johnson, A. E., Fairclough, R. H., and Cantor, C. R. (1977) in Nucleic Acid-Protein Recognition (Vogel, H., ed.) 469-490.

3. Lake, J. A. (1977) Proc. Natl. Acad. Sci. USA 74, 1903-1907.

4. Brot, N. (1977) in Molecular Mechanisms of Protein Biosynthesis (Weissbach, H. and Pestka, S., eds.) 375-411.

5. Furano, A. V. (1975) Proc. Natl. Acad. Sci. USA 72, 4780-4784.

6. Miller, D. L. and Weissbach, H. (1977) in Molecular Mechanisms of Protein Biosynthesis (Weissbach, H. and Pestka, S., eds.) 323-373.

7. Bosch, L., ed. (1972) The Mechanism of Protein Synthesis and Its Regulation.

8. Sprinzl, M. and Cramer, F. (1979) in Progress in Nucleic Acid Research and Molecular Biology 22, 1-69.

9. Jekowsky, E., Schimmel, P., and Miller, D. L. (1977) J. Mol. Biol. 114, 451-458.

10. Boutorin, A. S., Clark, B. F. C., Ebel, J. P., Kruse, T. A., Petersen, H. U., Remy, P., and Vassilenko, S. (1981) J. Mol. Biol. 152. 593-608.

11. Osterberg, R., Sjöberg, B., Ligaarden, R., and Elias, P. (1981) Eur. J. Biochem. 117, 155-159.

12. Beres, L. and Lucas-Lenard, J. (1973) Biochem. 12, 3998-4002.

13. Pingoud, A., Urbanke, C., Krauss, G., Peters, F., and Maass, G. (1977) Eur. J. Biochem. 78, 403-409.

14. Miller, D. L. and Weissbach, H. (1977) in Nucleic Acid-Protein Recognition (Vogel, H., ed.) 409-440.

15. Wagner, T. and Sprinzl, M. (1980) Eur. J. Biochem. 108, 213-221.

16. Pingoud, A. and Urbanke, C. (1980) Biochem. 19, 2108-2112.

17. Knowlton, R. G. and Yarus, M. (1980) J. Mol. Biol. 139, 721-732.

18. Ringer, D. and Chládek, S. (1975) Proc. Natl. Acad. Sci. USA 72, 2950-2954.

19. Jonák, J., Smrt, J., Holý, A., and Rychlík, I. (1980) Eur. J. Biochem. 105, 315-320.

20. Johnson, A. E., Miller, D. L., and Cantor, C. R. (1978) Proc. Natl. Acad. Sci. USA 75, 3075-3079.

21. Yamane, T., Miller, D. L., and Hopfield, J. J. (1981) Biochem. 20, 449-452.

22. Kruse, T. A., Clark, B. F. C., and Sprinzl, M. (1978) Nucleic Acids Res. 5, 879-892.

23. Weygand-Durasevic, I., Kruse, T. A., and Clark, B. F. C. (1981) Eur. J. Biochem. 116, 59-65.

24. Pingoud, A., Kownatzki, R., and Maass, G. (1977) Nucleic Acids Res. 4, 327-338.

25. Lotfield, R. B. and Vanderjagt, D. (1972) Biochem. J. 128, 1353-1356.

26. Grosjean, H. J., de Henau, S., and Crothers, D. M. (1978) Proc. Natl. Acad. Sci. USA 75, 610-614.

27. Yarus, M. (1979) Progress in Nucleic Acid Research and Molecular Biology 23, 195-225.

28. Hopfield, J. J. (1974) Proc. Natl. Acad. Sci. USA 71, 4135-4139.

29. Kurland, C. G., Rigler, R., Ehrenberg, M., and Blomberg, C. (1975) Proc. Natl. Acad. Sci. USA 72, 4248-4251.

30. Shulman, R. G., Hilbers, C. W., and Miller, D. L. (1974) J. Mol. Biol. 90, 601-607.

31. Gamble, R. C. and Schimmel, P. R. (1974) Proc. Natl. Acad. Sci. USA 71, 1356-1360.

32. Schwarz, U., Menzel, H. M., and Gassen, H. G. (1976) Biochem. 15, 2484-2490.

33. Takasaki, Y. and Imahori, K. (1973) J. Biochem. 74, 513-517.

34. Labuda, D. and Augustyniak, J. (1977) Eur. J. Biochem. 79, 303-307.

35. Urbanke, C. and Maass, G. (1978) Nucleic Acids Res. 5, 1551-1560.

36. Wintermeyer, W. and Zachau, H. G. (1971) FEBS Ltrs 18, 214-218.

37. Yang, C.-H. and Söll, D. (1974) Proc. Natl. Acad. Sci. USA 71, 2838-2842.

38. Wintermeyer, W. and Zachau, H. G. (1979) Eur. J. Biochem. 98, 465-475.

39. Kasai, H., Shindo-Okada, N., Noguchi, S., and Nishimura, S. (1979) Nucleic Acids Res. 7, 231-238.

40. Johnson, A. E., Adkins, H. J. Matthews, E. A., and Cantor, C. R. (1982) J. Mol. Biol. (in press).

41. Jones, C. R. and Kearns, D. R. (1975) Biochem. 14,2660-2665.

42. Liebman, M., Rubin, J., and Sundaralingam, M. (1977) Proc. Natl. Acad. Sci. USA 74, 4821-4825.

43. Wells, B. D. and Cantor, C. R. (1977) Nucleic Acids Res. 4, 1667-1680.

44. Nielsen, P. E. (1981) Biochem. Biophys. Acta 655, 89-95.

45. Craig, B. B., Odom, O. W., Foyt, D., White, J. M., and Hardesty, B. (1978) in Biomolecular Structure and Function (Agris, P. F., ed.) 545-553.

46. LePecq, J.-B. and Paoletti, C. (1967) J. Mol. Biol. 27, 87-106.

47. Crane, L. J. and Miller, D. L. (1974) Biochem. 13, 933-939.

48. Lehrer, S. S. and Leavis, P. C. (1978) in Methods Enzymol. 49, 222-236.

49. Yang, C.-H. and Söll, D. (1974) Biochem. 13, 3615-3621.

50. Uziel, M. and Gassen, H. G. (1969) Biochem. 8, 1643.

51. Dube, S. K., Marcker, K. A., and Clark, B. F. C., and Cory, S. (1969) Eur. J. Biochem. 8, 244.

52. Rich, A. and Kim, S.-H. (1978) Scientific American 238, 52.

53. Ofengand, J., Schwartz, I., Chinali, G., Hixson, S. S., and Hixson, S. H. (1977) in Methods Enzymol. 46 (Jakoby, W. and Wilchek, M., eds.) 683-702.

54. Randerath, E., Yu, C.-T., and Randerath, K. (1972) Anal. Biochem. 48, 172-198.

55. Johnson, A. E., Woodward, W. R., Herbert, E., and Menninger, J. R. (1976) Biochem. 15, 569-575.

56. Miller, D. L. and Weissbach, H. (1974) in Methods Enzymol. 30, 219-232.

57. Hatefi, Y. and Hanstein, W. G. (1969) Proc. Natl. Acad. Sci. USA 62, 1129-1136.

58. Wagner, T. and Sprinzl, M. (1979) in Methods Enzymol. 60, 615-628.

59. Ando, T., and Asai, H. (1980) J. Biochem. 88, 255-264.

60. Andrews, P. (1964) Biochem. J. 91, 222-223.

61. Eftink, M. R. and Ghiron, C. A. (1976) Biochem. 15, 672-679.

62. Hartig, P. R., Bertrand, N. J., and Sauer, K. (1977) Biochem. 16, 4275-4282.

63. Scatchard, G. (1949) Ann. N.Y. Acad. Sci. 51, 660-672.

64. Bittman, R. (1969) J. Mol. Biol. 46, 251-268.

65. Slobin, L. I. and Moller, W. (1976) Eur. J. Biochem. 69, 351-366.

66. Johnson, A. E. and Slobin, L. I. (1980) Nucleic Acids Res. 8, 4185-4200.

67. Iwasaki, K., Nagata, S., Kiyoshia, M., and Kaziro, Y. (1974) J. Biol. Chem. 249, 5008-5010.

68. Lee, J. C. and Timasheff, S. N. (1977) Biochem. 16, 1754-1764.

69. Nirmala, J. and Sastry, K. S. (1971) Indian J. Biochem. Biophys. 8, 263-265.

70. Crothers, D. M. and Cole, P. E. (1978) in Transfer RNA (Altman, S., ed.), 196-247.

71. Hirsch, D. (1971) J. Mol. Biol. 58, 439-458.

72. Hirsch, D. and Gold, L. (1971) J. Mol. Biol. 58, 459-468.

73. Vacher, J. and Buckingham, R. H. (1979) J. Mol. Biol. 129, 287-294.

74. Mercola, D. A., Morris, J. W. S., and Arguilla, E. R. (1972) Biochem. 11, 3860-3874.

75. Sprinzl, M. and Faulhammer, H. (1978) Nucleic Acids Res. 5, 4837-4853.

76. Kabsch, W., Gast, W. H., Schulz, G. E., and Leberman, R. (1977) J. Mol. Biol. 177, 999-1012.

77. Morikawa, K., La Cour, T. F. M., Nyborg, J., Rassmussen, K. M., Miller, D. L., and Clark, B. F. C. (1978) J. Mol. Biol. 125, 325-338.

78. Jurnak, F., McPherson, A., Wang, A. H. J., and Rich A. (1980) J. Biol. Chem. 225, 6751-6757.

79. Duffy, L. K., Gerber, L., Johnson, A. E., and Miller, D. L. (1981) Biochem. 20, 4663-4666.

80. Favre, A., Ballini, J. P., and Holler, E. (1979) Biochem. 18, 2887-2895.

81. Holler, E., Baltzinger, M., and Favre, A. (1981) Biochem. 20, 1139-1147.

82. Rigler, R., Nilsson, L., Wintermeyer, W., Pachmann, U., and Zachau, H. G. (1981) Nucleic Acids Res. 9, 1031-1044.

83. Dvorak, D. J., Kidson, C., and Chin, R. C. (1976) J. Biol. Chem. 251, 6730-6734.

84. Potts, R., Fournier, M. J., and Ford, N. C., Jr. (1977) Nature 268, 563-564.

85. Wong, Y. P., Reid, B. R., and Kearns, D. R. (1973) Proc. Natl. Acad. Sci. USA 70, 2193-2195.